Acidosis Activated GPR68
Promotes Vascular Smooth Muscle Cell Growth

Joshua S. Morgan

December 2020

Director of Dissertation: David A. Tulis, Ph.D., F.A.H.A.
Major Department: Department of Physiology

Abstract

Cardiovascular disease (CVD) is the primary cause of death in the United States and worldwide. Localized extracellular acidosis has been theorized as a possible contributor to CVD pathogenesis, but its precise impact remains unclear. G protein coupled receptors (GPCRs) are seven transmembrane receptors that have wide-ranging functions in cardiovascular physiology and pathophysiology. A sub-family of proton sensing GPCRs has been identified that senses changes in extracellular pH and are activated in acidic conditions. One proton sensing GPCR, GPR68, is primarily localized in vascular smooth muscle (VSM) and is thought to signal through stimulatory G_s signaling. The G_s pathway is known to activate cyclic AMP and its downstream effectors PKA and EPAC, yet the influence of GPR68 and its cyclic AMP signals on VSM cell (VSMC) growth in the context of CVD in not known. The hypothesis of this study was to determine that acidic activation of proton sensing GPR68 and its G_s signals regulates VSMC growth via decreased cell proliferation and increased cell death, in turn implicating GPR68 as a potential cytostatic target to control pathologic VSM growth. In primary VSMCs under growth stimulated,

normal pH conditions, loss of GPR68 (using GPR68 knockout (KO) models) results in increased proliferation with evidence pointing toward abbreviated cell cycle progression. Activation of GPR68 under acidic conditions suggests stimulation of G_s signaling through cAMP and the downstream effectors EPAC1, Rap1A/1B, and ERK1/2. Activation of GPR68 under acidic conditions also shows possible influence on intracellular calcium and the cytokine IL-6. In comparison, our in vivo arterial injury studies that mimic acidic vascular conditions suggest a decrease in GPR68 activation and that lack of GPR68 minimalizes remodeling and neointimal growth of VSMCs. Importantly these novel findings highlight the importance of GPR68 and G_s signaling in context-specific regulation of VSMC growth under both normal and acidic conditions. Clinically, a more complete understanding of possible biased signaling for GPR68 could elucidate contextual G_s signaling for deterring the proliferative hallmarks of occlusive CVD.

Acidosis Activated GPR68
Promotes Vascular Smooth Muscle Cell Growth

A Dissertation

Presented to the Faculty of the Department of Physiology

East Carolina University

In Partial Fulfillment of the Requirements for the Degree

Doctorate of Philosophy in Physiology

by

Joshua S. Morgan

December 2020

Acidosis Activated GPR68

Promotes Vascular Smooth Muscle Cell Growth

by

Joshua Morgan

APPROVED BY:

DIRECTOR OF DISSERTATION:_____

(David Tulis, Ph.D.)

COMMITTEE MEMBER:_____

(Johanna Hannan, Ph.D.)

COMMITTEE MEMBER:_____

(Robert Lust, Ph.D.)

COMMITTEE MEMBER:_____

(Kelsey Fisher-Wellman, Ph.D.)

COMMITTEE MEMBER:_____

(Li Yang, Ph.D.)

CHAIR OF THE DEPARTMENT OF PHYSIOLOGY:_____

(Robert Lust, Ph.D.)

DEAN OF THE GRADUATE SCHOOL:_____

(Paul Gemperline, Ph.D.)

TABLE OF CONTENTS

LIST OF FIGURES

LIST OF ABBREVIATIONS

AC,	Adenylyl cyclase
AE,	Anion exchanger
AMPK,	AMP-activated protein kinase
ASIC,	Acid-sensing ion channel
ASM,	Arterial smooth muscle
ATP,	Adenosine triphosphate
CAF,	Cancer associated fibroblasts
cAMP,	3’,5’-Cyclic adenosine monophosphate
cAMP-GEF,	Cyclic AMP guanine nucleotide exchange factor
Cdc-25HD,	Cell division cycle 25 homology domain
CNBD-B	cAMP-nucleotide binding-B domain
CNG,	Cyclic nucleotide-gated
CVD,	Cardiovascular disease
DEP,	Disheveled/EGL-10/pleckstrin
ddC_t	Delta delta C_t
DMEM,	Dulbecco's modified eagle medium
Elk-1	ETS like-1 protein
EPAC,	Exchange protein activated by cAMP
EPCs,	Endothelial progenitor cells
FBS,	Fetal bovine serum
G2A,	G2 accumulating protein
GPCR,	G-protein coupled receptor
G_i,	Inhibitory form of the G alpha subunit
G_s,	Stimulatory form of the G alpha subunit
H,	Histidine
HHBS,	Hanks buffer with 20mM HEPES
HR,	Heart rate

HRP,	Horseradish peroxidase
HSC,	Hemopoietic stem cells
IBMX,	3-Isobutyl-1-Methylxanthine
IL-6,	Interleukin 6
KO,	Knockout
KA,	Knockout cells in acidic media
KN,	Knockout cells in normal media
LCA,	Left carotid artery
LPA,	Lysophosphatidic acid
MAP,	Mean arterial pressure
MKP-1	Mitogen-activated protein kinase phosphatase 1
MLEC,	Mouse lung endothelial cell
MMRRC,	Mutant Mouse Resource & Research Center
MTT,	3-(4,5-dimethylthiazol-2-yl)-2,5-diphenyltetrazolium bromide
NBC,	Na^+-coupled HCO_3^- transporter
OGR1,	Ovarian cancer G protein coupled receptor 1
PAM,	Positive allosteric modulator
PDE,	Phosphodiesterase
PKA,	Protein kinase A
POPDC,	Popeye domain-containing proteins
PVDF,	Polyvinylidene fluoride
PP,	Pulse pressure
PP_i,	Pyrophosphate
RA,	Ras associated
Rap1,	Ras associated protein 1
REM,	Ras exchange motif
RPP,	Rate pressure product
RQ,	Relative quantity

Sap-1a	Stress activated protein 1a
SBP,	Systolic blood pressure
SDS-PAGE,	Sodium dodecyl sulfate-polyacrylamide gel electrophoresis
SEM,	Standard error of the mean
Skp2	S-phase kinase associated protein 2
TBST,	Tris-buffered saline+Tween-20
TDAG8,	T-cell death-associated gene 8
TRPV1	Transient receptor potential cation channel subfamily V member 1
US,	United States
VSM,	Vascular smooth muscle
VSMC,	Vascular smooth muscle cells
VVG,	Verhoeff vanGieson
WA,	Wild type cells in acidic media
WN,	Wild type cells in normal media
WT,	Wild type

CHAPTER 1

Background and Literature Review

Cardiovascular disease is a significant health problem

In the United States and globally, cardiovascular disease (CVD) is the primary cause of morbidity and mortality[1,2]. Cardiovascular disease comprises a large family of related disorders and includes as examples angina pectoris, myocardial and systemic ischemia and/or infarct, coronary heart disease, heart failure, arteriosclerosis and atherosclerosis, hypertension, diabetes, metabolic syndrome, and stroke. Cardiovascular disease is truly considered a significant global pandemic that demands our attention[2]. Just as disconcerting is age-dependency of CVD: its prevalence in adults older than 20 years of age exceeds 121 million, accounting for almost half of the entire US population[3]. In the US alone, more than 100 deaths a day are caused by heart attack, stroke, or other cardiovascular event[4]. Cardiovascular disease accounts for nearly 30% of all global deaths, which totaled around 17.8 million for the year 2017[1]. These CVD-related deaths have been consistently on the rise, with a 21% increase in the year 2017 compared to 10 years earlier[1]. More concerning, deaths worldwide from CVD are on pace to exceed 22 million by the year 2030[1]. The world economic forum in 2011 cited that CVD represents about half of the global deaths attributed to non-communicable diseases[1,2,5]. Economically, the annual direct and indirect costs of CVD in the US alone currently exceeds $351 billion and are projected to approach $1.1 trillion by 2035, with direct costs alone reaching $749 billion[1]. With the human and economic damage that CVD has created over many years, there is an absolute need for improved and expanded efforts to combat CVD and the host of issues it brings to the

world's economy and everyday lives.

Within cardiovascular tissues, the arterial system represents the primary site for many CVD pathologies. The artery wall is made up of three distinct layers: the tunica intima, tunica media and tunica adventitia. While the intima is comprised of endothelial cells and the adventitia is the collagen-rich, outermost connective tissue covering, the media is made up primarily of vascular smooth muscle cells (VSMCs). Aberrant or uncontrolled growth of vascular smooth muscle (VSM) has been shown to contribute to the progression of vascular proliferative disorders. This uncontrolled growth, along with alterations in programmed cell death (apoptosis), other forms of cell death, cell migration, and matrix modulation[6] are instrumental in the pathogenesis of CVD[1,7-9]. These cellular growth processes often operate in positive feedback, eventually remodeling the vessel wall and creating marked lumen stenosis with compromised regional or downstream tissue blood flow[10]. Given its central roles in the pathogenesis of CVD and other vascular disorders and its potential to serve as a rate-limiter for disease maintenance and/or progression, pathologic VSM growth presents an essential focus for continued study and targeted therapeutic intervention.

Fully effective therapies for resolution of CVD are lacking due to an incomplete understanding of its many diverse causes. Prophylactic lifestyle choices include smoking cessation, weight control, and eating a well-balanced, nutritional diet. Pharmacological interventions can include antiplatelet therapies, antihypertension medication, calcium signal blockers and non-prescribed (i.e., over the counter) forms of prophylaxis (e.g., baby aspirin, multi-vitamins) that can be suitable in both treatment and prevention of CVD. Lastly, surgical options to treat existing CVD can include

angioplasty, atherectomy, stenting, and bypass grafting, possibly allowing blocked blood vessels to be mechanically cleared in an effort to re-establish blood flow. Many of these therapies, while useful to some degree, can result in adverse side effects, and these ensuing complications can be even more significant than the original disorder. Therefore, these treatments and in particular their underlying cellular/molecular/biochemical mechanisms need to be studied more extensively to ensure more effective and complete treatments against CVD.

Localized acidosis is a common feature of CVD

In CVD, stenotic vascular growth can eventuate in compromised blood flow and can result in nutrient deprivation and tissue hypoxia/oxygen desaturation that leads to dysregulated and primarily glycolytic cellular metabolism. This largely anerobic glycolytic environment leads to an increase in localized lactic acid levels. This increase in lactic acid results in an increase in CO_2 which, via carbonic anhydrase, is converted into H^+ and HCO_3^-[11]. There are also various other transporters that are utilized for sustained regulatory effects, including alkali cation-H^+ exchangers such as Na^+-H^+ and Na^+-H^+ antiporters, lactate-H^+ cotransporters such as monocarboxylate transporters, bicarbonate transporters such as Na^+-coupled HCO_3^- transporters (NBCs), and acid-loading transporters such as Cl^--HCO_3^- anion exchangers (AEs)[12]. The imbalance H^+ and HCO_3^-, such as by carbonic anhydrase inhibition, in turn, results in extracellular H^+ transport and decreased extracellular pH[11-13]. Modulation of extracellular pH as a central facet of cardiac and vascular function has been known for over a century[14] and dysregulation of pH is a feature of both tissue repair and tumor growth[15].

In the vascular system, normal pH levels are tightly regulated in the range 7.35 to 7.45. Any pH below 7.35 down to 7 is considered moderately acidotic[17], and anything below 7.0 is considered severe acidosis[18]. However, tissue pH levels < 6.0 have been recorded in localized regions of diseased vasculature[16]. In cardiac muscle, a similar range of acidosis, pH 6.8 to 7.2, can cause a reduction of the contractile state[19-23]. Even isolated cardiac muscle in vitro will exhibit decreased contractile forces during either metabolic or respiratory acidosis[19-23].

The reduction of blood pH or use of acid solutions has been shown to induce blood vessel dilation[24], increase blood flow, and evoke VSM relaxation[17]. This occurs when acidic pH, created by increasing CO_2 or H^+, causes vascular cell hyperpolarization, which in turn increases nitric oxide[25] and/or opening of potassium channels[25,26]. This contributes to the hyperpolarization of VSMCs which inhibits calcium influx through the voltage-sensitive calcium channels, leading to vasodilation[26,27]. This phenomenon, the so-called 'acidic-metabolic vasodilation', has been suggested to contribute to the regulation of local blood flow, mediating vasodilation that occurs during hypoxia or ischemia or during increased metabolic activity in order to fulfill the need for energy and oxygen[17].

Vascular smooth muscle cells within the vessel wall experience disease-induced pH changes, and acidosis-mediated events have been suggested to include provoking cell death, inhibiting cell proliferation and inhibiting cell migration[28]. In vivo, extracellular acidosis has been reported to significantly exaggerate vascular injury and contribute to the pathogenesis of CVD[29-32]. Intriguingly and underlying our premise, acidosis-related

processes have been proposed as therapeutic targets against inflammation, stenosis and ischemia, and diverse vascular disorders[31-33].

Acid-sensing G protein-coupled receptors

G protein-coupled receptors (GPCRs) play wide-ranging and important roles in the body and specifically in VSM, where they help control numerous functions from vascular reactivity to proliferation[34-37]. G protein-coupled receptors are characterized by seven transmembrane protein alpha helical segments that make up the intracellular and extracellular loop regions[38]. The GPCR family is the largest known in the human genome, with over 850 family members discovered thus far[38]. GPCRs are present in various tissue types and can be activated by numerous stimuli to consequently activate or inhibit diverse downstream signaling pathways[34].

Upon activation by an agonist, GPCRs undergo conformational changes in their α, β, and γ subunits, leading to the exchange of GTP for GDP that is bound to the G_{α} subunit and allowing dissociation with $G_{\beta\gamma}$. Both the G_{α} and the $G_{\beta\gamma}$ subunits can then activate and modulate downstream signaling processes[39]. The signaling pathways that accompany GPCRs are physiologically essential and control countless cardiovascular functions[38]. G-protein coupled receptors are important clinically and serve as therapeutic targets for ~30% of all FDA approved drugs[40]. In fact, more than half of the drugs that are on the market today act either directly or indirectly through GPCRs[15].

Within this extensive family, a unique sub-family of pH-sensing GPCRs has been identified and characterized as extracellular proton sensors, and these proton sensing GPCRs detect extracellular H^+ and in turn stimulate many cellular activities through their

various intracellular G proteins[34]. This family of proton sensing GPCRs is comprised of GPR4, GPR65 (TDAG8), GPR68, also known as ovarian cancer G protein-coupled receptor 1 (OGR1), and GPR132 (G2A)[33,41,42,43]. These GPCRs are fully activated when extracellular pH drops below physiological range of 6.9, normally by the protonation of several histidine (H) residues (H17, H20, H84, H169, and H269 in GPR68[41,44]; H79,H165, and H269 in GPR4[45]; H10 and H14 in TDAG8[46,47]; and H174 in human, arginine, lysine in mouse and rat in G2A)[48,47] that are present[15,33,42,49].

GPR4 is located in the highest proportion in the lungs, with lower levels in the heart, liver, and intestine[50]. It is activated by both isocapnic and hypercapnic acidosis[31]. Activation of GPR4 elicits a wide variety of responses, from suppression of tumor growth via reduction of cell migration and invasion to endothelial cell inflammatory responses via upregulation of pro-inflammatory cytokines and chemokines[51,52,53].

GPR65, also known as T-cell death-associated gene 8 (TDAG8), is located primarily in immune cells but can also be found in other cells and organs[54,55,56]. It has been associated with anti-inflammatory cAMP signaling and inhibition of pro-inflammatory cytokines and chemokines[57].

GPR132, also known as G2 accumulating protein (G2A) is located in highest levels in lymphoid tissues and macrophages. Its initial role was defined as an antiproliferative cell cycle regulator, in which it induces cell cycle arrest at the G_2/M stage, resulting in G_2 accumulation[58]. Besides impacting the cell cycle, G2A also has roles in oncogenesis, immunity and inflammation[59,60].

Finally, GPR68 becomes fully activated at pH 6.8 and below while becoming inactivated at pH levels above 7.8[49]. GPR68 reportedly can form weak homodimers and heterodimers with the other proton sensing GPCRs[61]. It is also highly homologous across many species, including human, rat, mouse, etc., and shares closest protein sequence homology with GPR4 at around 50%, with transmembrane domain sharing the highest homology.[61,62]. GPR68 has been extensively studied in the tumor microenvironment as well as in the brain and neurological system[63,64]. While it has been reported that VSMCs express primarily GPR68[42,65], expression of GPR4 has also been observed in VSM[42].

These proton sensing GPCRs have been known activate a vast number of downstream pathways, including the G_s or G_i pathways leading to respective activation or inhibition of cAMP synthesis, the G_q pathway and activation of PLC/Ca^{2+}, and the $G_{12/13}$ pathway for Rho and Rac signaling[33]. GPR68, along with GPR4, GPR65 and GPR132, sense through histidine residues in relatively weak or neutral pH settings between 6.0-8.0. Others, like transient receptor potential cation channel subfamily V member 1 (TRPV1) and acid sensing ion channels (ASICs), tend to sense much lower pH levels between pH 4.0-7.0[34,57].

Reported involvement of proton sensing GPCRs in VSM physiology and/or pathology in the scientific literature is scarce. Previous studies involving GPR68 in VSM have given us an introduction into potential roles of proton sensing GPCRs in VSM, but much more work needs to be done in order to get a better understanding of the impact of proton sensing GPCRs in cardiovascular tissues and specifically, of GPR68 in VSM. While our colleagues[31-33,43] and others[30,42] have theorized that acid-sensing GPCRs

may play key roles and serve therapeutic utility in pathogenesis of a variety of disorders, the mechanisms responsible for extracellular acidosis initiating aberrant VSM growth in CVD remain unclear.

VSM growth in CVD

Normal adult VSMCs exist in a fully differentiated state which exhibits low rates of proliferation, migration and cellular death[66]. By contrast, during development, proliferation and migration are important events that are part of normal cell growth in the vessel; moreover, they can be involved in responses to damage and/or injury that can progress to wound healing in the vessel. In response to pathologic insult, VSMCs switch from a homeostatic and contractile phenotype to a synthetic, migratory and proliferative phenotype[7-9,67]. This phenotypic conversion results in reduced vessel function and contractility and a reorganized vessel structure that leads to medial wall remodeling with possible stenotic neointima development. Although this vascular remodeling initially serves as an adaptation to the injurious stimulus, it can soon progress to an uncontrolled, pathologic, and self-perpetuating cascade with severe clinical repercussions such as ischemic luminal obstruction. As such, abnormal proliferation and migration play integral parts in diseased and pathological conditions such as neointimal hyperplasia, atherosclerosis, and hypertension amongst others[68]. Clearly, the impact of pathologic VSM growth and its phenotypic modulation in CVD and other vascular disorders is highly critical and of utmost importance.

In a normal healthy cardiovascular system, cell death, such as apoptosis, is essential in maintenance of homeostasis and for the shaping and sculpting of both cardiac and vascular tissues. In CVD however, changes in blood flow, tissue hypoxia,

and/or cell death impact these processes. While both proliferation and migration have clear outcomes in CVD and studies have implicated apoptosis in CVD[69-71], the precise mechanisms for cell death in CVD remains unclear. In CVD, pathologic cell death can be responsible for the weakening of an aneurysm site, but whether cell death including apoptosis is solely responsible for the formation and eventual rupture of the aneurysm is still up for debate[72]. It has been shown that arterial aneurysmal tissue in an ex vivo environment shows a large number of apoptotic VSMCs and increased expression of pro-apoptotic factors[73]. In atherosclerotic lesions, VSMC apoptosis is implicated as an underlying factor for destabilization and rupture of the fibrotic cap[72]. In neointimal hyperplasia, proliferation of VSMCs is counterbalanced by apoptotic cell death, and an imbalance of this proliferation/cell death can determine a stenotic vessel versus luminal expansion of the vessel[74].

Apoptosis is the primary mode of cell death that offsets VSM growth during CVD. This is particularly true when focusing on ischemic vascular diseases. However, since the discovery of apoptosis, there have been other forms of cell death that have come to light, including autophagy and necroptosis, that have been implicated in CVD. Autophagy is a programmed form of cell death in which cytoplasmic material is broken down and/or recycled by lysosomes and appears to play a role in the heart as well as in the vasculature[75]. Necroptosis is a programmed form of necrosis which triggers necrosis-like morphologic changes and inflammation in surrounding tissues[76]. Information involving necroptosis in CVD and especially in VSM is just now starting to come to light. Studies have been done in the areas of myocardial infarction, atherosclerosis, and abdominal aortic aneurysm that implicate necroptosis as an

underlying mechanism in these pathologies[77-80]. However, the exact role that necroptosis plays in ischemic vascular disease has yet to be determined.

Cyclic AMP signaling in VSM Growth

G protein-coupled receptors are responsible for activation of numerous signaling pathways. The stimulatory GPCR (G_s) is responsible for the synthesis of purine 3',5'-cyclic adenosine monophosphate (cyclic AMP or cAMP). Cyclic AMP is an important and ubiquitous second messenger that is involved in a wide variety of biological processes. The synthesis of cAMP can occur via multiple mechanisms including stimulation of adenylyl cyclase (AC), direct ligand agonism, by β-adrenergic induction, or by GPCRs coupled to G_s. When stimulated, AC synthesizes cAMP by dephosphorylating adenosine triphosphate (ATP), which yields cAMP and pyrophosphate (PP_i)[34]. Conversely, cyclic AMP synthesis is inhibited by activation of inhibitory G proteins (G_i), and synthesized mature cAMP is degraded by a family of phosphodiesterases (PDEs) including primarily PDE3 for cAMP[99].

In the vasculature, cAMP has some duality in regard to its impact on cellular growth that is largely context-specific and dependent on cell or tissue type. Activated cAMP has been shown to reduce both VSMC proliferation[81] and migration[82-84], thereby reducing vascular growth[85]. It can play this inhibitory role by blocking the MAPK pathway[85] or by partially stimulating AMP-activated protein kinase (AMPK)[83]. There are numerous studies that show that cAMP inhibits VSMC proliferation by interrupting the cell cycle, where it disrupts the progress of cells from G_1 into S phase [86], which is responsible for synthesis of new DNA[87-91]. The cAMP pathway and its downstream effector cAMP-dependent protein kinase (PKA) have also been implicated in both pro

and anti-apoptotic responses[87,92]. It was thought that the anti-proliferative effect was largely attributed to its primary effector, PKA[93-95]. Studies have also highlighted other downstream effectors, such as exchange protein directly activated by cAMP (EPAC)[95], in the modulation of growth in VSM. In addition to reducing the effects of cell proliferation and cell death, cAMP is important in regulating vessel tone and cell migration[68,81]. On the other hand, some studies indicate that cAMP is essential in increasing proliferation[96] and migration[97] in promotion of cellular growth[98]. Truly, this diverse, context-specific nature of cAMP signaling including its diverse downstream effectors in cellular growth, and particularly in VSM, renders its impact in CVD pathology unclear.

Once cAMP becomes activated, it can then activate PKA, a serine/threonine kinase that can modulate, via phosphorylation, varied effects within the cell[34]. Protein kinases are required for a large number of both normal physiological and pathophysiological processes, and along with GPCRs, represent a significant amount of the human genome at around 2% with over 500 protein kinases identified in the human body to date[99,100]. In terms of its molecular/cellular mechanism, ATP binds to an active site in a conserved catalytic domain around 250 amino acids in length. This is located between one lobe of N-terminal β-sheets and a second lobe of C-terminal α-helices[101]. Following binding, a set of conserved residues in the catalytic domain transfers the terminal γ-phosphate of ATP to the hydroxyl oxygen of the receiving residue (Ser/Thr) on the target[102.103]. This allows release of the downstream substrate, the remaining ADP is removed, and phosphorylation-driven activation or inactivation of the downstream effector commences. The resulting post-translational modification of these

corresponding downstream proteins then dictates other enzymatic and protein expression/activities and functions that include those critical in both cardiac and vascular diseases.

There are a number studies suggesting that this PKA pathway is pro-apoptotic[104-107] and a number of reports suggesting that it is anti-apoptotic[87,108-111], with this dichotomy largely dependent on cell type and the mechanisms by which apoptosis is induced[112,113]. In rat aortic VSM cells, activation of PKA alone was insufficient in helping mediate cAMP-dependent cell cycle arrest[68], indicating that an alternate cAMP effector might be involved. In addition to working subsequent to cAMP activation and yet by operating synergistically with EPAC in reducing cell proliferation, it is also important to note that PKA activation has conversely been implicated in increased proliferative signaling in VSM cells[96,114]. This increased proliferation may involve a transient activation and not a sustained activation of PKA, which has been thought to be essential in the proliferative response[96]. Additional results point to the involvement of cAMP sensors, such as EPAC, as essential in the inhibition of cell proliferation as opposed to cAMP itself. For example, a PKA selective cAMP analogue (6BNZ-cAMP) was not sufficient to significantly inhibit VSM cell proliferation[115], indicating biological limitations of the cAMP/PKA pathway. This shows the large and complex role by which PKA, and other downstream effectors including EPAC, play in the modulation of vascular growth.

Cyclic AMP can also operate through a variety of non-canonical pathways such as cyclic nucleotide -gated (CNG) ion channels, by binding to Popeye domain-containing (POPDC) proteins as well as through EPAC[34]. One of these pathways, EPAC, comes to the forefront because cAMP has been suggested to inhibit cell

proliferation through EPAC activation[115-119]. Also, findings have identified EPAC as an intracellular effector of G protein signaling in VSMCs[31]. In fact, PKA has been shown to work synergistically with EPAC to reduce VSMC proliferation and migration[115].

EPAC, also known as cyclic AMP guanine nucleotide exchange factor (cAMP-GEF), is made up of two isoforms, EPAC1 and EPAC2. Guanine nucleotide exchange factors are responsible for the release of GDP, allowing binding of GTP to the small GTPase, therefore regulating the transition from the inactive to the active state. These GEFs for Ras-like GTPases include proteins such as Rap1/2. The first isoform, EPAC1, is ubiquitously expressed but is particularly abundant in cardiovascular tissues such as the heart, kidneys, and blood vessels[68,120]. In humans, EPAC1 is encoded by the RAPGEF3 gene[120]. The other isoform, EPAC2, is encoded by the RAPGEF4 gene in humans[68]. However, unlike EPAC1, EPAC2 is not ubiquitously expressed, and along with its three isoforms from alternative splicing, EPAC2A, EPAC2B, and EPAC2C, is more often expressed in the brain, adrenal glands, pituitary, and liver[120-124]. With this in mind, we will focus our discussion specifically on EPAC1 (EPAC) as it relates to the cardiovascular system and specifically VSM.

EPACs are made up of two specific regions, an N-terminal regulatory region and a C-terminal catalytic region[68]. The catalytic region is similar in all EPAC isoforms and consists of a Ras-exchange motif (REM), a Ras association (RA) domain and a cell division cycle 25 homology domain (Cdc25-HD)[120,125-128]. The regulatory region creates the differences between the EPAC isoforms but at its core consists of two domains. The first is the disheveled/EGL-10/pleckstrin (DEP) domain which is responsible for translocation of EPAC from the cytosol to the membrane[129]. The second domain is a

cAMP-nucleotide binding-B domain (CNBD-B), which serves as the binding site for cAMP. Activation of EPAC, in short, goes like this: in the inactive state, the regulatory region blocks the catalytic region of Rap, a downstream protein, from binding to the Cdc25-HD domain. Binding by cAMP to CNBD causes a conformational change which then removes the inhibition by the regulatory region and allows RA to bind to the Cdc25-HD motif[125,129,130], resulting in EPAC activation.

EPAC has been suggested to play significant roles in cell proliferation in a variety of tissues. Aside from working synergistically with PKA, EPAC can inhibit cell proliferation in a PKA-independent manner and has been shown to promote opposing effects on cell proliferation when compared to PKA[131-133]. Although EPAC's downstream activation of Rap1 seems to actually increase cell cycle progression[134], it can also exert inhibitory effects on the cell cycle in a Rap1-independent manner[134]. While the identity of the EPAC effector involved in cell cycle arrest and reduced proliferation is currently unknown, there is possibility that activated EPAC acts as a positive modulator for PKA signaling[81]. In fact, a microarray analysis study of VSMCs stimulated with a selective EPAC agonist (8-pCPT-2′-*O*-Me-cAMP) for 8 hours did not reveal any significantly regulated genes; rather, EPAC activation modulated expression of PKA specific genes like Egr1, which plays a central role in the regulation of VSMC proliferation[135]. These observations indicate that EPAC and PKA signals converge in order to modulate expression of genes that are involved in cell proliferation. However, there are a few instances in which EPAC has been suggested to be anti-apoptotic, although these targets not well defined[87] and, as the authors stated, "may reflect distinct compartmentation of EPAC signaling under different circumstances"[92]. While many

studies implicate EPAC signaling in reduced VSM growth[115-118], to date no studies exist that describe the role of EPAC in acidic vascular tissues much less its involvement in proliferation and migration (in the presence of acidosis) in the context of CVD.

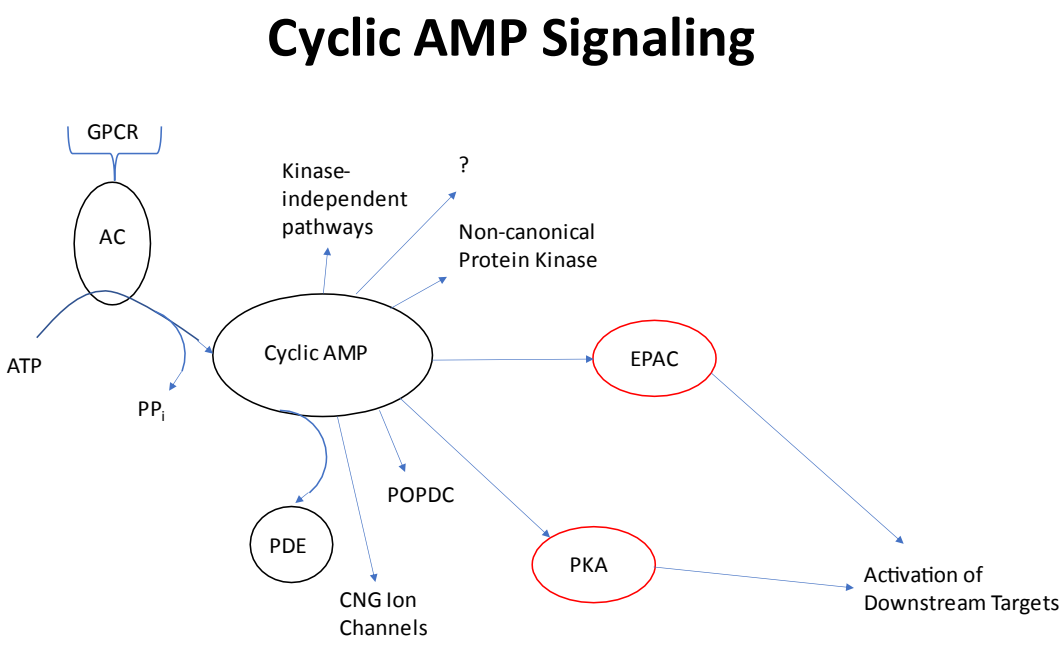

Figure 1. Cyclic AMP Signaling pathway. Overview of cyclic AMP signaling pathway. Activation of GPCR results in synthesis of cAMP by Adenyl Cyclase (AC) by dephosphorylation of ATP, resulting in cAMP and pyrophosphate (PP_i). The resulting cAMP can then activate a host of downstream effectors, including cyclic nucleotide gated (CNG) ion channels, popeye domain containing proteins (POPDC), kinase-independent pathways, non-canonical protein kinases, and many yet to be identified effectors. The primary downstream effector, protein kinase A (PKA), along with exchange protein activated by cAMP (EPAC) both have been implicated in VSMC proliferation and cell death and are responsible for activation of a variety of downstream targets. Degradation of cAMP occurs via a family of proteins called phosphodiesterases.

The regulatory influence of cAMP and its two primary downstream effectors, PKA and EPAC, as well as other potential downstream proteins, on cell growth is not clear. Growth-related outcomes of these proteins and their signals have not been clearly defined to date, and studies on VSM in particular are still needed to discern potential outcomes across a variety of physiological conditions.

Acidosis-induced GPR68 in VSM dysfunction

Relatively little is known regarding acid sensing GPR68 in vascular tissues. Most of the published data involving GPR68 has focused on other major systems or tissues, including the brain, where S100β-positive cells from the rat anterior pituitary gland upregulated IL-6 and proopiomelanocortin in response to GPR68 activation via extracellular acidification[63]. In bone, the lack of GPR68 increases density and increased cell turnover[136]. In gastrointestinal tissues, GPR68 has been implicated in the regulation of ER stress through the IRE1α-JNK signaling pathway and as blockage of autophagosomal degradation[137]. Most notable in the literature is a role for GPR68 in tumorigenesis[49], where GPR68 has been shown to reduce migration and proliferation of cancer cells[138]. In the cardiovascular system, GPR68 is thought to be primarily localized in VSM[6,65,139]; however, at the time of this writing a PubMed search for "GPR68 AND vascular" yielded only 5 original manuscripts and 1 review article on the subject.

In the seminal study on GPR68 in VSMCs[139], acidic pH ranging from 6.8 to 6.3 was found to markedly elevate cAMP (suggested to occur via $G_s/G_q/G_{11}$) and to increase intracellular calcium and prostacyclin within 30 minutes following treatment in human cultured VSMCs, yet the discrete molecular mechanisms involved, the exact roles for GPR68 in mediating these events, and the impact of chronically elevated acidosis in VSM were not addressed in this work. Only a single follow-up journal article exists examining GPR68 specifically in VSMCs[65], and in this report by Liu et al., the investigators examined effects of long-term extracellular acidification on GPR68 signals in human VSMCs[65]. Results from this follow-up study seemed to affirm elevated levels of cAMP secondary to GPR68 activation in human VSMCs. They also concluded that extracellular acidification, whether through GPR68 or some other yet undiscovered

mechanism, and Lysophosphatidic acid (LPA), through the LPA_1 receptor, may play important roles in the initiation and chronic progression of inflammatory diseases[65]. Liu et al. also suggested that the OGR1/COX-2/Prostaglandin I2 (PGI_2) pathway does not play a critical role in acidic media-induced inhibition of DNA synthesis and cell proliferation. Their conclusion was based on the lack of effect after knocking down OGR1 expression, using OGR1 siRNA or by the inhibition of $G_{q/11}$ and COX-2 by their respective antagonists, YM-254890 and indomethacin[65]. Overall, Liu et al. were able to find that responses to acidic pH can be placed into two different categories: an OGR1 (GPR68)-dependent pathway and an OGR1-independent pathway. They found that while extracellular acidification and subsequent GPR68 expression play a role in COX-2 expression, the same could not observed for PGI_2 expression, Mitogen-activated protein kinase phosphatase 1 (MKP-1) expression, and cAMP accumulation. While they did ascertain that cAMP accumulation is tied to acidic pH induced GPR68 expression, they surmised that inhibition of proliferation as well as the regulation of PAI-1 expression are mediated by pathways independent of GPR68[65]. Finally, these authors suggested that an in vivo study using GPR68 deficient mice would help to clarify the roles of proton sensing GPR68 in vascular remodeling and atherogenesis[65].

Another important study[140] that was recently published highlighted GPR68 in vascular dysfunction but did not specifically address GPR68 in VSM. Instead, this work was related to in vivo and ex vivo models of intact blood vessels and involved GPR68 activation in response to shear stress in the microvasculature. However, this experimental design focused on microvascular endothelial cells in response to shear stress and the impact of GPR68 in microvessel remodeling and dilation in response to

shear stress[140]. Acidification in general has been reported to increase VSM-mediated vessel dilation and decrease growth[141,142], yet to date no studies exist documenting regulatory actions of acid-sensing GPR68 on VSM growth including proliferation.

In summary, this project will determine as of yet untested mechanisms in pH-sensing GPR68 and downstream effectors EPAC and PKA as crucial controllers of abnormal VSM growth as an underpinning of CVD. Our general hypothesis is that acidosis activates VSM GPR68, stimulating cAMP-driven PKA and EPAC and in turn deterring VSMC proliferation and increasing cell death as basic elements of abnormal vascular growth in CVD.

BACKGROUND REFERENCES

1. Heart Disease and Stroke Statistics – 2020 Update. A Report from the American Heart Association. On behalf of the American Heart Association Statistics Committee and Stroke Statistics Subcommittee. *Circulation* 1: e138-e596, 2020; https://doi.org/10.1161/CIR.0000000000000757.

2. World Health Organization; World Heart Federation; World Stroke Organization. Global atlas on cardiovascular disease prevention and control: Policies, strategies and interventions. ISBN: 9789241564373, 2011.

3. National Center for Health Statistics. National Health and Nutrition Examination Survey (NHANES) public use data files. Centers for Disease Control and Prevention website. Accessed August 11th, 2020. https://www.cdc.gov/nchs/nhanes/.

4. Ritchey MD, Wall HK, Owens PL, Wright JS. Vital Signs: State-level variation in nonfatal and fatal cardiovascular events targeted for prevention by million hearts 2022. *MMWR Morb Mortal Wkly Rep*. 2018;67(35):974-982. Published 2018 Sep 7. doi:10.15585/mmwr.mm6735a3.

5. Bloom, D.E., Cafiero, E.T., Jané-Llopis, E., Abrahams-Gessel, S., Bloom, L.R., Fathima, S., Feigl, A.B., Gaziano, T., Mowafi, M., Pandya, A., Prettner, K., Rosenberg, L., Seligman, B., Stein, A.Z., & Weinstein, C. The global economic burden of noncommunicable diseases. *Geneva: World Economic Forum.* 2011.

6. Braun-Dullaeus RC, Mann MJ, Dzau VJ. Cell cycle progression: new therapeutic target for vascular proliferative disease. *Circulation*. 1998;98(1):82-89. doi:10.1161/01.cir.98.1.82.

7. Ross, R. The pathogenesis of atherosclerosis: a perspective for the 1990s. *Nature* 362: 801-809, 1993.

8. Tulis, D.A. Novel Cyclic nucleotide signals in the control of pathologic vascular smooth muscle growth, *Cardiovascular Disease II*, 1st Edition, Chapter 9, pp. 175-200, iCONCEPT Press, Ltd., ISBN 978-1-922227-560; https://www.iconceptpress.com/books/042-2-1/cardiovascular-disease-ii/; 2014.

9. Holt, D., Tulis, D. Vascular smooth muscle as a therapeutic target in disease pathology. *Muscle Cell and Tissue*, Chapter 1, pp. 3-26, Ed. K. Sakuma, InTech Open Access Publishers, ISBN 978-953-51-2156-5, doi: 10.5772/60878; http://www.intechopen.com/ articles/show/title/vascular-smooth-muscle-as-a-therapeutic-target-in-disease-pathology, 2015.

10. Tulis DA. Novel protein kinase targets in vascular smooth muscle therapeutics. *Curr Opin Pharmacol*. 2017;33:12-16. doi:10.1016/j.coph.2017.03.003.

11. Lee JY, Alexeyev M, Kozhukhar N, Pastukh V, White R, Stevens T. Carbonic anhydrase IX is a critical determinant of pulmonary microvascular endothelial cell pH regulation and angiogenesis during acidosis. *Am J Physiol Lung Cell Mol Physiol*. 2018;315(1):L41-L51. doi:10.1152/ajplung.00446.2017.

12. Casey JR, Grinstein S, Orlowski J. Sensors and regulators of intracellular pH. *Nat Rev Mol Cell Biol*. 2010;11(1):50-61. doi:10.1038/nrm2820.

13. Kato Y, Ozawa S, Miyamoto C, et al. Acidic extracellular microenvironment and cancer. *Cancer Cell Int*. 2013;13(1):89. Published 2013 Sep 3. doi:10.1186/1475-2867-13-89.

14. Gaskell, W.H. On the tonicity of the heart and blood vessels. *J. Physiology* 3: 48-92, 1880.

15. Weiß KT, Fante M, Köhl G, et al. Proton-sensing G protein-coupled receptors as regulators of cell proliferation and migration during tumor growth and wound healing. *Exp Dermatol*. 2017;26(2):127-132. doi:10.1111/exd.13209.

16. Xiong, Z.G., Zhu, X.M., Chu, X.P., Minami, M., Hey, J., Wei, W.L., MacDonald, J.F., Wemmie, J.A., Price, M.P., Welsh, M.J., Simon, R.P. Neuroprotection in ischemia: blocking calcium-permeable acid-sensing ion channels. *Cell* 118: 687-698, 2004.

17. Celotto AC, Capellini VK, Baldo CF, Dalio MB, Rodrigues AJ, Evora PR. Effects of acid-base imbalance on vascular reactivity. *Braz J Med Biol Res*. 2008;41(6):439-445. doi:10.1590/s0100-879x2008005000026.

18. Kimmoun A, Novy E, Auchet T, Ducrocq N, Levy B. Hemodynamic consequences of severe lactic acidosis in shock states: from bench to bedside [published correction appears in Crit Care. 2017 Feb 21;21(1):40]. *Crit Care*. 2015;19(1):175. Published 2015 Apr 9. doi:10.1186/s13054-015-0896-7.

19. Vaughan Williams EM. The individual effects of CO2, bicarbonate and pH on the electrical and mechanical activity of isolated rabbit auricles. *J Physiol*. 1955;129(1):90-110. doi:10.1113/jphysiol.1955.sp005340.

20. McElroy WT Jr, Gerdes AJ, Brown EB Jr. Effects of CO2, bicarbonate and pH on the performance of isolated perfused guinea pig hearts. *Am J Physiol*. 1958;195(2):412-416. doi:10.1152/ajplegacy.1958.195.2.412.

21. Ng ML, Levy MN, Zieske HA. Effects of changes of pH and of carbon dioxide tension on left ventricular performance. *Am J Physiol*. 1967;213(1):115-120. doi:10.1152/ajplegacy.1967.213.1.115.

22. Opie L. Effect of extracellular pH on function and metabolism of isolated perfused rat heart. *Am J Physiol*. 1965;209(6):1075-1080. doi:10.1152/ajplegacy.1965.209.6.1075.

23. Pannier JL, Brutsaert DL. Contractility of isolated cat papillary muscle and acid-base changes. *Arch Int Pharmacodyn Ther*. 1968;172(1):244-246.

24. Zsoter T, Banderman L, Chappel CI. The effect of "local" pH changes on blood flow in the dog. *Am Heart J*. 1961;61:777-782. doi:10.1016/0002-8703(61)90462-8.

25. Celotto AC, Restini CB, Capellini VK, Bendhack LM, Evora PR. Acidosis induces relaxation mediated by nitric oxide and potassium channels in rat thoracic aorta. *Eur J Pharmacol*. 2011;656(1-3):88-93. doi:10.1016/j.ejphar.2011.01.053.

26. Ishizaka H, Kuo L. Acidosis-induced coronary arteriolar dilation is mediated by ATP-sensitive potassium channels in vascular smooth muscle. *Circ Res*. 1996;78(1):50-57. doi:10.1161/01.res.78.1.50.

27. Siegel G, Emden J, Wenzel K, Mironneau J, Stock G. Potassium channel activation in vascular smooth muscle. *Adv Exp Med Biol*. 1992;311:53-72. doi:10.1007/978-1-4615-3362-7_5.

28. Brenninkmeijer L, Kuehl C, Geldart AM, Arons E, Christou H. Heme oxygenase-1 does not mediate the effects of extracellular acidosis on vascular smooth muscle cell proliferation, migration, and susceptibility to apoptosis. *J Vasc Res*. 2011;48(4):285-296. doi:10.1159/000321555.

29. Naghavi, M., John, R., Naguib, S., Siadaty, M.S., Grasu, R., Kurian, K.C., van Winkle, W.B., Soller, B., Litovsky, S., Madjid, M., Willerson, J.T., Casscells, W. pH heterogeneity of human and rabbit atherosclerotic plaques; a new insight into detection of vulnerable plaque. *Atherosclerosis* 164: 27-35, 2002.

30. Capellini, V.K., Restini, C.B.A., Bendhack, L.M., Evora, P.R.B., Celotto, A.C. The effect of extracellular pH changes on intracellular pH and nitric oxide concentration in endothelial and smooth muscle cells from rat aorta. *PLoS ONE* 8(5): e62887. doi:10.1371/journal.pone.0062887.

31. Chen, A., Dong, L., Leffler, N.R., Asch, A.S., Witte, O.N., T, L.V. Activation of GPR4 by acidosis increases endothelial cell adhesion through the cAMP/Epac pathway. *PLoS ONE* 6(11): e27586. doi:10.1371/journal.pone.0027586; PMID: 22110680, 2011.

32. Dong, L., Li, Z., Leffler, N.R., Asch, A.S., Chi, J.T., Yang, L.V. Acidosis activation of the proton-sensing GPR4 receptor stimulates vascular endothelial cell inflammatory responses revealed by transcriptome analysis. *PLoS ONE* 8(4): e61991. doi:10.1371/journal.pone.0061991. PMID: 23613998; 2013.

33. Justus, C.R., Dong, L., Yang, L.V. Acidic tumor microenvironment and pH-sensing G protein-coupled receptors*. Front. Physiol.* 4:354. doi:10.3389/fphys.2013.00354. 2013.

34. Holland NA, Francisco JT, Johnson SC, et al. Cyclic Nucleotide-directed protein kinases in cardiovascular inflammation and growth. *J Cardiovasc Dev Dis*. 2018;5(1):6. Published 2018 Jan 23. doi:10.3390/jcdd5010006.

35. Maguire JJ, Davenport AP. Regulation of vascular reactivity by established and emerging GPCRs. *Trends Pharmacol Sci*. 2005;26(9):448-454. doi:10.1016/j.tips.2005.07.007.

36. Kaur H, Carvalho J, Looso M, et al. Single-cell profiling reveals heterogeneity and functional patterning of GPCR expression in the vascular system [published correction appears in Nat Commun. 2019 Mar 28;10(1):1448]. *Nat Commun*. 2017;8:15700. Published 2017 Jun 16. doi:10.1038/ncomms15700.

37. Iyinikkel J, Murray F. GPCRs in pulmonary arterial hypertension: tipping the balance. *Br J Pharmacol*. 2018;175(15):3063-3079. doi:10.1111/bph.14172.

38. Rosenbaum DM, Rasmussen SG, Kobilka BK. The structure and function of G-protein-coupled receptors. *Nature*. 2009;459(7245):356-363. doi:10.1038/nature08144.

39. Neves SR, Ram PT, Iyengar R. G protein pathways. *Science*. 2002;296(5573): 1636-1639. doi:10.1126/science.1071550.

40. Hauser A.S., Attwood M.M., Rask-Andersen M., Schioth H.B., Gloriam D.E. Trends in GPCR drug discovery: new agents, targets and indications. *Nat Rev Drug Discov.,*16: 829-842, 2017.

41. Ludwig, M.G., Vanek, G., Guerini, D., Gasser, J.A., Jones, C.E., Junker, U., Hofstetter, H., Wolf, R.M., Seuwen, K. Proton-sensing G-protein-coupled receptors. *Nature* 425: 93-98, 2003.

42. Tomura, H., Mogi, C., Sato, K., Okajima, F. Proton-sensing and lysolipid-sensitive G-protein-coupled receptors: a novel type of multi-functional receptors. *Cell. Signal.* 17: 1466-1476, 2005.

43. Yang, L.V., Radu, C.G., Roy, M., Lee, S., McLaughlin, J., Teitell, M.A., Iruela-Arispe, M.L., Witte, O.N. Vascular abnormalities in mice deficient for the G protein-coupled receptor GPR4 that functions as a pH sensor. *Mol. Cell Biol.* 27:1334-1347, 2007.

44. Sato K, Mogi C, Mighell AJ, Okajima F. A missense mutation of Leu74Pro of OGR1 found in familial amelogenesis imperfecta actually causes the loss of the pH-sensing mechanism. *Biochem Biophys Res Commun*. 2020;526(4):920-926. doi:10.1016/j.bbrc.2020.04.005

45. Liu JP, Nakakura T, Tomura H, et al. Each one of certain histidine residues in G-protein-coupled receptor GPR4 is critical for extracellular proton-induced stimulation of multiple G-protein-signaling pathways. *Pharmacol Res*. 2010;61(6):499-505. doi:10.1016/j.phrs.2010.02.013.

46. Wang JQ, Kon J, Mogi C, et al. TDAG8 is a proton-sensing and psychosine-sensitive G-protein-coupled receptor. *J Biol Chem*. 2004;279(44):45626-45633. doi:10.1074/jbc.M406966200.

47. Radu CG, Nijagal A, McLaughlin J, Wang L, Witte ON. Differential proton sensitivity of related G protein-coupled receptors T cell death-associated gene 8 and G2A expressed in immune cells. *Proc Natl Acad Sci U S A*. 2005;102(5):1632-1637. doi:10.1073/pnas.0409415102.

48. Murakami N, Yokomizo T, Okuno T, Shimizu T. G2A is a proton-sensing G-protein-coupled receptor antagonized by lysophosphatidylcholine. *J Biol Chem*. 2004;279(41):42484-42491. doi:10.1074/jbc.M406561200.

49. Wiley SZ, Sriram K, Salmerón C, Insel PA. GPR68: An Emerging Drug Target in Cancer. *Int J Mol Sci*. 2019;20(3):559. Published 2019 Jan 28. doi:10.3390/ijms20030559.

50. Sanderlin EJ, Leffler NR, Lertpiriyapong K, et al. GPR4 deficiency alleviates intestinal inflammation in a mouse model of acute experimental colitis. *Biochim Biophys Acta Mol Basis Dis*. 2017;1863(2):569-584. doi:10.1016/j.bbadis.2016.12.005.

51. Castellone RD, Leffler NR, Dong L, Yang LV. Inhibition of tumor cell migration and metastasis by the proton-sensing GPR4 receptor. *Cancer Lett*. 2011;312(2):197-208. doi:10.1016/j.canlet.2011.08.013.

52. Chen A, Dong L, Leffler NR, Asch AS, Witte ON, Yang LV. Activation of GPR4 by acidosis increases endothelial cell adhesion through the cAMP/Epac pathway. *PLoS One*. 2011;6(11):e27586. doi:10.1371/journal.pone.0027586.

53. Dong L, Li Z, Leffler NR, Asch AS, Chi JT, Yang LV. Acidosis activation of the proton-sensing GPR4 receptor stimulates vascular endothelial cell inflammatory responses revealed by transcriptome analysis. *PLoS One*. 2013;8(4):e61991. Published 2013 Apr 16. doi:10.1371/journal.pone.0061991.

54. Im DS, Heise CE, Nguyen T, O'Dowd BF, Lynch KR. Identification of a molecular target of psychosine and its role in globoid cell formation. *J Cell Biol*. 2001;153(2):429-434. doi:10.1083/jcb.153.2.429.

55. Lassen KG, McKenzie CI, Mari M, et al. Genetic Coding Variant in GPR65 Alters Lysosomal pH and Links Lysosomal Dysfunction with Colitis Risk. *Immunity*. 2016;44(6):1392-1405. doi:10.1016/j.immuni.2016.05.007.

56. Ishii S, Kihara Y, Shimizu T. Identification of T cell death-associated gene 8 (TDAG8) as a novel acid sensing G-protein-coupled receptor. *J Biol Chem*. 2005;280(10):9083-9087. doi:10.1074/jbc.M407832200.

57. Okajima F. Regulation of inflammation by extracellular acidification and proton-sensing GPCRs. *Cell Signal*. 2013;25(11):2263-2271. doi:10.1016/j.cellsig.2013.07.022.

58. Weng Z, Fluckiger AC, Nisitani S, et al. A DNA damage and stress inducible G protein-coupled receptor blocks cells in G2/M. *Proc Natl Acad Sci U S A*. 1998;95(21):12334-12339. doi:10.1073/pnas.95.21.12334.

59. Tobo M, Tomura H, Mogi C, et al. Previously postulated "ligand-independent" signaling of GPR4 is mediated through proton-sensing mechanisms. *Cell Signal*. 2007;19(8):1745-1753. doi:10.1016/j.cellsig.2007.03.009.

60. Kabarowski JH. G2A and LPC: regulatory functions in immunity. *Prostaglandins Other Lipid Mediat*. 2009;89(3-4):73-81. doi:10.1016/j.prostaglandins.2009.04.007.

61. Zaslavsky A, Singh LS, Tan H, Ding H, Liang Z, Xu Y. Homo- and hetero-dimerization of LPA/S1P receptors, OGR1 and GPR4. *Biochim Biophys Acta*. 2006;1761(10):1200-1212. doi:10.1016/j.bbalip.2006.08.011.

62. Xu Y, Casey G. Identification of human OGR1, a novel G protein-coupled receptor that maps to chromosome 14. *Genomics*. 1996;35(2):397-402. doi:10.1006/geno.1996.0377.

63. Horiguchi K, Higuchi M, Yoshida S, et al. Proton receptor GPR68 expression in dendritic-cell-like S100β-positive cells of rat anterior pituitary gland: GPR68 induces interleukin-6 gene expression in extracellular acidification. *Cell Tissue Res*. 2014;358(2):515-525. doi:10.1007/s00441-014-1958-x.

64. Khan MZ, He L. Neuro-psychopharmacological perspective of orphan receptors of rhodopsin (class A) family of G protein-coupled receptors. *Psychopharmacology (Berl)*. 2017;234(8):1181-1207. doi:10.1007/s00213-017-4586-9.

65. Liu JP, Komachi M, Tomura H, et al. Ovarian cancer G protein-coupled receptor 1-dependent and -independent vascular actions to acidic pH in human aortic smooth muscle cells. *Am J Physiol Heart Circ Physiol*. 2010;299(3):H731-H742. doi:10.1152/ajpheart.00977.2009.

66. Newby AC, Zaltsman AB. Molecular mechanisms in intimal hyperplasia. *J Pathol*. 2000;190(3):300-309. doi:10.1002/(SICI)1096-9896(200002)190:3<300::AID-PATH596>3.0.CO;2-I.

67. Holt, D., de Castro Brás, L., Tulis, D. Cyclic Nucleotide-driven Protein Kinase Signaling in Arterial Smooth Muscle (Patho)physiology, *Coronary Artery Disease – Causes, Symptoms & Treatments*, 1st Edition, iCONCEPT Press, Ltd., ISBN:978-1-922227-92-8. iConcept Press, 2016.

68. Wehbe N, Nasser SA, Al-Dhaheri Y, et al. EPAC in Vascular Smooth Muscle Cells. *Int J Mol Sci*. 2020;21(14):5160. Published 2020 Jul 21. doi:10.3390/ijms21145160.

69. Haunstetter A., Izumo S., Apoptosis: basic mechanisms and implications for cardiovascular disease. *Circulation* 84: 1111-1129, 1998.

70. Perlman H, Maillard L, Krasinski K, Walsh K. Evidence for the rapid onset of apoptosis in medial smooth muscle cells after balloon injury. *Circulation*. 1997;95:981–987.

71. Han DK, Haudenschild CC, Hong MK, Tinkle BT, Leon MB, Liau G. Evidence for apoptosis in human atherogenesis and in a rat vascular injury model. *Am J Pathol*. 1995;147:267–277.

72. Clarke M, Bennett M, Littlewood T. Cell death in the cardiovascular system. *Heart*. 2007;93(6):659-664. doi:10.1136/hrt.2006.088203.

73. López-Candales A, Holmes DR, Liao S, Scott MJ, Wickline SA, Thompson RW. Decreased vascular smooth muscle cell density in medial degeneration of human abdominal aortic aneurysms. *Am J Pathol*. 1997;150(3):993-1007.

74. McLaughlin R, Kelly CJ, Kay E, Bouchier-Hayes D. The role of apoptotic cell death in cardiovascular disease. *Ir J Med Sci*. 2001;170(2):132-140. doi:10.1007/BF03168827.

75. Nemchenko A, Chiong M, Turer A, Lavandero S, Hill JA. Autophagy as a therapeutic target in cardiovascular disease. *J Mol Cell Cardiol*. 2011;51(4):584-593. doi:10.1016/j.yjmcc.2011.06.010.

76. Ruan ZH, Xu ZX, Zhou XY, Zhang X, Shang L. Implications of necroptosis for cardiovascular diseases. *Curr Med Sci*. 2019;39(4):513-522. doi:10.1007/s11596-019-2067-6.

77. Zhang T., Zhang Y., Cui M., Jin L., Wang Y., Lv F., Liu Y., Zheng W., Shang H., Zhang J., Zhang M., et al., CaMKII is a RIP3 substrate mediating ischemia- and oxidative stress-induced myocardial necroptosis, *Nat. Med.* 22: 175–182, 2016.

78. Li Q., Li G., Lan X., Zheng M., Chen K.H., Cao C.M., Xiao R.P., Receptor interacting protein 3 suppresses vascular smooth muscle cell growth by inhibition of the phosphoinositide 3-kinase-Akt axis, *J. Biol. Chem*. 285: 9535–9544, 2010.

79. Wang Q., Liu Z., Ren J., Morgan S., Assa C., Liu B., Receptor-interacting protein kinase 3 contributes to abdominal aortic aneurysms via smooth muscle cell necrosis and inflammation, *Circ. Res.*116: 600–611, 2015.

80. Gupta K, Phan N, Wang Q, Liu B. Necroptosis in cardiovascular disease - a new therapeutic target. *J Mol Cell Cardiol*. 2018;118:26-35. doi:10.1016/j.yjmcc.2018.03.003

81. Smith SA, Newby AC, Bond M. Ending restenosis: inhibition of vascular smooth muscle cell proliferation by cAMP. *Cells*. 2019;8(11):1447. Published 2019 Nov 16. doi:10.3390/cells8111447.

82. Palmer D, Tsoi K, Maurice DH. Synergistic inhibition of vascular smooth muscle cell migration by phosphodiesterase 3 and phosphodiesterase 4 inhibitors. *Circ Res*. 1998;82:852–861.

83. Stone JD, Narine A, Tulis DA. Inhibition of vascular smooth muscle growth via signaling crosstalk between AMP-activated protein kinase and cAMP-dependent protein kinase. *Front Physiol*. 2012;3:409. Published 2012 Oct 29. doi:10.3389/fphys.2012.00409.

84. Hayashi S, Morishita R, Matsushita H, et al. Cyclic AMP inhibited proliferation of human aortic vascular smooth muscle cells, accompanied by induction of p53 and p21. *Hypertension*. 2000;35(1 Pt 2):237-243. doi:10.1161/01.hyp.35.1.237.

85. Schmitt JM, Stork PJ. Cyclic AMP-mediated inhibition of cell growth requires the small G protein Rap1. *Mol Cell Biol*. 2001;21(11):3671-3683. doi:10.1128/MCB.21.11.3671-3683.2001.

86. Fukumoto S, Koyama H, Hosoi M, et al. Distinct role of cAMP and cGMP in the cell cycle control of vascular smooth muscle cells: cGMP delays cell cycle transition through suppression of cyclin D1 and cyclin-dependent kinase 4 activation. *Circ Res*. 1999;85(11):985-991. doi:10.1161/01.res.85.11.985.

87. Insel P.A., Zhang L., Murray F., Yokouchi H., Zambon A.C., Cyclic AMP is both a pro-apoptotic and anti-apoptotic second messenger. *Acta Physiol* 204:277-287*,* 2012.

88. Southgate K, Newby AC. Serum-induced proliferation of rabbit aortic smooth muscle cells from the contractile state is inhibited by 8-Br-cAMP but not 8-Br-cGMP. *Atherosclerosis*. 1990;82(1-2):113-123. doi:10.1016/0021-9150(90)90150-h.

89. Bittinger MA, McWhinnie E, Meltzer J, et al. Activation of cAMP response element-mediated gene expression by regulated nuclear transport of TORC proteins. *Curr Biol*. 2004;14(23):2156-2161. doi:10.1016/j.cub.2004.11.002.

90. Kronemann N, Nockher WA, Busse R, Schini-Kerth VB. Growth-inhibitory effect of cyclic GMP- and cyclic AMP-dependent vasodilators on rat vascular smooth muscle cells: effect on cell cycle and cyclin expression. *Br J Pharmacol*. 1999;126(1):349-357. doi:10.1038/sj.bjp.0702305.

91. Assender JW, Southgate KM, Hallett MB, Newby AC. Inhibition of proliferation, but not of Ca2+ mobilization, by cyclic AMP and GMP in rabbit aortic smooth-muscle cells. *Biochem J*. 1992;288 (Pt 2)(Pt 2):527-532. doi:10.1042/bj2880527.

92. Lezoualc'h F, Fazal L, Laudette M, Conte C. cyclic AMP sensor EPAC proteins and their role in cardiovascular function and disease. *Circ Res*. 2016;118(5):881-897. doi:10.1161/CIRCRESAHA.115.306529.

93. Wu YJ, Bond M, Sala-Newby GB, Newby AC. Altered S-phase kinase-associated protein-2 levels are a major mediator of cyclic nucleotide-induced inhibition of vascular smooth muscle cell proliferation. *Circ Res*. 2006;98(9):1141-1150. doi:10.1161/01.RES.0000219905.16312.28.

94. Hayashi S, Morishita R, Matsushita H, et al. Cyclic AMP inhibited proliferation of human aortic vascular smooth muscle cells, accompanied by induction of p53 and p21. *Hypertension*. 2000;35(1 Pt 2):237-243. doi:10.1161/01.hyp.35.1.237.

95. Indolfi C, Avvedimento EV, Di Lorenzo E, et al. Activation of cAMP-PKA signaling in vivo inhibits smooth muscle cell proliferation induced by vascular injury. *Nat Med*. 1997;3(7):775-779. doi:10.1038/nm0797-775.

96. Hogarth DK, Sandbo N, Taurin S, Kolenko V, Miano JM, Dulin NO. Dual role of PKA in phenotypic modulation of vascular smooth muscle cells by extracellular ATP. *Am J Physiol Cell Physiol*. 2004;287(2):C449-C456. doi:10.1152/ajpcell.00547.2003.

97. Kim MO, Ryu JM, Suh HN, et al. cAMP promotes cell migration through cell junctional complex dynamics and actin cytoskeleton remodeling: implications in skin wound healing. *Stem Cells Dev*. 2015;24(21):2513-2524. doi:10.1089/scd.2015.0130.

98. Hochbaum D, Hong K, Barila G, Ribeiro-Neto F, Altschuler DL. Epac, in synergy with cAMP-dependent protein kinase (PKA), is required for cAMP-mediated mitogenesis. *J Biol Chem*. 2008;283(8):4464-4468. doi:10.1074/jbc.C700171200.

99. S.P. Adderley, C.N. Joshi, D.N. Martin, S. Mooney, D.A. Tulis. Multiple kinase involvement in the regulation of vascular growth. advance in protein kinases. Chapter 6. G. Da Silva Zavier (Ed.), InTech Open Access Publishers ISBN 978-953-51-0633-3 (2012), pp. 131-150.

100. Manning G, Whyte DB, Martinez R, Hunter T, Sudarsanam S. The protein kinase complement of the human genome. *Science*. 2002;298(5600):1912-1934. doi:10.1126/science.1075762.

101. Knighton DR, Zheng JH, Ten Eyck LF, Xuong NH, Taylor SS, Sowadski JM. Structure of a peptide inhibitor bound to the catalytic subunit of cyclic adenosine monophosphate-dependent protein kinase. *Science*. 1991;253(5018):414-420. doi:10.1126/science.1862343.

102. Ubersax JA, Ferrell JE Jr. Mechanisms of specificity in protein phosphorylation [published correction appears in Nat Rev Mol Cell Biol. 2007 Aug;8(8):665]. *Nat Rev Mol Cell Biol*. 2007;8(7):530-541. doi:10.1038/nrm2203.

103. Francis SH, Corbin JD. Structure and function of cyclic nucleotide-dependent protein kinases. *Annu Rev Physiol*. 1994;56:237-272. doi:10.1146/annurev.ph.56.030194.001321.

104. Zambon AC, Zhang L, Minovitsky S, et al. Gene expression patterns define key transcriptional events in cell-cycle regulation by cAMP and protein kinase A. *Proc Natl Acad Sci U S A*. 2005;102(24):8561-8566. doi:10.1073/pnas.0503363102.

105. Carie AE, Sebti SM. A chemical biology approach identifies a beta-2 adrenergic receptor agonist that causes human tumor regression by blocking the Raf-1/Mek-1/Erk1/2 pathway. *Oncogene*. 2007;26(26):3777-3788. doi:10.1038/sj.onc.1210172.

106. Zhang J, Wang Q, Zhu N, et al. Cyclic AMP inhibits JNK activation by CREB-mediated induction of c-FLIP(L) and MKP-1, thereby antagonizing UV-induced apoptosis. *Cell Death Differ*. 2008;15(10):1654-1662. doi:10.1038/cdd.2008.87.

107. Benz PM, Feller SM, Sickmann A, Walter U, Renné T. Prostaglandin-induced VASP phosphorylation controls alpha II-spectrin breakdown in apoptotic cells. *Int Immunopharmacol*. 2008;8(2):319-324. doi:10.1016/j.intimp.2007.10.004.

108. Krakstad C, Christensen AE, Døskeland SO. cAMP protects neutrophils against TNF-alpha-induced apoptosis by activation of cAMP-dependent protein kinase, independently of exchange protein directly activated by cAMP (Epac). *J Leukoc Biol*. 2004;76(3):641-647. doi:10.1189/jlb.0104005.

109. Leone V, di Palma A, Ricchi P, et al. PGE2 inhibits apoptosis in human adenocarcinoma Caco-2 cell line through Ras-PI3K association and cAMP-dependent kinase A activation. *Am J Physiol Gastrointest Liver Physiol*. 2007;293(4):G673-G681. doi:10.1152/ajpgi.00584.2006.

110. Torella D, Gasparri C, Ellison GM, et al. Differential regulation of vascular smooth muscle and endothelial cell proliferation in vitro and in vivo by cAMP/PKA-activated p85alphaPI3K. *Am J Physiol Heart Circ Physiol*. 2009;297(6):H2015-H2025. doi:10.1152/ajpheart.00738.2009.

111. Cribbs JT, Strack S. Reversible phosphorylation of Drp1 by cyclic AMP-dependent protein kinase and calcineurin regulates mitochondrial fission and cell death. *EMBO Rep*. 2007;8(10):939-944. doi:10.1038/sj.embor.7401062.

112. Franklin RA, McCubrey JA. Kinases: positive and negative regulators of apoptosis. *Leukemia*. 2000;14(12):2019-2034. doi:10.1038/sj.leu.2401967.

113. Vermeulen K, Berneman ZN, Van Bockstaele DR. Cell cycle and apoptosis. *Cell Prolif*. 2003;36(3):165-175. doi:10.1046/j.1365-2184.2003.00267.x.

114. Taurin S, Sandbo N, Yau DM, Sethakorn N, Dulin NO. Phosphorylation of beta-catenin by PKA promotes ATP-induced proliferation of vascular smooth muscle

cells. *Am J Physiol Cell Physiol*. 2008;294(5):C1169-C1174. doi:10.1152/ajpcell.00096.2008.

115. Hewer RC, Sala-Newby GB, Wu YJ, Newby AC, Bond M. PKA and Epac synergistically inhibit smooth muscle cell proliferation. *J Mol Cell Cardiol*. 2011;50:87–98. doi: 10.1016/j.yjmcc.2010.10.010.

116. McKean JS, Murray F, Gibson G, Shewan DA, Tucker SJ, Nixon GF.The cAMP-producing agonist beraprost inhibits human vascular smooth muscle cell migration via exchange protein directly activated by cAMP. *Cardiovasc Res*. 2015;107:546–555. doi: 10.1093/cvr/cvv176.

117. Mayer P, Hinze AV, Harst A, von Kügelgen I. A2B receptors mediate the induction of early genes and inhibition of arterial smooth muscle cell proliferation via Epac. *Cardiovasc Res*. 2011;90:148–156. doi: 10.1093/cvr/cvq371.

118. Roscioni SS, Dekkers BG, Prins AG, Menzen MH, Meurs H, SchmidtM, Maarsingh H. cAMP inhibits modulation of airway smooth muscle phenotype via the exchange protein activated by cAMP (Epac) and protein kinase A. *Br J Pharmacol*. 2011;162:193–209. doi:10.1111/j.1476-5381.2010.01011.x.

119. Adderley SP, Martin DN and Tulis DA. Exchange protein activated by cAMP (EPAC) controls migration of vascular smooth muscle cells in concentration and time-dependent manner. *Arch Physiol*. 2015; 2:2. http://dx.doi.org/10.7243/2055-0898-2-2.

120. de Rooij J, Zwartkruis FJ, Verheijen MH, et al. Epac is a Rap1 guanine-nucleotide-exchange factor directly activated by cyclic AMP. *Nature*. 1998;396(6710):474-477. doi:10.1038/24884.

121. Kawasaki H, Springett GM, Mochizuki N, et al. A family of cAMP-binding proteins that directly activate Rap1. *Science*. 1998;282(5397):2275-2279. doi:10.1126/science.282.5397.2275.

122. Hoivik EA, Witsoe SL, Bergheim IR, et al. DNA methylation of alternative promoters directs tissue specific expression of Epac2 isoforms. *PLoS ONE*. 2013;8(7):e67925. Published 2013 Jul 4. doi:10.1371/journal.pone.0067925.

123. Aumo L, Rusten M, Mellgren G, Bakke M, Lewis AE. Functional roles of protein kinase A (PKA) and exchange protein directly activated by 3',5'-cyclic adenosine 5'-monophosphate (cAMP) 2 (EPAC2) in cAMP-mediated actions in adrenocortical cells. *Endocrinology*. 2010;151(5):2151-2161. doi:10.1210/en.2009-1139.

124. Ueno H, Shibasaki T, Iwanaga T, et al. Characterization of the gene EPAC2: structure, chromosomal localization, tissue expression, and identification of the liver-specific isoform. *Genomics*. 2001;78(1-2):91-98. doi:10.1006/geno.2001.6641.

125. Robichaux WG 3rd, Cheng X. Intracellular cAMP Sensor EPAC: Physiology, pathophysiology, and therapeutics development. *Physiol Rev*. 2018;98(2):919-1053. doi:10.1152/physrev.00025.2017.

126. Boriack-Sjodin PA, Margarit SM, Bar-Sagi D, Kuriyan J. The structural basis of the activation of Ras by Sos. *Nature*. 1998;394(6691):337-343. doi:10.1038/28548.

127. Liu C, Takahashi M, Li Y, et al. Ras is required for the cyclic AMP-dependent activation of Rap1 via Epac2. *Mol Cell Biol*. 2008;28(23):7109-7125. doi:10.1128/MCB.01060-08.

128. Popovic M, Rensen-de Leeuw M, Rehmann H. Selectivity of CDC25 homology domain-containing guanine nucleotide exchange factors. *J Mol Biol*. 2013;425(15):2782-2794. doi:10.1016/j.jmb.2013.04.031.

129. de Rooij J, Rehmann H, van Triest M, Cool RH, Wittinghofer A, Bos JL. Mechanism of regulation of the Epac family of cAMP-dependent RapGEFs. *J Biol Chem*. 2000;275(27):20829-20836. doi:10.1074/jbc.M001113200.

130. Niimura M, Miki T, Shibasaki T, Fujimoto W, Iwanaga T, Seino S. Critical role of the N-terminal cyclic AMP-binding domain of Epac2 in its subcellular localization and function. *J Cell Physiol*. 2009;219(3):652-658. doi:10.1002/jcp.21709.

131. Sherr CJ, Roberts JM. CDK inhibitors: positive and negative regulators of G1-phase progression. *Genes Dev*. 1999;13(12):1501-1512. doi:10.1101/gad.13.12.1501.

132. Mayer P, Hinze AV, Harst A, von Kügelgen I. A_2B receptors mediate the induction of early genes and inhibition of arterial smooth muscle cell proliferation via Epac. *Cardiovasc Res*. 2011;90(1):148-156. doi:10.1093/cvr/cvq371.

133. Bond M, Wu YJ, Sala-Newby GB, Newby AC. Rho GTPase, Rac1, regulates Skp2 levels, vascular smooth muscle cell proliferation, and intima formation in vitro and in vivo. *Cardiovasc Res*. 2008;80(2):29.

134. Li Q, Teng Y, Wang J, Yu M, Li Y, Zheng H. Rap1 promotes proliferation and migration of vascular smooth muscle cell via the ERK pathway. *Pathol Res Pract*. 2018;214(7):1045-1050. doi:10.1016/j.prp.2018.04.007.

135. Kimura TE, Duggirala A, Hindmarch CC, et al. Inhibition of Egr1 expression underlies the anti-mitogenic effects of cAMP in vascular smooth muscle cells. *J Mol Cell Cardiol*. 2014;72(100):9-19. doi:10.1016/j.yjmcc.2014.02.001.

136. Krieger NS, Yao Z, Kyker-Snowman K, Kim MH, Boyce BF, Bushinsky DA. Increased bone density in mice lacking the proton receptor OGR1. *Kidney Int*. 2016;89(3):565-573. doi:10.1016/j.kint.2015.12.020.

137. Maeyashiki C, Melhem H, Hering L, Baebler K, Cosin-Roger J, Schefer F, Weder B, Hausmann M, Scharl M, Rogler G, de Vallière C, Ruiz PA. Activation of pH-sensing receptor OGR1 (GPR68) induces ER stress via the IRE1α/JNK pathway in an intestinal epithelial cell model. *Sci Rep*. 2020 Jan 29;10(1):1438. doi: 10.1038/s41598-020-57657-9. PMID: 31996710; PMCID: PMC6989664.

138. Li J., Guo B., Wang J., Cheng X., Xu Y., Sang J. Ovarian cancer G protein coupled receptor 1 suppresses cell migration of MCF7 breast cancer cells via a Gα12/13-Rho-Rac1 pathway. *J Mol Signal* 10: 1-8, 2013.

139. Tomura, H., Wang, J.Q., Komachi, M., Damirin, A., Mogi, C., Tobo, M., Kon, J., Misawa, N., Sato, K., Okajima, F. Prostaglandin I(2) production and cAMP accumulation

in response to acidic extracellular pH through OGR1 in human aortic smooth muscle cells. *J. Biol. Chem.* 280: 34458- 34464, 2005.

140. Xu J, Mathur J, Vessières E, et al. GPR68 senses flow and is essential for vascular physiology. *Cell*. 2018;173(3):762-775.e16. doi:10.1016/j.cell.2018.03.076.

141. Guan, J., Wu, X., Arons, E., Christou, H. The p38 mitogen-activated protein kinase pathway is involved in the regulation of heme oxygenase-1 by acidic extracellular pH in aortic smooth muscle cells. J*. Cell. Biochem*. 105: 1298–1306, 2008.

142. Rios, E.J., Fallon, M., Wang, J., Shimoda, L.A. Chronic hypoxia elevates intracellular pH and activates Na+/H+ exchange in pulmonary arterial smooth muscle cells. *Am. J. Physiol. Lung Cell Mol. Physiol.* 289: L867-L874, 2005.

CHAPTER 2

Materials and Methods

Materials

3-Isobutyl-1-methylxanthine (IBMX) was purchased from Sigma-Aldrich (Saint Louis, MO). 8-CPT-2Me-cAMP was purchased from Tocris Bioscience (Bristol, UK). Primary antibodies were purchased from Invitrogen (Carlsbad, CA), Cell Signaling (Danvers, MA), or EMD Millipore (Burlington, MA), and secondary antibodies were purchased from Rockland (Gilbertsville, PA). Breeding pairs of GPR68 KO mice were purchased (from cryopreserve) from Mutant Mouse Resource & Research Center (MMRRC), Chapel Hill, NC[1]. Wild type (WT) C57BL/6J mice were purchased from Jackson Laboratories (Bar Harbor, ME). GPR68 Taqman primers and custom GPR68 SYBR Green primers were purchased from Thermo Fisher Scientific (Waltham, MA) and GAPDH primers were purchased from BioRad Laboratories (Hercules, CA). Powdered Dulbecco's Modified Eagle Medium (DMEM) and high glucose DMEM were purchased from Gibco (Waltham, MA). Fetal Bovine Serum (FBS) was purchased from Atlanta Biologicals/Bio-Techne (Minneapolis, MN). Milliplex MAP Cytokine/Chemokine Panel was purchased from EMD Millipore (Billerica, MA). cAMP Complete ELISA, PKA protein kinase activity, and FLUOFORTE calcium assay kits were purchased from Enzo Life Sciences (Farmingdale, NY). Bradford protein assay kit was purchased from Thermo Fisher Scientific (Waltham, MA). Verhoeff vanGieson (VVG) stain was purchased from Richard Allen Scientific through Thermo Fisher Scientific (Waltham, MA). RNeasy Plus Mini Kit and QiaShredder were purchased from Qiagen (Hilden, Germany). Superscript VILO IV Mastermix was purchased from Thermo Fisher Scientific (Waltham, MA). Trans-Blot

Turbo Midi PVDF Transfer Kit, Precision Plus Protein All Blue protein standards, and Criterion TGX Stain-Free precast gels were purchased from Bio-Rad Laboratories. (Hercules, CA). Super Signal West Pico substrates were purchased from Thermo Fisher Scientific (Waltham, MA). Primocin was purchased from InvivoGen (San Diego, CA). Reagent Packs for Vi-Cell were purchased from Beckman Coulter (Brea, CA). Sterile 6-0 Prolene blue monofilament suture was purchased from Ethicon (Somerville, NJ). Vetbond Tissue Adhesive was purchased through 3M Animal Care Products (Saint Paul, MN).

Methods

Mouse Ligation Injury Model

This investigation was approved by the Institutional Animal Care and Use Committee and conformed to the Guide for the Care and Use of Laboratory Animals (National Research Council, revised 2011). Mouse carotid artery ligation injury was performed as we've previously described[2,3]. Briefly, male and female adult age-matched (age range 3–10 months, n=17) C57BL/6J WT and GPR68 KO mice were given buprenorphine (0.05-0.1 mg/kg; SC) or meloxicam (5-10 mg/kg, PO) as an analgesic 10 minutes prior to being anesthetized by isoflurane (0.25-2%) supplied by the Department of Comparative Medicine, Brody School of Medicine, East Carolina University, Greenville, NC. Once anesthesized, the neck area was shaved of hair and swabbed with 3 alternating scrubs of surgical iodine and 70% alcohol. The animal was laid supine on a heated operating table, and legs and head were retracted carefully. The skin was opened with a midline incision along the ventral aspect of the neck. Underlying tissues were blunt dissected to expose the common carotid and external

carotid artery branch. Using blunt dissection, the area immediately surrounding the carotid bifurcation was cleared, and sterile 6-0 Prolene suture was double tied around the common carotid artery just proximal to the bifurcation. The overlying tissues were closed in layers, and the skin was closed using non-absorbable non-braided sutures or commercially available, veterinary-grade Vetbond tissue adhesive. The area surrounding the skin incision was swabbed with an antiseptic/antimicrobial agent, the animal was provided supplementary fluids and kept on a heated surface under supervision until full recovery. Upon gaining sternal recumbency animals were returned to their individual cages and were monitored closely for the first 24 hours, then twice daily thereafter while being provided analgesic every day for up to 3 days. Animals were routinely observed for at least 3 days, or until shorter time points were reached to ensure their full recovery. Standard mouse chow and water were provided through the duration of the study.

Rat Balloon Injury Model

This investigation was approved by the Institutional Animal Care and Use Committee and conformed to the Guide for the Care and Use of Laboratory Animals (National Research Council, revised 2011). Rat carotid artery balloon injury was performed as we've previously described[3-5]. Briefly, male and female adult Sprague-Dawley rats (age range 3-6 months, n=6) were given buprenorphine (0.01-0.05 mg/kg; SC) or meloxicam (1 mg/kg, PO) as an analgesic 10 minutes prior to being anesthetized by isoflurane (induction 3-5%; maintenance 1-3%) supplied by the Department of Comparative Medicine, Brody School of Medicine, East Carolina University, Greenville, NC. Once anesthetized, the neck area was shaved of hair and swabbed with 3

alternating scrubs of surgical iodine and 70% alcohol. The animal was laid supine on a heated operating table, and legs and head were retracted carefully. The skin was opened with a midline incision along the ventral aspect of the neck. Underlying tissues were blunt dissected to expose the common carotid and external carotid artery branch. Using blunt dissection, the area immediately surrounding the carotid bifurcation was cleared, and a Fogarty 2-Fr embolectomy catheter was introduced through an external carotid arteriotomy site and advanced through the left common carotid artery to the aortic arch, inflated, and withdrawn with rotation three times to achieve arterial distension injury. Following injury, the catheter was removed, the external carotid arteriotomy was double tied closed with 4-0 sterile suture, overlying tissues and skin were closed in layers, and the skin was sealed with non-absorbable non-braided sutures or commercially available, veterinary-grade Vetbond tissue adhesive. Animals, upon gaining sternal recumbency, were returned to their individual cages and were monitored closely for the first 24 hours, then twice daily thereafter and provided analgesic every day for up to 3 days. Animals were routinely observed for at least 3 days, or until shorter time points were reached to ensure their full recovery. Standard rat chow and water were provided through the duration of the study.

Tissue Processing and Staining

Following our established protocols[4,5], fourteen days after balloon injury in rats or twenty-eight days after ligation injury in mice, animals were deeply anesthetized with isoflurane and euthanized by pneumothorax and exsanguination. Briefly, isotonic saline was perfused transcardially immediately followed by perfusion of 10% formalin buffer in saline. Common carotid arteries were harvested, post-fixed in 10% formalin, and stored

in 70% ethanol until processing. Vessels were processed in graded alcohols and xylenes and embedded upright in liquid paraffin. Five µm artery cross-sections were cut and mounted on charged slides before deparaffinization and rehydration steps were performed to prepare samples for staining. Verhoeff-van Gieson staining of elastic tissue was accomplished per manufacturer's instructions using elastic staining solution containing alcoholic hematoxylin, ferric chloride, and Weigert's iodine. Slides were differentiated in ferric chloride and van Gieson-counterstained. Slides were coverslipped and allowed to dry in desiccating oven for at least 24 hours prior to image analysis. Images were captured microscopically (Leica DM5000B; Leica, Wetzlar, Germany) and analyzed using NIH Image J software. Lumen, neointimal, and medial wall areas were measured, and their ratios calculated (as neointimal area/medial wall area) as a standard measure of arterial remodeling. Also, perimeters of the internal and external elastic laminae were measured to obtain vessel circumferences.

Seeding of Cell plates

WT C57BL/6J and/or GPR68 KO mouse VSMCs were seeded in either 6-well plates at 100,000 cells per well or in 12-well plates at 50,000 cells per well in DMEM supplemented with FBS (10%), 2 mM L-glutamine, and 1:500 dilution of 50 ug/mL Primocin at 37°C in 95% air/5% CO_2 for 36-48 hours. Media was removed and quiescent media containing 0.2% FBS was added 24 hours prior to start of each experiment.

Cell harvest

Primary VSMCs were isolated from thoracic aorta of male C57BL/6J (~25 g; Charles River Labs) by collagenase and elastase digestion and characterized morphologically as previously described[6]. The VSMCs were cultured in DMEM supplemented with FBS (0.5–10%), 2 mM L-glutamine, and 1:500 dilution of 50 ug/mL Primocin at 37°C in 95% air/5% CO_2.

Acidic media

Media was made following protocols set forth by Gibco for DMEM powder high pyruvate high glucose media. The powdered medium was added to room temperature deionized water and gently stirred using a magnetic stir bar. Sodium bicarbonate was added and, based on Henderson-Hasselbach equation, brought to a pH of 6.4 using exactly 3.84 ml of a 7.5% NaOH solution (Gibco) added to the media. The media was taken to a pH of 6.1-6.2 using ≈300 ul of 6N HCl. Finally, the acidic media was filtered through a 0.22 µM filter (Corning, Inc.) to achieve media with a final pH of 6.4. Then, 10% FBS was added to the media to achieve a pH range ≈6.5-6.7, and the media was then stored for subsequent experiments. A pH measurement was taken with each new experiment at the beginning, middle, and end of the experiment in order to establish consistency and maintenance of appropriate pH in the acidic media[7-9].

Milliplex Assay

WT C57BL/6J mouse vascular smooth muscle cells (VSMCs) and GPR68 KO mouse VSMCs were seeded in 6-well plates at 100,000 cells per well. After 36-48 hours, growth media containing 10% FBS was removed and “quiescent media” containing 0.2% FBS was added. After 24 hours, the quiescent media was removed

and either normal growth media or acidic growth media (pH≈6.5-6.7) containing both 10% FBS and IBMX was added to plates accordingly. Over the course of a 5-hour time point, pH was taken of both normal and acidic media at the beginning (time 0 hrs), middle (time 2.5 hrs) and end (time 5 hrs) in order to establish consistency of the acid/base balance of the media and to allow averaging of the measured pH levels over the duration of the 5-hour time point. If pH values varied from the desired levels, either HCl or NaOH was carefully titrated to achieve desired pH. The pH was measured using InLab Micro pH electrode probes and an InLab Micro pH reader (Mettler-Toledo). After 5 hours, cells were trypsinized and placed into 1.5mL Eppendorf tubes. Cells were lysed in RIPA buffer supplemented with protein phosphatase and protease inhibitor cocktail (1:100; Thermo Fisher Scientific). Protein was isolated according to manufacturer's instructions and protein content was determined using the Bradford Protein Assay Kit (Thermo Fisher Scientific). After loading 25µl of protein, the concentration of IL-6 was measured utilizing a Milliplex MAP Cytokine/Chemokine Panel (EMD Millipore, Billerica, MA) according to the manufacturer's instructions. Protein samples from the WT and KO samples with normal or acidic media were run on a MagPix system (Luminex, Austin, TX). All results were analyzed using the Milliplex Analyst software (Version 5.1, EMD Millipore, Billerica, MA).

Viability Assay

WT C57BL/6J mouse VSMCs and GPR68 KO mouse VSMCs were seeded in 12-well plates at 50,000 cells per well and incubated in DMEM supplemented with FBS (10%), 2 mM L-glutamine, and 1:500 dilution of 50 ug/mL Primocin at 37°C in 95% air/5% CO_2 for 36-48 hours. Media was removed and quiescent media containing 0.2%

FBS was added 24 hours prior to start of experiment. At the start of the experiment, quiescent media was removed, and treatment was initiated in either complete growth media or acidic growth media (pH≈6.5-6.7) containing 10% FBS for periods of 0 hours, 24 hours, 48 hours. At each time point cells were trypsinized, and viability was assessed through trypan blue exclusion staining along with automated cell counting (ViCell, Beckman Coulter).

cAMP assay

WT C57BL/6J mouse VSMCs and GPR68 KO mouse VSMCs were seeded in 6-well plates at 100,000 cells per well. After 36-48 hours, growth media containing 10% FBS was removed and quiescent media containing 0.2% FBS was added. After 24 hours, the quiescent media was removed and either normal growth media or acidic growth media (pH≈6.5-6.7) containing both 10% FBS and IBMX was added to plates accordingly. Over the course of a 5 hour time point, pH was taken of both normal and acidic media at the beginning (time 0 hrs), middle (time 2.5 hrs) and end (time 5 hrs) of the 5 hour time point to maintain consistency of pH levels and to average the measured pH levels over time. The pH was measured using InLab Micro pH electrode probes and an InLab Micro pH reader (Mettler-Toledo). Cells were lysed in 0.1M HCL, protein was isolated according to manufacturer's instructions, and protein content was determined using the Bradford Protein Assay Kit (Thermo Fisher Scientific). After the addition of 25 µL of crude lysate to each well of a cAMP Complete ELISA kit (Enzo Life Sciences; Farmingdale, NY), absorbance was read at 450 nm using a bottom-read plate reader (Tecan Infinite M200) and normalized to total protein loaded per well. Total cAMP activity and non-specific binding were used as controls.

PKA Activity Assay

WT C57BL/6J mouse VSMCs and GPR68 KO mouse VSMCs were seeded in 6-well plates at 100,000 cells per well. After 36-48 hours, growth media containing 10% FBS was removed and quiescent media containing 0.2% FBS was added. After 24 hours, the quiescent media was removed and either normal growth media or acidic growth media (pH≈6.5-6.7) containing both 10% FBS and IBMX was added to plates accordingly. Over the course of a 5 hour time point, pH was taken of both normal and acidic media at the beginning (time 0 hrs), middle (time 2.5 hrs) and end (time 5 hrs) of the 5 hour time point to maintain consistency of pH and to average measured pH levels over the time point. The pH was measured using InLab Micro pH electrode probes and an InLab Micro pH reader (Mettler-Toledo). Cells were trypsinized and placed into 1.5 mL Eppendorf tubes. Cells were lysed in RIPA buffer supplemented with protein phosphatase and protease inhibitor cocktail (1:100; Thermo Fisher Scientific). Protein was isolated according to manufacturer's instructions and content determined using the Bradford Protein Assay Kit (Thermo). Then, 30 µL of crude lysate totaling 1µg was loaded into each corresponding well of a 96 well plate that was part of a PKA protein kinase activity kit (Enzo Life Sciences; Farmingdale, NY). Absorbance was read at 450 nm using a bottom-read plate reader (Tecan Infinite M200). RIPA buffer in media was used a negative control.

Cell proliferation assay

Cultured VSMCs were plated in 6-well plates at 100,000 cells/well in complete media containing DMEM and supplemented with 10% FBS until 50% confluent. Cells were quiesced in 0.2% FBS for 24 hours followed by treatment in complete growth

media for 48 hours as described above. Cells were trypsinized, and proliferation and viability were assessed through automated cell counting with trypan blue exclusion staining as an estimate of cell viability (ViCell, Beckman).

Cell Cycle Analysis

Cells were plated in 12-well plates at 25,000 cells/well in complete media until ~50% confluent. Cells were quiesced in 0.2% FBS for 24 hours followed by treatment in complete growth media (DMEM, 20% FBS; Primocin) for 12 hours. Cells were trypsinized, fixed, and stained with propidium iodide for flow cytometry. The fraction of cells in each phase of the cell cycle was assessed by flow cytometry[6].

PCR

Cells were seeded in 6-well plates at 100,000 cells per well. After 36-48 hours, growth media containing 10% FBS was removed and quiescent media containing 0.2% FBS was added. After 24 hours, the quiescent media was removed and either normal growth media or acidic growth media (pH≈6.5-6.7) containing both 10% FBS and IBMX was added to plates accordingly. Over the course of a 5 hour time point, pH was taken of both normal and acidic media at the beginning (time 0 hrs), middle (time 2.5 hrs) and end (time 5 hrs) of the 5 hour time point to maintain pH consistency and to average pH over time. The pH was measured InLab Micro pH electrode probes and an In Lab Micro pH reader (Mettler-Toledo). Total RNA was extracted and isolated using RNeasy Plus Mini kit and QIAShredder (Qiagen) according to manufacturer's instructions. Total RNA was measured using NanoDrop (Thermo Fisher Scientific) to quantify total RNA. Between 1-2ug of RNA, unless otherwise noted, were reversed transcribed using the

SuperScript IV VILO Mastermix (Thermo Fisher Scientific) and a thermal cycler (Bio-Rad) for the synthesis of cDNA from RNA according to manufacturer's instructions. RT-qPCR was perform using Taqman or SYBR green primers (Thermo Fisher Scientific) for GPR68 (s: TGAGCTGGGAGTGTACCTGT; as: AGGATGCCCTGGTAGGAGG) and the housekeeper GAPDH on QuantStudio 6 Real-Time PCR System (Life Technologies). Results and calculations for quality controls were collected, produced, and analyzed using QuantStudio 6 Real Time PCR Software (Life Technologies).

Western Blots

Whole VSMC lysates were subjected to sodium dodecyl sulfate-polyacrylamide gel electrophoresis (SDS-PAGE). Separated protein was transferred to polyvinylidene fluoride (PVDF) membranes with TransBlot Turbo transfer packs (Bio-Rad) using the TransBlot Turbo Transfer System (Bio-Rad) at a mixed molecular weight setting (7 minutes at 2.5A up to 25V). Membranes were blocked for 1 hour at room temperature in 5% dry milk solution containing 0.1% Tris-buffered saline+Tween-20 (TBST). Following blocking, membranes were incubated at 4°C in 5% BSA in 0.1% TBST using 1:1000 primary antibodies (unless otherwise noted) with gentle agitation overnight. Membranes were washed in TBST and incubated for 1 hour at room temperature in 5% dry milk+TBST using 1:5000 horseradish peroxidase (HRP) conjugated anti-rabbit secondary antibody (Rockland; Limerick, PA), unless otherwise noted, with gentle agitation. Membranes were washed and developed using Super Signal West Pico substrates (Thermo Fisher Scientific) per manufacturer's instructions. Chemiluminescent signal was detected and analyzed using Bio-Rad's ChemiDocIt imaging system and software[10].

Calcium Assays

T75 flasks containing WT C57BL/6J mouse VSMCs and GPR68 KO VSMCs were trypsinized and the cell slurry was placed into 15 ml conical tubes. Total viable cell numbers were counted using Vi-Cell automated cell counter (Beckman Coulter). Cells were seeded in 96-well plates at 40,000 cells per well. Plates were allowed to sit overnight (18 hrs) in incubator to allow cells to attach and spread. Cell growth medium containing 10% FBS was then removed. Fluoforte Calcium Assay kit (Enzo Life Sciences) was used to determine intracellular calcium levels. Fluoforte Dye-loading Solution was made, using either normal Hanks buffer with 20mM HEPES (HHBS) or acidic HHBS with 20mM HEPES (pH≈6.4) were added to well plates accordingly. Following manufacturer's instructions, the plates then incubated at room temperature for 1 hour. The assay was then run on a plate reader for a total of 4 hours at Ex=490nm/Em=525nm with readings taken every hour that were taken from both the top and the bottom of the well plate.

Blood Pressure and Heart Rate Measurements

All animals underwent conditioning to the placement and recording for 2 days in the blood pressure tail cuff restraining device (SC1000, Hatteras Instruments), per manufacturer's recommendations. At various ages, animals were placed in the restrainer on a pre warmed (100°F) platform. Blood pressure and heart rate recordings were performed once a day (at the same time each day) for each animal for a maximum of 3 recording sessions. A single recording session lasted no longer than 10 minutes per animal. Once recordings were complete, animals were returned to their cages.

Statistical Analysis

Results are presented as mean ± standard error of the mean (SEM). Statistical analyses were performed with one-way analysis of variance (ANOVA) followed by Tukey's post-hoc multiple comparison tests for comparisons of three or more groups. Two-way ANOVA was used when two different independent variables impacted one continuous dependent variable. Student's t-test were performed for unpaired groups using Graphpad Prism (v7). A p-value < 0.05 was considered statistically significant for all comparisons.

MATERIAL AND METHODS REFERENCES

1. Huang XP, Karpiak J, Kroeze WK, et al. Allosteric ligands for the pharmacologically dark receptors GPR68 and GPR65. *Nature*. 2015;527(7579):477-483. doi:10.1038/nature15699

2. Yuan Y, Liao L, Tulis DA, Xu J. Steroid receptor coactivator-3 is required for inhibition of neointima formation by estrogen. *Circulation*. 2002;105(22):2653-2659. doi:10.1161/01.cir.0000018947.95555.65

3. Holt AW, Tulis DA. Experimental rat and mouse carotid artery surgery: injury & remodeling studies. *ISRN Minim Invasive Surg*. 2013;2013:167407. doi:10.1155/2013/167407

4. Tulis DA. Histological and morphometric analyses for rat carotid balloon injury model. *Methods Mol Med*. 2007;139:31-66. doi:10.1007/978-1-59745-571-8_2

5. Tulis DA. Rat carotid artery balloon injury model. *Methods Mol Med*. 2007;139:1-30. doi:10.1007/978-1-59745-571-8_1

6. Joshi CN, Martin DN, Fox JC, Mendelev NN, Brown TA, Tulis DA. The soluble guanylate cyclase stimulator BAY 41-2272 inhibits vascular smooth muscle growth through the cAMP-dependent protein kinase and cGMP-dependent protein kinase pathways. *J Pharmacol Exp Ther*. 2011;339(2):394-402. doi:10.1124/jpet.111.183400

7. Chen A, Dong L, Leffler NR, Asch AS, Witte ON, Yang LV. Activation of GPR4 by acidosis increases endothelial cell adhesion through the cAMP/Epac pathway. *PLoS One*. 2011;6(11):e27586. doi:10.1371/journal.pone.0027586

8. Dong L, Li Z, Leffler NR, Asch AS, Chi JT, Yang LV. Acidosis activation of the proton-sensing GPR4 receptor stimulates vascular endothelial cell inflammatory responses revealed by transcriptome analysis. *PLoS ONE*. 2013;8(4):e61991. Published 2013 Apr 16. doi:10.1371/journal.pone.0061991

9. Dong L, Krewson EA, Yang LV. Acidosis activates endoplasmic reticulum stress pathways through GPR4 in human vascular endothelial cells. *Int J Mol Sci*. 2017;18(2):278. Published 2017 Jan 27. doi:10.3390/ijms18020278

10. Holt AW, Martin DN, Shaver PR, et al. Soluble guanylyl cyclase-activated cyclic GMP-dependent protein kinase inhibits arterial smooth muscle cell migration independent of VASP-serine 239 phosphorylation. *Cell Signal*. 2016;28(9):1364-1379. doi:10.1016/j.cellsig.2016.06.012

CHAPTER 3

In Vitro Studies on GPR68

Confirmation of the genetic makeup of our GPR68 knockout (KO) and C57BL/6J wild type (WT) mice was performed before their initial use and subsequently during specific experiments. Vascular smooth muscle cells (VSMCs) from the thoracic aorta of KO and WT mice were harvested, and RT-qPCR was performed using Taqman Advanced Master Mix to determine the relative quantities (RQ) of GPR68 mRNA normalized to the housekeeper GAPDH. Results from our RT-qPCR experiments in Figure 2 show statistically significant and complete ablation of GPR68 mRNA in the KO mouse VSMCs compared to C57BL/6J WT mouse VSMCs.

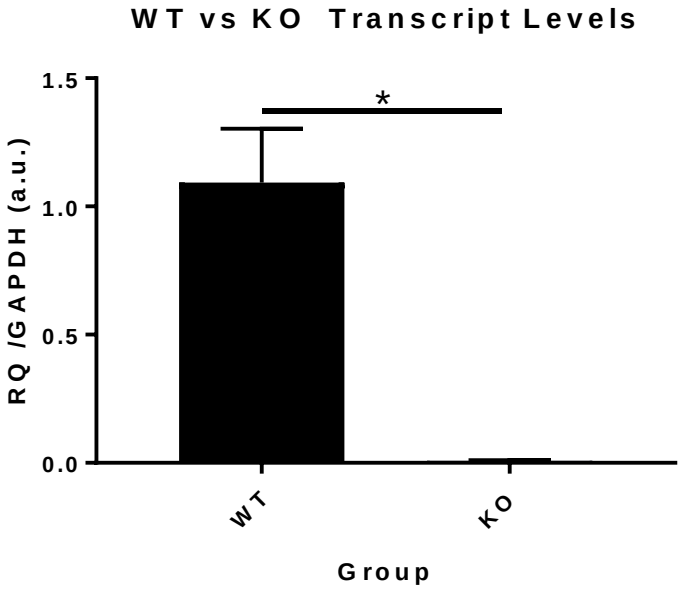

Figure 2. Confirmation of the genetic makeup of our GPR68 knockout (KO) mice and their C57BL/6J wild type (WT) counterparts. WT and GPR68 KO vascular smooth muscle cells (VSMCs) were compared using RT-qPCR to confirm the presence or absence of GPR68 mRNA expression. GPR68 KO cells showed a significant reduction in relative quantification (RQ) of GPR68 mRNA transcript compared to WT cells; n=3 biological replicates in triplicate for each group; *p<.05.

For our RT-qPCR protocols, quality control and primer efficiencies were evaluated on our custom GPR68 and GAPDH primers using SYBR Green reagents,

and results were automatically calculated and quantified using QuantStudio 6 Real-Time PCR System (Life Technologies). As shown in Figure 3, a relative efficiency above 90% validates our use of ΔΔCt and therefore RQ as a scientifically accurate means with which to quantify our observed RT-qPCR mRNA expression values.

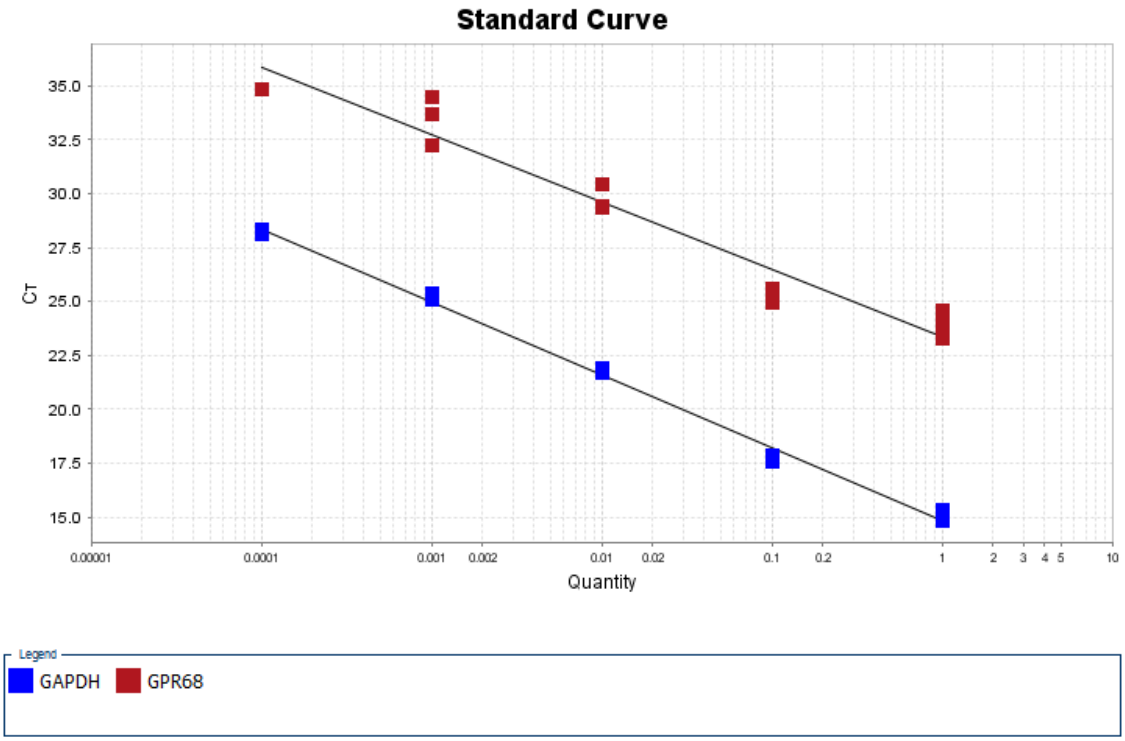

Figure 3. Standard curve shows validity of SYBR Green assay. A standard curve was performed on GPR68 and housekeeping GAPDH primers, and results verified use of both GPR68 and housekeeper GAPDH primers for ΔΔCt and RQ using SYBR Green. Calculations for primer efficiency were performed using QuantStudio 6 software; n=3 biological replicates per group in triplicate.

For our RT-qPCR protocols, quality control and primer validation was also performed using melt curve analysis on our custom GPR68 and GAPDH primers using SYBR Green reagents, and results were automatically calculated using QuantStudio 6 Real-Time PCR System (Life Technologies). Melt curves should contain a single peak, and multiple peaks indicate that the custom primers may be producing multiple PCR

products or primer dimers. From our results shown in Figure 4, there are single peaks for our GPR68 custom primers and for our housekeeper GAPDH primers.

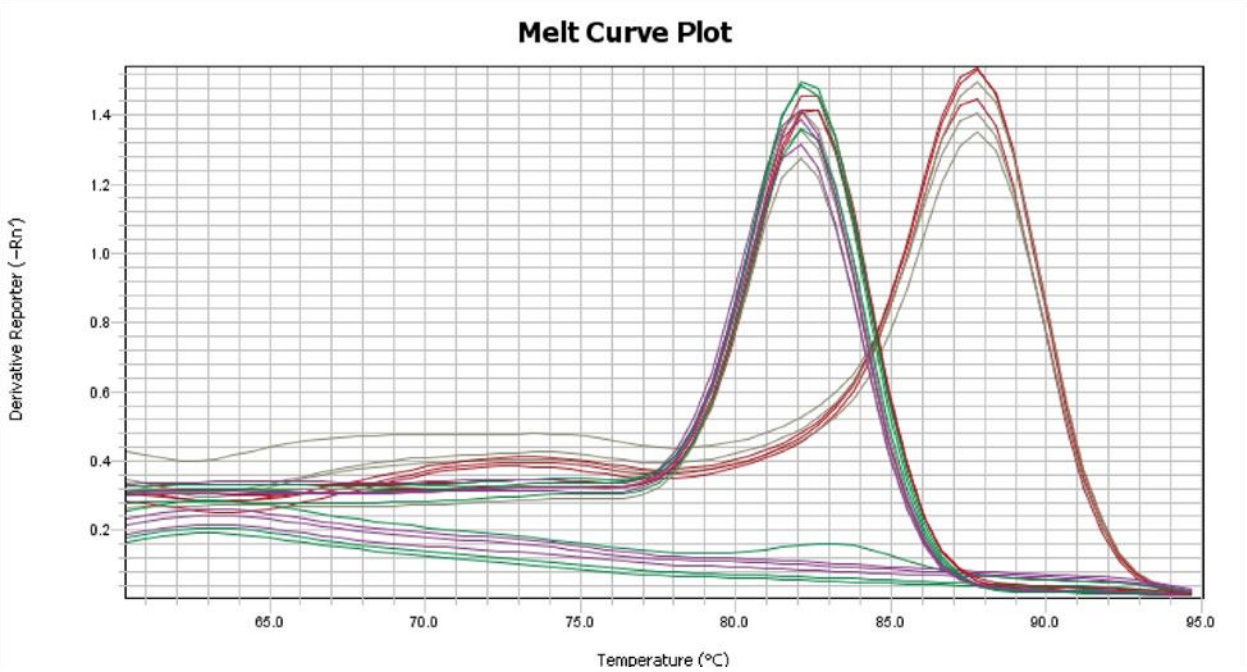

Figure 4. Melt Curve shows validity for SYBR Green. Melt curve plot showing both GPR68 and GAPDH primers in primary WT VSMCs with both containing single peaks. The first set of peaks is for GPR68 primers. The second set of peaks is for KO housekeeper GAPDH primers. Calculations for melt curve were performed using QuantStudio 6 software; n=3 biological replicates in triplicate for each group.

Genotyping confirmation was then performed by the external automatic genotyping vendor Transnetyx. Genotyping was performed by Transnetyx on our male and female GPR68 KO mice and C57BL/6J WT mice using both tail snips and primary VSMCs and probing for both GPR68 and neomycin and using c-JUN as a housekeeping gene. During generation of our KO mice, the neomycin gene was inserted for use as a positive control. As seen in Figure 5, our GPR68 KO mice and VSMCs showed a statistically significant decrease in GPR68 expression compared to the WT mice and VSMCs. Conversely, the GPR68 KO mice showed a statistically significant increase in neomycin expression compared to WT mice and VSMCs. Results shown in Figure 5 are combined data from male and female mouse tail snips and male

and female VSMCs in one graph as their individual data were identical. In sum, these results confirmed GPR68 genotypes of both our WT and GPR68 KO mice and VSMCs.

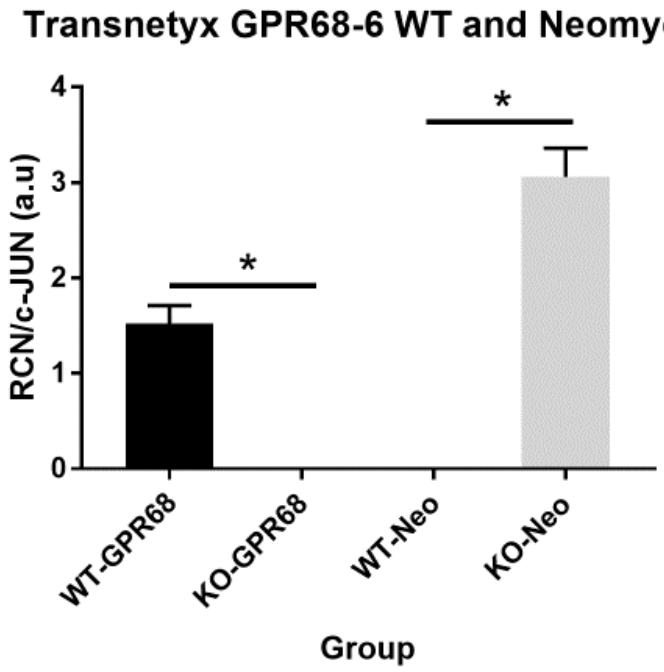

Figure 5. Transnetyx confirmation of GPR68 KO animals. Both WT and GPR68 KO tail snips and VSMCs from both male and female animals were sent to external automatic genotyping vendor Transnetyx for genotyping and confirmation of genetic modification. Significant decrease in GPR68 mRNA expression in the GPR68 KO animals compared to WT controls was observed. Further, a significant increase in positive control neomycin was evident in the KO models compared to the WT controls. Results were from combined male and female tail snips and male and female VSMCs; n=8-10 biological replicates for each group.

Cell viability was then assessed starting from addition of growth media (time 0) through 48 hours in serum-stimulated (10% FBS) primary VSMCs from C57BL/6J WT and GPR68 KO mice. Using trypan blue exclusion staining and automated viability and cell number counting (ViCell), results shown in Figure 6 indicate stable viability for the GPR68 KO cells (~80%) through 24 hours; however, WT cells showed a statistically significant reduction in viability compared to KO cells at the 48 hour time point (Fig. 6C). A timeline for cell viability for both WT and GPR68 KO VSMCs is shown in Figure 6D.

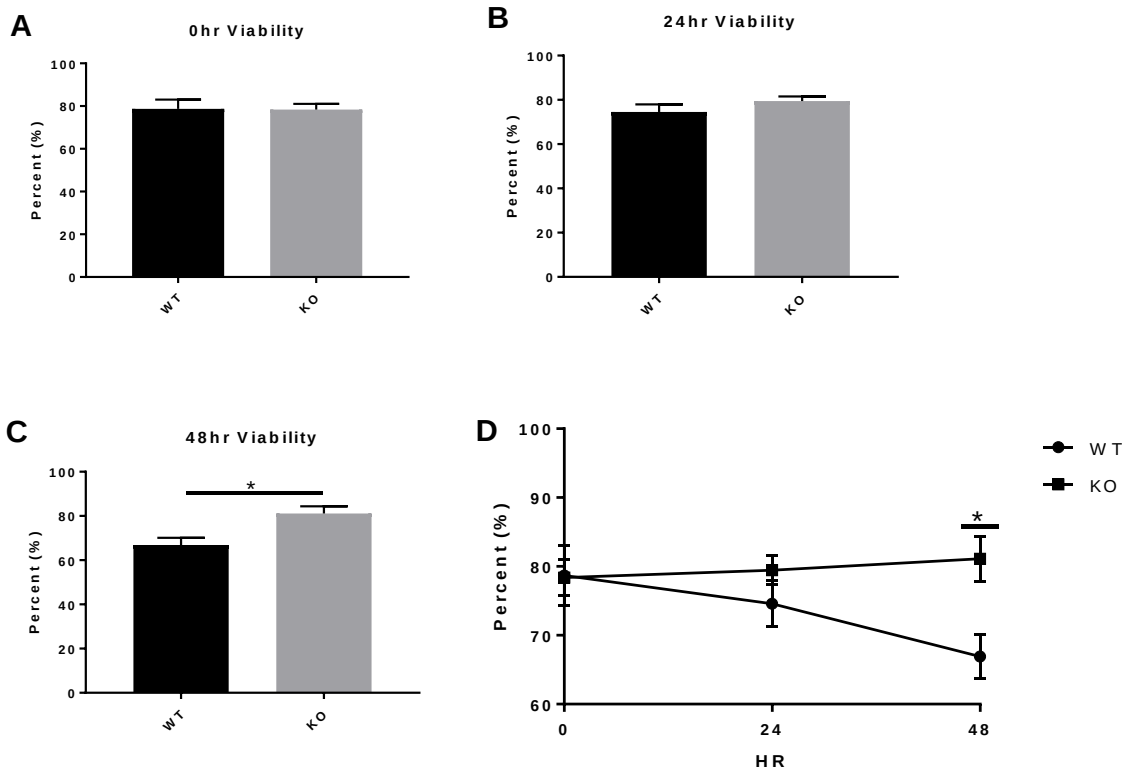

Figure 6. WT and GPR68 KO VSMCs show a difference in cell viability after 48 hours. **A**: There are no significant differences between the WT control VSMCs compared to the GPR68 KO cells at the addition of DMEM with 10% FBS growth media (time 0hr); **B**: After 24 hours, there are no significant differences in viability between the WT and KO groups; **C**: After 48 hours in growth media the viability of the WT cells is significantly decreased compared to the GPR68 KO VSM cells; **D**: Timeline of the viability of WT VSMCs compared to GPR68 KO cells over 48 hours; n=6-10 technical replicates for each group.

Cell circularity, an indirect readout of the contractile state of the cell, cell spreading including the presence of membrane protrusions, and/or cell motility, was evaluated using an automated ViCell cell viability analyzer in serum-stimulated (10% FBS) primary VSMCs from C57BL/6J WT and GPR68 KO mice from addition of growth media (time 0) through 48 hours (Fig. 7). As seen in Figure 7D, although both WT and KO cells showed slight, not significant, reductions in circularity after 24 hours, likely due to acute cell spreading following addition of growth media, no major differences in cell circularity between WT and KO cells were observed over the span of 48 hours. A timeline for cell circularity for both WT and GPR68 KO VSMCs is shown in Figure 7D.

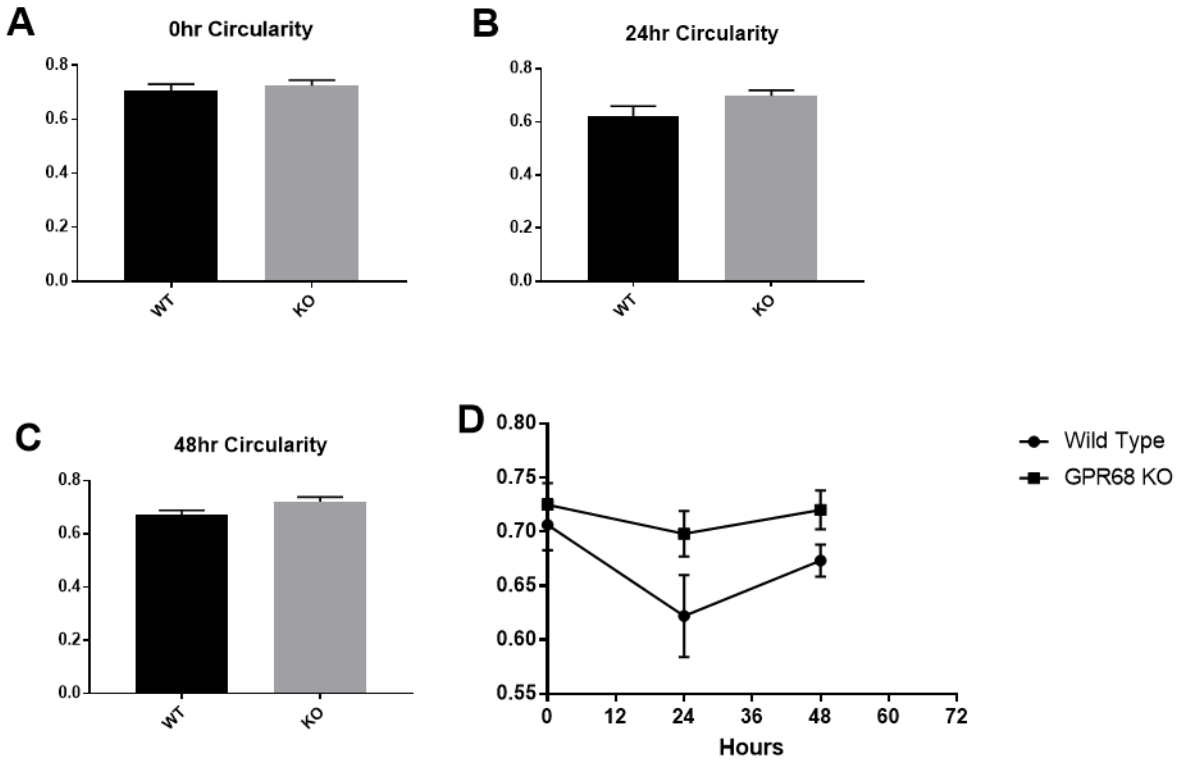

Figure 7. WT and GPR68 KO VSMCs show no significant differences in cell circularity. A: There are no significant differences between the WT control VSMCs compared to the GPR68 KO cells at the addition of DMEM with 10% FBS growth media (time 0); **B**:After 24 hours in growth media there are no significant differences between the WT cells compared to the GPR68 KO VSMCs; **C**: After 48hours, there are no significant differences between the WT and KO groups; **D**: Timeline of the circularity of WT VSMCs compared to GPR68 KO cells over 48 hours; n=6-10 technical replicates for each group

Cell diameter, a marker of cell size and indicative of degree of protein synthesis and cell cycle stage, were assessed using an automated ViCell cell viability analyzer following the addition of growth media (time 0) through 48 hours in serum-stimulated (10% FBS) primary VSMCs 48-hour period. No significant differences in cell diameter between WT and GPR68 KO cells were observed at any time. A timeline for cell diameter for both WT and GPR68 KO VSMCs is shown in Figure 8D.

Cell numbers, a direct measure of hyperplastic cell proliferation, were counted using the automated ViCell cell viability analyzer from addition of growth media (time 0) through 48 hours in serum (10%)-stimulated primary VSMCs from C57BL/6J WT and

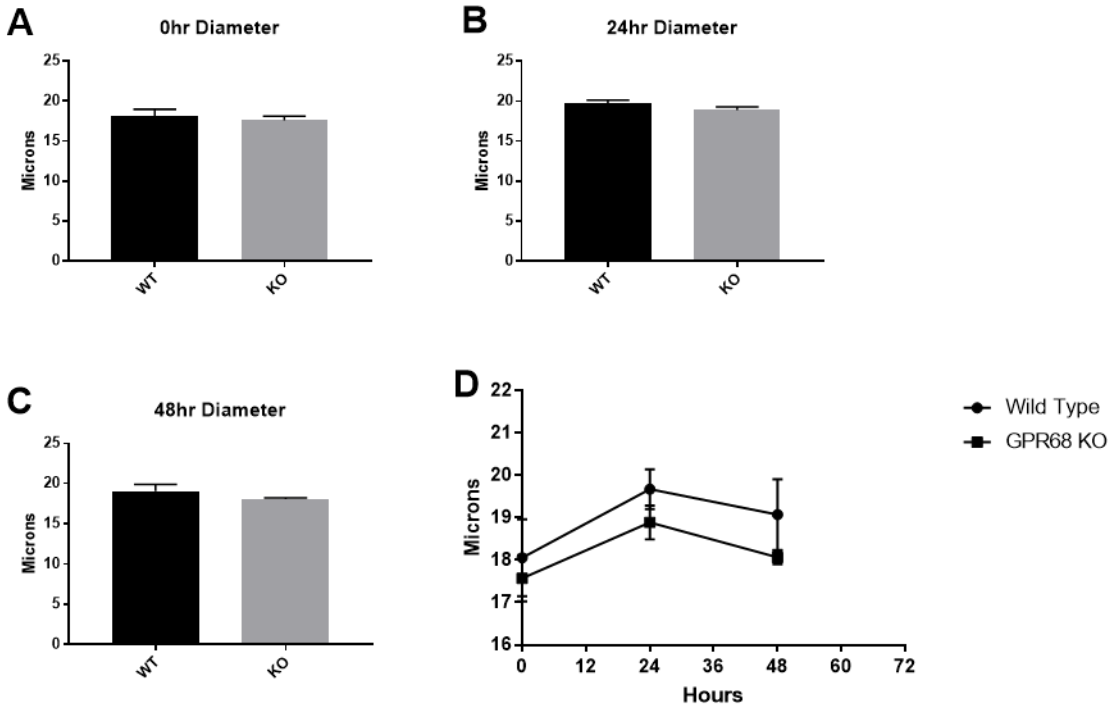

Figure 8. WT and GPR68 KO VSMCs show no significant difference in cell diameter. A: There are no significant differences between the WT control VSMCs compared to the GPR68 KO cells at the addition of DMEM with 10% FBS growth media; **B**:After 24 hours in growth media there are no significant differences between WT cells compared to the GPR68 KO VSMCs; **C**:After 48 hours, there are no significant differences between the two groups; **D**: Timeline of the diameter of WT VSMCs compared to GPR68 KO cells over 48 hours; n=6-10 technical replicates for each group.

GPR68 KO mice. As shown in Figure 9, at addition of growth media (time 0) and after 24 hours, cell numbers from WT and KO mice were the same (Figs. 9A, 9B); however, after 48 hours, there were statistically significant increases in cell numbers in the GPR68 KO group compared to their WT counterparts (Fig. 9C). A timeline for cell numbers for both WT and GPR68 KO VSMCs is shown in Figure 9D.

Cell cycle progression, estimated with flow cytometry as a component of cell proliferation, was determined every 4 hours from plating (time 0) through 12 hours in serum (10%)-stimulated primary VSMCs from C57BL/6J WT and GPR68 KO mice. As seen in Figure 10A, results at plating (time 0) showed no significant differences between

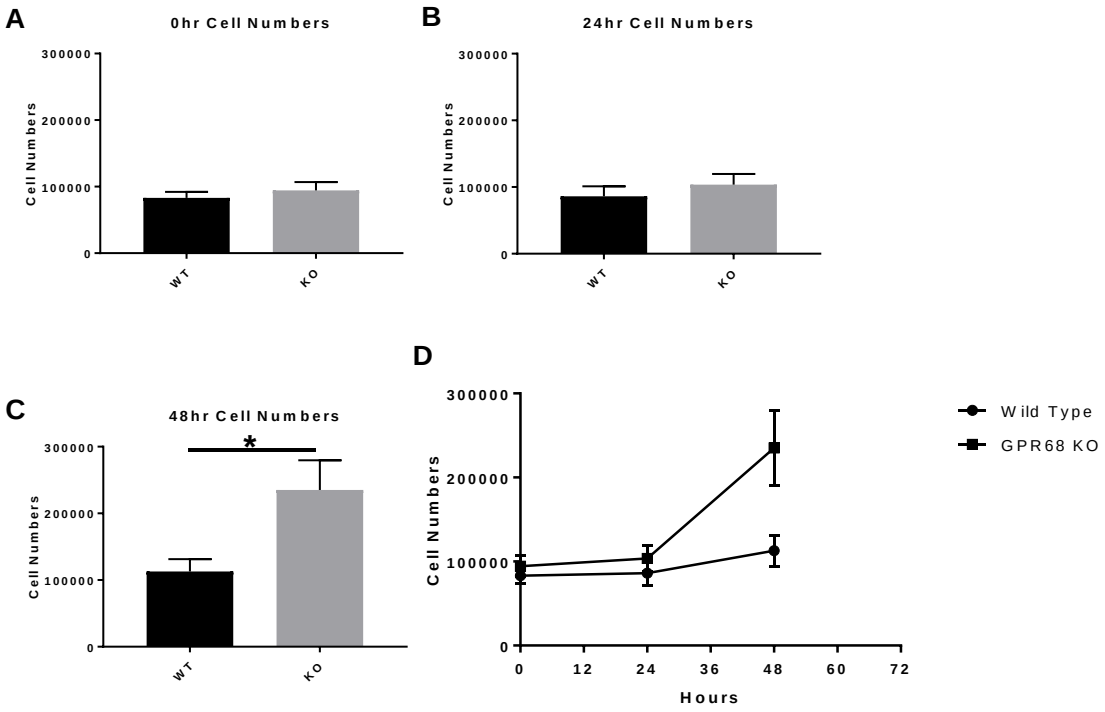

Figure 9. GPR68 KO VSMCs show an increase in cell numbers compared to WT controls after 48 hours. A: There are no significant differences between the WT control VSMCs compared to the GPR68 KO cells at the addition of DMEM with 10% FBS growth media; **B**:After 24 hours in growth media cell numbers of WT cells do not change compared to the GPR68 KO VSMCs; **C**:After 48 hours, there is a significant increase in GPR68 KO cell numbers compared to their WT VSMCs controls; **D**: Timeline of the cell numbers of WT VSMCs compared to GPR68 KO cells over 48 hours; n=6-10 technical replicates for each group.

WT and KO cells throughout the cell cycle; however, trends for reduced KO cells in G_0/G_1 (p=.08) and for increased KO cells in G_2/M (p=.06) compared to WT cells were observed. At the 4-hour time point (Fig. 10B) there was a significant decrease in KO cell numbers in the G_0/G_1 phase compared to WT cells (with no marked differences between WT and KO cells in the other phases) the 8-hour time point (Fig. 10C), no significant differences in the cell cycle phases between the two groups were observed, although a trend for increased KO cells in G_2/M (p=.08) compared to WT cells was noted. After 12 hours (Fig. 10D), no statistically significant differences between the WT and KO groups for any cell cycle phase were observed, although the GPR68 KO cells were trending

(p=.21) toward a higher number of cells in G_0/G_1 and lower cell numbers in S phase (p=.14) compared to WT cells at this time point.

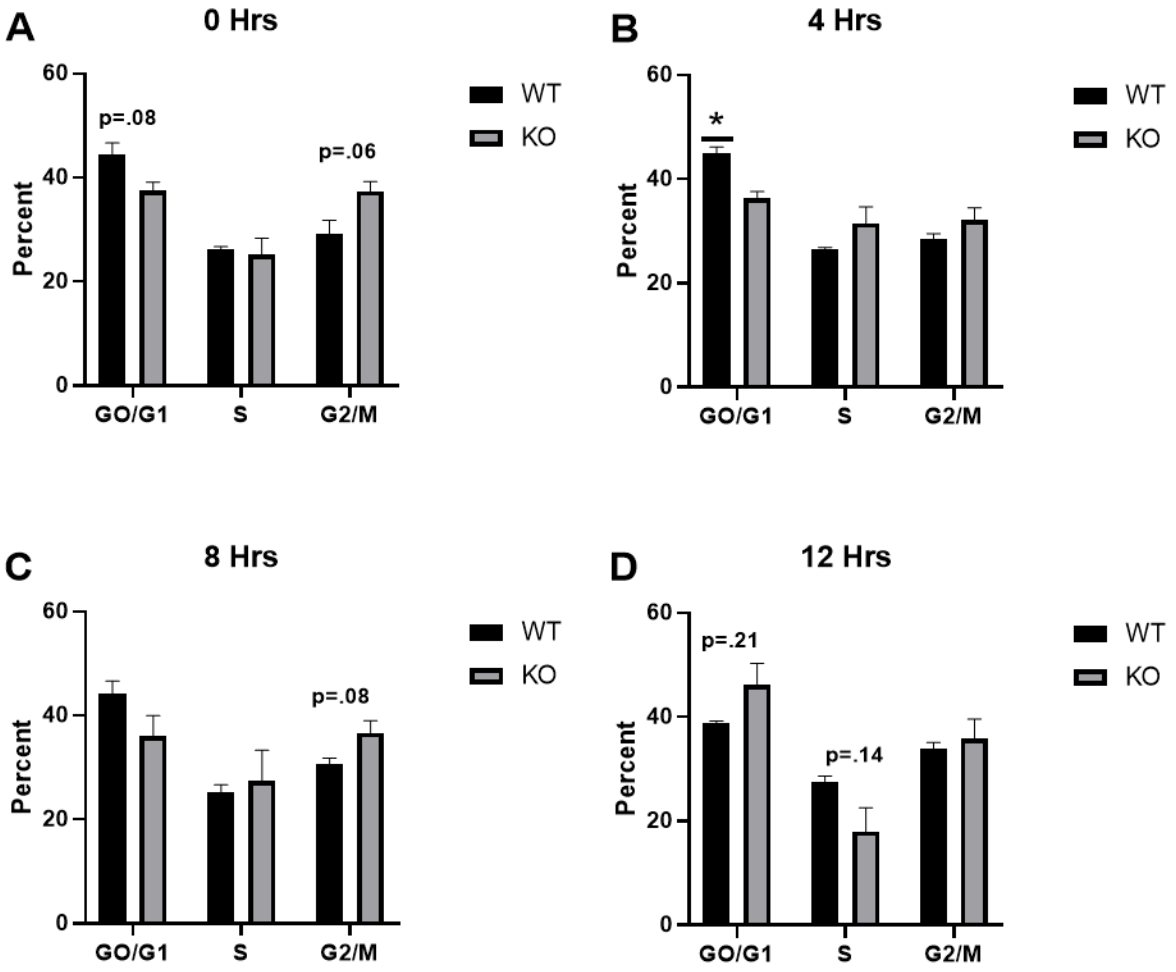

Figure 10. Flow cytometry for cell cycle analysis suggests GPR68 plays a role in a shortened cell cycle. C57BL/6J WT and GPR68 KO VSMCs underwent cell cycle analysis every 4 hours for a total of 12 hours. **A: 0hrs** showed no difference between the WT and KO VSMCs; **B: 4hrs** showed a statistically significant decrease in the KO VSMCs at the G_0/G_1 when compared to its WT counterpart**; C: 8 hrs** showed no difference between the WT and the KO VSMCs **D: 12hrs** While no statistical significance between the two groups was found, it is interesting to note the trending increase at G_0/G_1 for the KO VSMCs compared to the WT VSMCs; n=3 technical replicates for each group.

In experiments using specially-prepared cell culture media with either acidic (pH≈6.5-6.7) pH, as a model of extracellular acidosis, or physiologically normal (pH≈7.4-7.6) pH, we first confirmed biological validity of our custom media by probing for GPR68

and GAPDH mRNA expression. Primary VSMCs from C57BL/6J WT mice were incubated in normal (pH≈7.4-7.6) or acidic (pH≈6.5-6.7) media for 5 hours, and cell lysates were probed for GPR68 mRNA expression using RT-qPCR with both Taqman and SYBR green technologies. As seen in Figure 11, when using Taqman reagents WT cells showed a statistically significant ~4-fold increase in the Relative Quantity (RQ) (normalized to housekeeping GAPDH) of GPR68 mRNA in acidic media compared to WT cells in normal media. The process was then repeated using SYBR green reagents and the results similarly produced a statistically significant ~4-fold increase in the RQ for GPR68/GAPDH in WT cells in acidic media compared to cells in normal media.

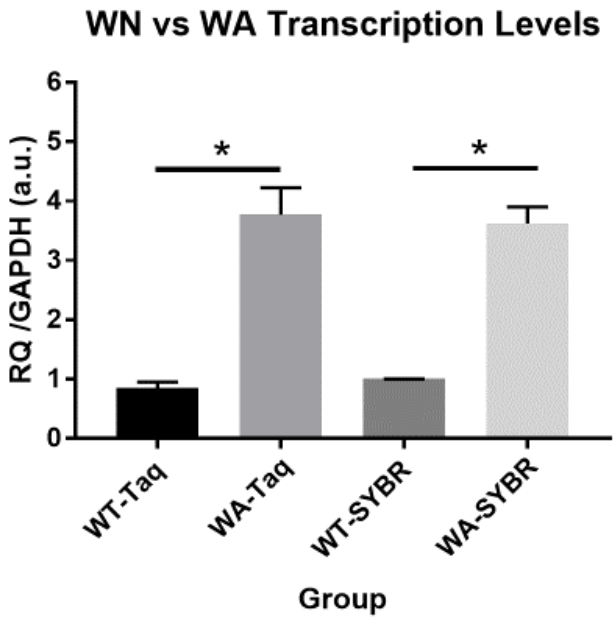

Figure 11. Acidic media shows increase in GPR68 levels compared to normal media in WT animals with Taqman and SYBR Green Reagents; Mouse WT VSMCs were incubated for 5 hours either in normal (pH ≈7.4-7.6) or acidic (pH ≈6.5-6.7) media. Then, RT-qPCR, using both Taqman and SYBR Green technology, was performed. WT cells that were incubated in acidic media (WA) showed a significant 4-fold increase in relative quantification (RQ) of GPR68 mRNA transcript as compared to WT cells that were incubated in normal media (WN) with Taqman reagents. WT cells that were incubated in acidic media as compared to normal media showed a very similar significant 4 fold increase in relative quantification (RQ) of GPR68 transcript as compared to WT cells that were incubated in normal media with SYBR Green reagents; n=3 biological replicates in triplicate for each group.

Using incubation in acidic growth media (pH≈6.5-6.7), to mimic extracellular

acidosis, or normal growth media (pH≈7.4-7.6), and using trypan blue exclusion staining we evaluated the viability of WT and GPR68 KO VSMCs over a period of 48 hours. In general, over the 48-hour time frame, viabilities for both WT and KO cells ranged between 60% and 80%. Results shown in Figure 12A indicate no overt differences in viability in any group at the initial addition of either normal or acidic growth media (time 0). After incubation for 24 hours, WT cells showed significantly increased viability in acidic media (WA) compared to normal media (WN), while no differences were observed in KO cells in acidic (KA) versus normal (KN) media (Fig. 12B). After 48

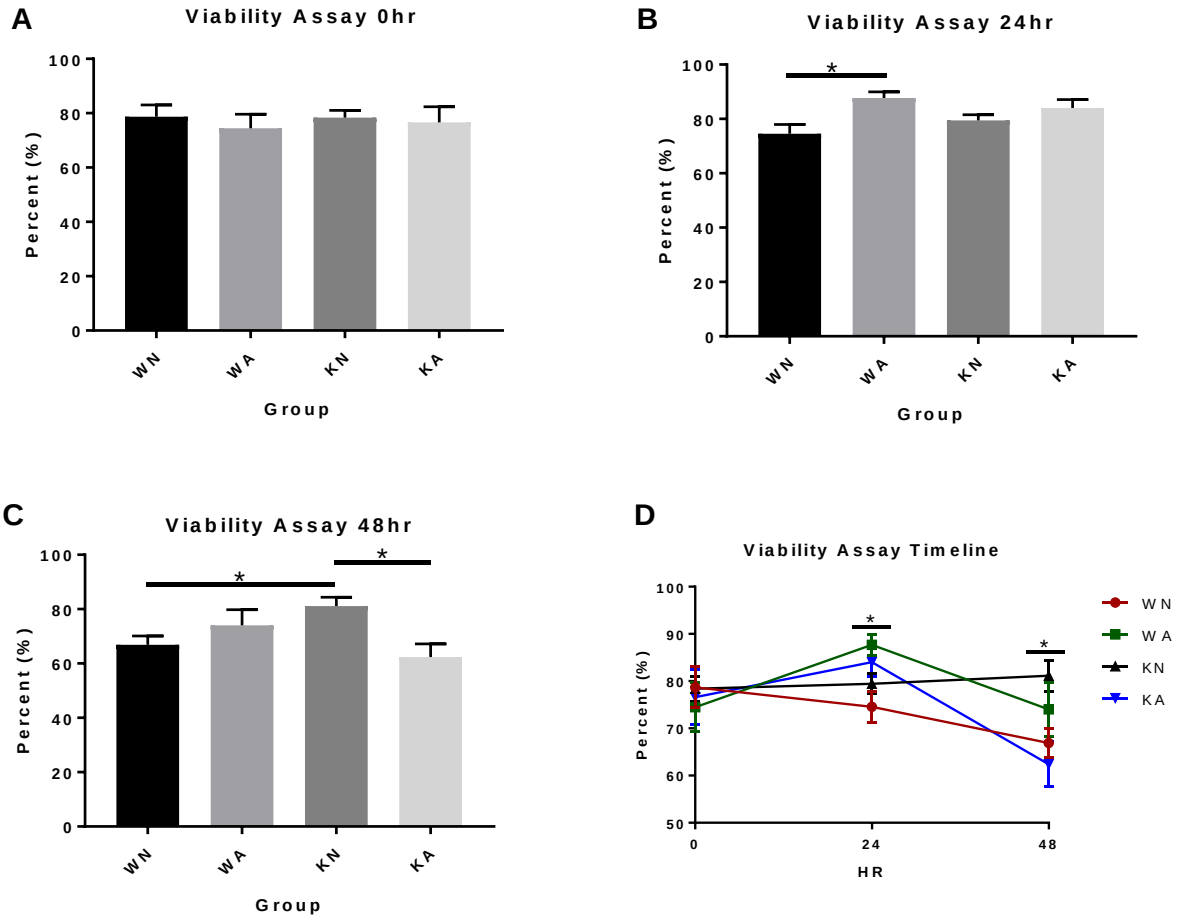

Figure 12. VSMC Viability does not change until 48 hours in acidic vs normal media. A: WT or GPR68 KO VSMC viability over 48 hours in either normal media or acidic media; **B**: Viability from either WT or KO VSMC groups prior to the addition of normal or acidic media at time 0hr; **C**: after 24hours ; **D**: after 48 hours; n= 7-16 technical replicates per group.

hours, KO cells in normal media were more viable compared to both their WT counterparts in normal media (WN) and KO cells in acidic media (KA) (Fig. 12C). A timeline for cell viability for both WT and GPR68 KO VSMCs is shown in Figure 12D.

To determine potential changes in cAMP levels following incubation of WT and GPR68 KO VSMCs in normal or acidic media for 5 hours, a cAMP Complete ELISA was performed. Results in Figure 13 show a significant decrease in cAMP content (normalized to protein per sample) in WT cells in acidic media (WA) compared to their WT counterparts in normal media (WN). No differences in cAMP content were detected in GPR68 KO cells in acidic (KA) versus normal (KN) media. Also, the levels of cAMP in both the KN and KA groups are consistent with the levels of cAMP observed in the

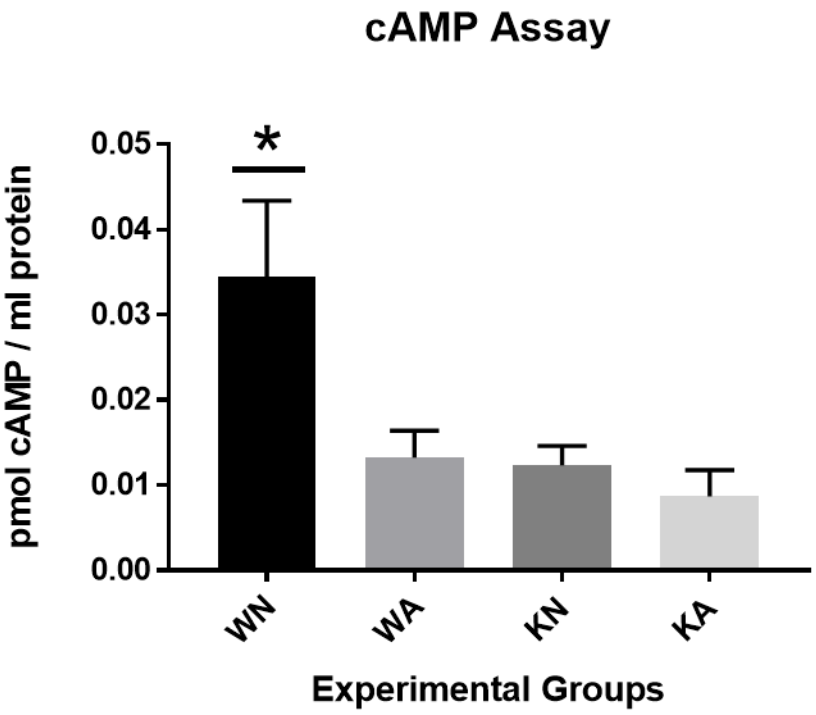

Figure 13. cAMP content decreases in WT cells in acidic media but does not change in GPR68 KO cells. Quantification of cAMP in either WT or GPR68 KO mouse VSMCs in normal (pH ≈7.4-7.6) or acidic (pH ≈6.5-6.7) media. Content of cAMP was normalized to total protein, and results show a significant reduction in cAMP in WT VSMCs following 5 hours in acidic media (WA) as compared to the normal media (WN) control. Content of cAMP in GPR68 KO cells did not significantly change in acidic media compared to normal media but levels were significantly lower than the WT VSMCs in normal media (WN); n=9 technical replicates for each group; * p<.05 versus control.

WA group.

A cAMP-dependent protein kinase (PKA) activity assay was performed to determine changes in the primary cAMP effector PKA following incubation of cells in normal or acidic media. WT and GPR68 KO VSMCs in either normal (pH≈7.4-7.6) or acidic (pH≈6.5-6.7) media, with or without the PDE inhibitor IBMX, were incubated for 5 hours, after which PKA activity was determined (Enzo Life Sciences). Results were quantified and normalized to determine nanograms of PKA per milliliter of homogenate. Results in Figure 14 showed no major differences between groups that contained IBMX versus the groups that did not contain IBMX. Further, PKA activity was unchanged

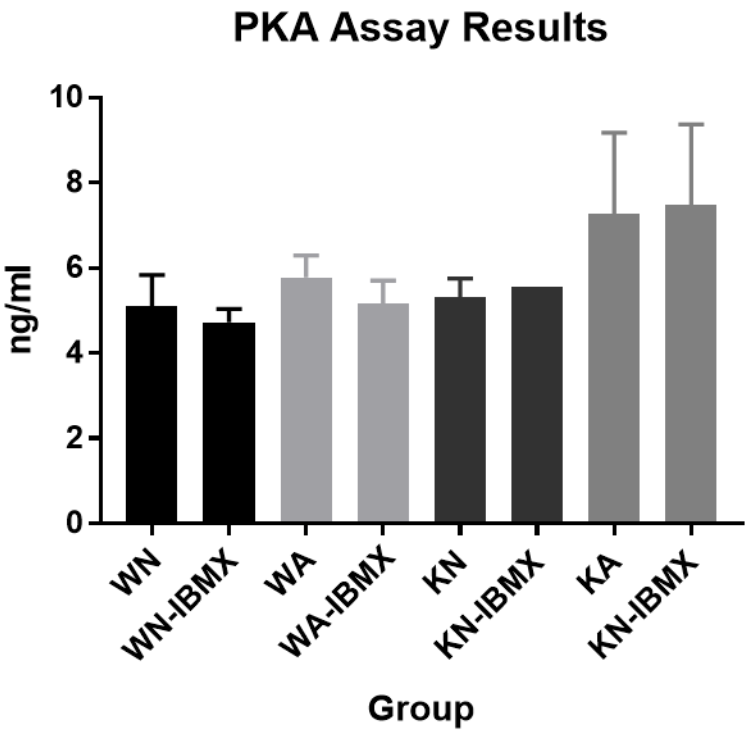

Figure 14. PKA activity remains unchanged between WT and GPR68 KO cells in normal or acidic media with/without the addition of IBMX. Quantification of PKA activity in either WT or GPR68 KO mouse VSM cells in normal (pH ≈7.4-7.6) or acidic (pH ≈6.5-6.7) media. PKA activity was normalized to total protein loaded, and results show no differences in WT and GPR68 KO VSMCs following 5 hours in incubated with or without IBMX in both acidic media or normal media. Activity of PKA with or without IBMX in GPR68 KO cells also did not change in acidic media or normal media; n=1-3 technical replicates for each group.

between WT cells in acidic (WA) versus normal (WN) media, and.a non-significant increase in PKA activity is observed in the KA cohort compared to KN cohort.

Protein expression for Rap1A/1B, a downstream effector of cAMP in the G_s pathway, was probed by Western blotting in WT and GPR68 KO mouse VSMCs incubated in either normal (pH≈7.4-7.6) or acidic media (pH≈6.5-6.7) with the addition of the PDE inhibitor IBMX for 5 hours. As shown in Figure 15, results indicate significant reduction in Rap1A/1B expression in WT cells in acidic media (WA) compared to WT cells in normal media (WN). In GPR68 KO cells, a slight (not significant) reduction in Rap1A/1B expression under acidic (KA) versus normal (KN) conditions is observed.

Protein expression for Rap1A/1B was probed by Western blotting in WT and GPR68 KO mouse VSMCs incubated in either normal (pH≈7.4-7.6) or acidic media (pH≈6.5-6.7), in the presence of IBMX for 5 hours and with the addition of ogerin, a positive allosteric modulator (PAM) of GPR68[1]. Results illustrated in Figure 16 show a very similar dataset compared to cells without the addition of ogerin (see Fig. 15): a marked (p=0.25) reduction in Rap1A/1B expression in WT cells in acidic (WA) versus normal (WN) media, with no significant changes observed in GPR68 KO cells in acidic (KA) versus normal (KN) conditions.

As a test of scientific rigor considering that ogerin works as a PAM of GPR68 and knowing that GPR68 was completely ablated in our GPR68 KO mice, Rap1A/1B was probed via Western blotting in GPR68 KO cells in normal or acidic media with/without the addition of ogerin. Results in Figure 17 showed no significant differences in

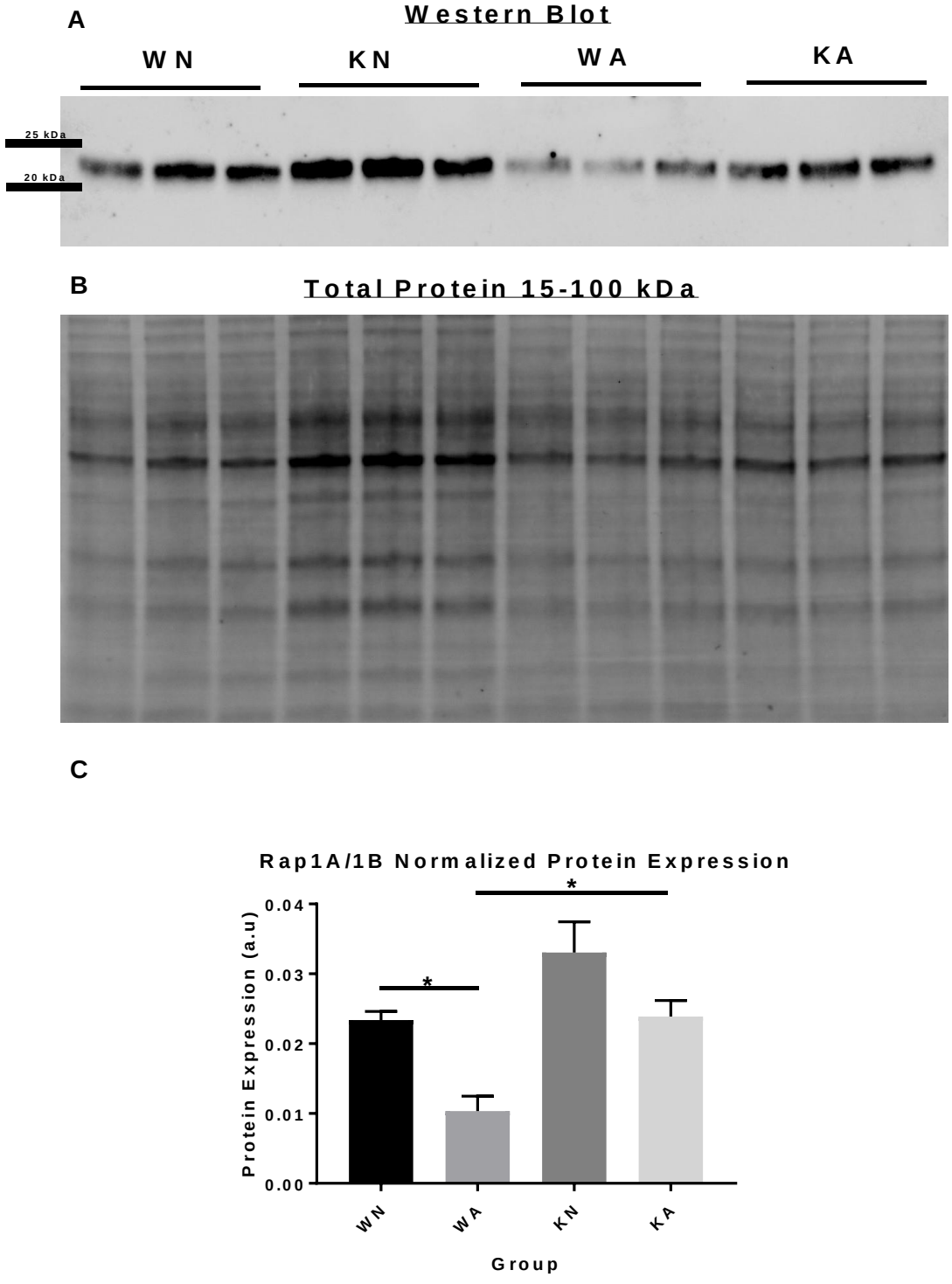

Figure 15. Rap1A/1B expression decreases in WT VSMCs but not in KO cells in acidic media. A: Rap1A/1B expression of C57B6J WT mouse or GPR68 KO mouse VSMCs in either normal (pH ≈7.4-7.6) or acidic (pH ≈6.5-6.7) media; **B**: Total protein (15-100 kDa) used as a loading control ; **C** Quantification of Rap1A/1B expression (normalized to total protein) shows a significant decrease in Rap1A/1B expression in WT group in acidic media (WA) as compared to its WT counterpart in normal media (WN) and also compared to KO groups in normal (KN) or acidic (KA) media; n=6 technical replicates for each group; *p<.05.

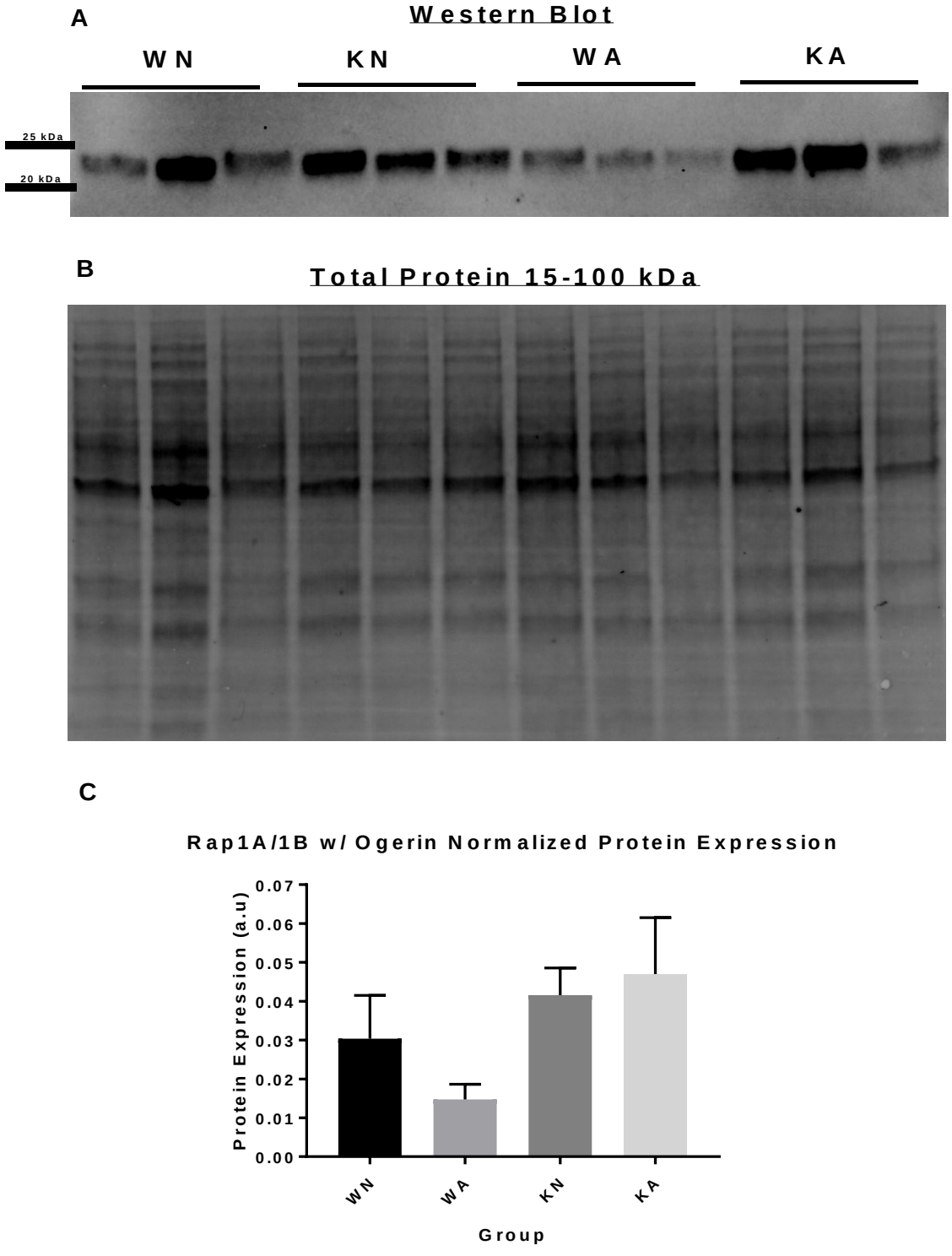

Figure 16. Ogerin does not change Rap1A/1B levels in WT or KO VSMCs in either acidic or normal media. A: Rap1A/1B expression of C57B6J WT mouse or GPR68 KO mouse VSMCs with or without the GPR68 positive modulator ogerin in either normal or acidic (pH ≈6.6) media; **B**: Total protein (15-100 kDa) used as a loading control ; **C** Quantification of Rap1A/1B shows a decreasing trend in the WT group in acidic media (WA) as compared to all other groups; n=3 technical replicates for each group.

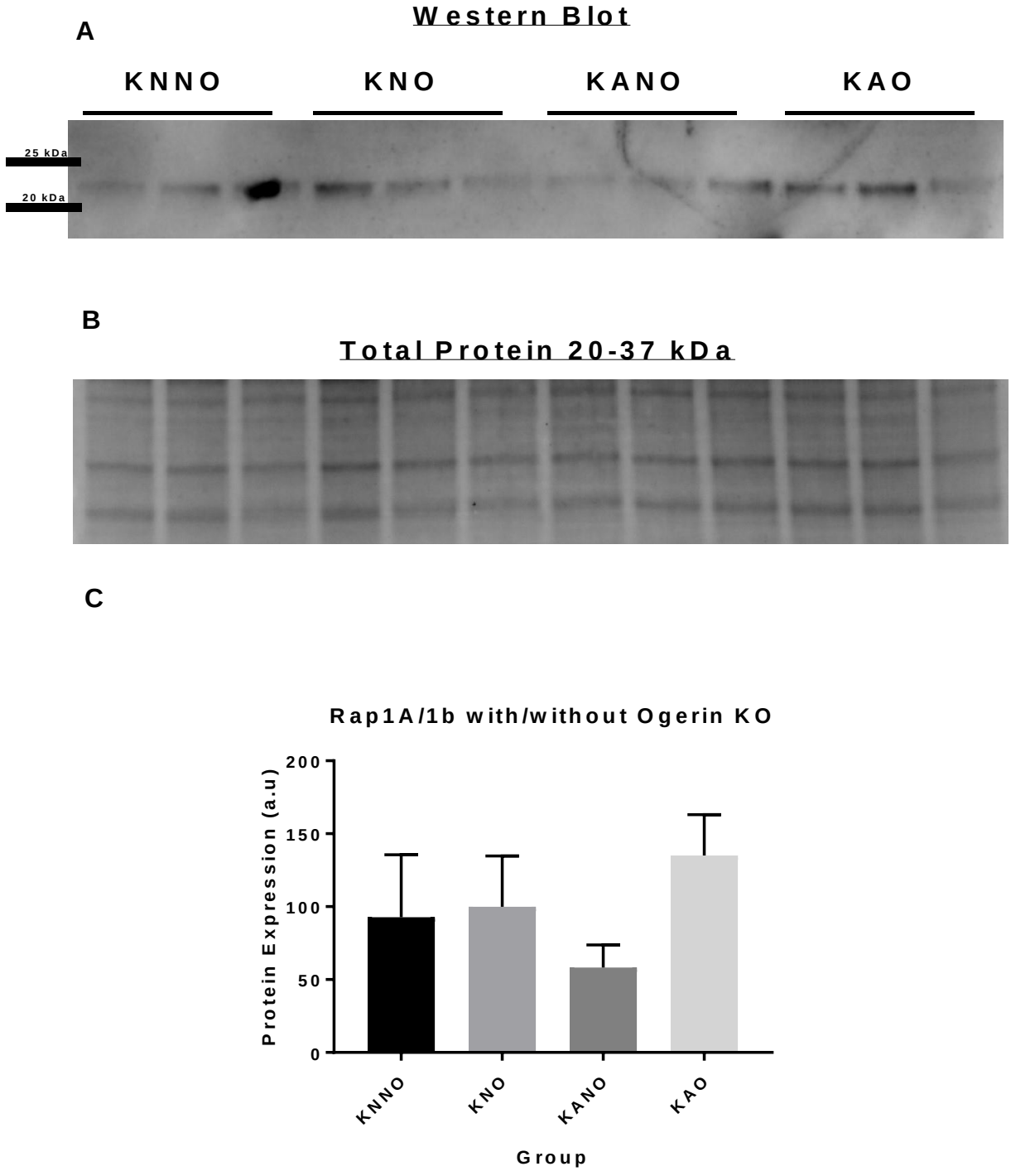

Figure 17. Ogerin does not change Rap1A/1B levels in KO VSMCs in either acidic or normal media. A: Rap1A/1B expression of GPR68 KO mouse VSMC with or without ogerin in either normal (pH ≈7.4-7.6) or acidic (pH ≈6.5-6.7) media; **B**: Total protein (20-37 kDa) used as a loading control ; **C** Neither acidic media nor ogerin makes a significant difference among groups; n=3 technical replicates for each group.

Rap1A/1B expression between any of the groups, confirming reliance on GPR68 for the

positive actions of the GPR68-specific PAM ogerin.

Protein expression for phosphorylated ERK1/2, total ERK1/2 and pERK/totalERK1/2, a downstream effector of cAMP/EPAC in the G_s pathway, was probed by Western blotting in WT and GPR68 KO mouse VSMCs incubated in either normal (pH≈7.4-7.6) or acidic media (pH≈6.5-6.7) with the addition of IBMX for 5 hours. As shown in Figure 18A, results show significant reduction in phospho-ERK1/2

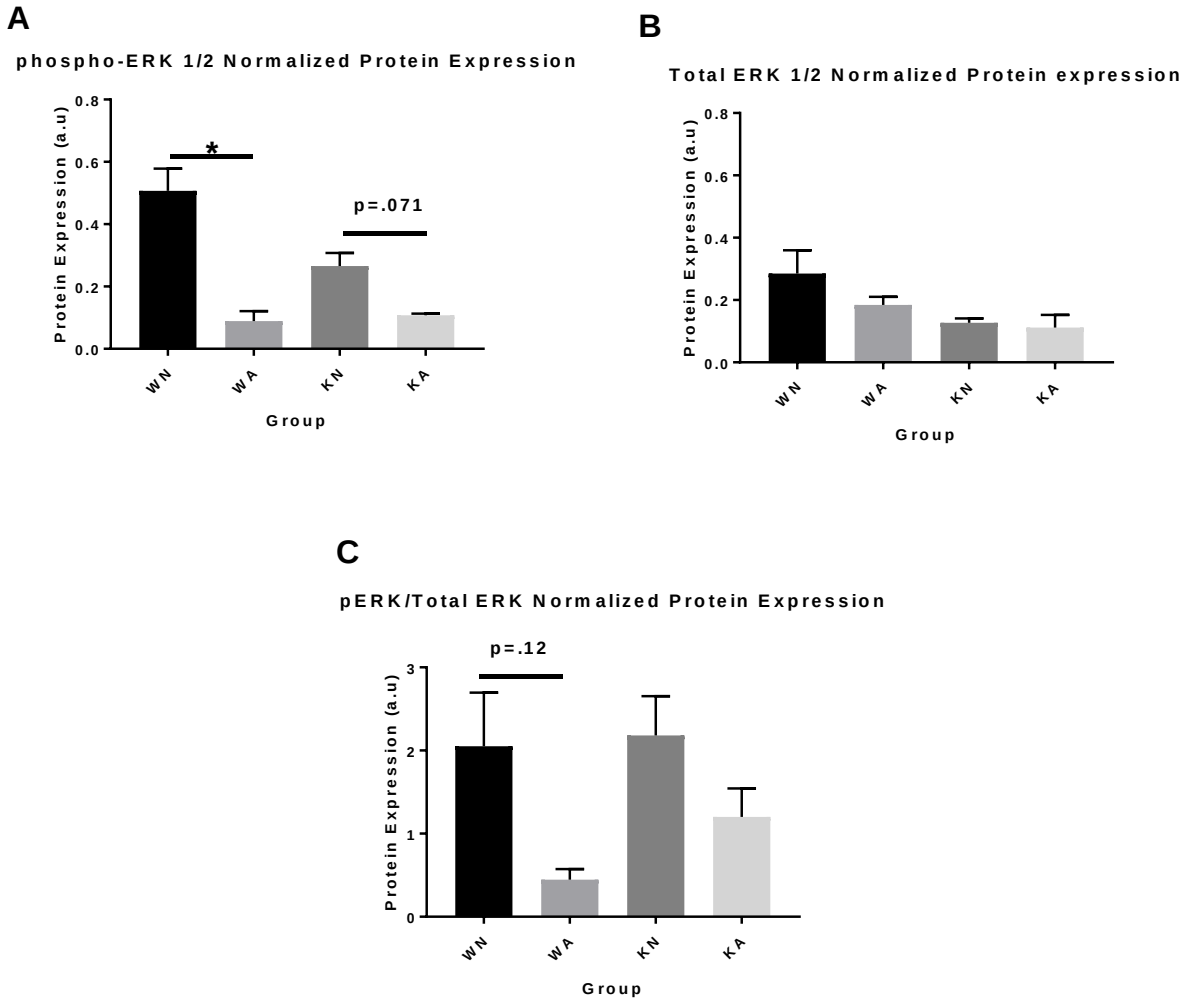

Figure 18. ERK 1/2 expression decreases in WT VSMCs but not in KO cells in acidic media . **A**: Results show significant reduction in phospho-ERK1/2 expression (normalized to total protein) in WT cells in acidic media (WA) compared to WT cells in normal media (WN). In GPR68 KO cells, a marked (p=.071) reduction in phospho-ERK1/2 expression under acidic (KA) versus normal (KN) conditions is observed; **B**: Total ERK expression shows a slight (p=.27) but not significant decrease in WT cells in acidic media compared to WT cells in normal media. No changes is total ERK were seen in KO cells in acidic and normal media; **C**: Normalized pERK1/2/total ERK1/2 expression shows a marked but not significant (p=.12) reduction in WT cells in acidic media as compared to normal media. A slight, also not significant (p=.44) reduction in KO cells in acidic media compared to normal media; n=3 technical replicates for each group *p<.05 versus WT

expression (normalized to total protein) in WT cells in acidic media (WA) compared to WT cells in normal media (WN). In GPR68 KO cells, a slight but not significant (p=.071) reduction in phospho-ERK1/2 expression under acidic (KA) versus normal (KN) conditions is observed (Fig. 18A). Results for total ERK expression (normalized to total protein) showed a slight but not significant (p=.27) reduction in WT cells in acidic media compared to WT cells in normal media (Fig. 18B). In GPR68 KO cells, no significant differences were seen in total ERK expression (Fig. 18B). Normalized pERK1/2/total ERK1/2 expression showed a marked but not significant (p=.12) reduction in WT cells in cidic media as compared to normal media (Fig 18C), with a slight, also not significant (p=.18) reduction in KO cells in acidic media compared to normal media (Fig. 18C).

Intracellular calcium levels were measured via 'top reading' in real-time using a plate reader and a Fluorforte Calcium Assay (Enzo) in WT and GPR68 KO VSMCs incubated in normal or acidic media over a 4-hour time point (following a 1 hour incubation period per the protocol). In Figure 19, results from top read calcium determination showed that the GPR68 KO cells exhibited consistent and significantly higher levels of intracellular calcium (normalized to background fluorescence) in the normal media compared to all other groups at each time point (except after 1 hour; p=.06 for KN to KA comparison). Figure 19A shows a timeline for top read calcium measurements in WT and GPR68 KO VSMCs from time 0 through 4 hours. After the initial top read following the 1 hour incubation period (Fig. 19B), there was no difference between the WT groups in acidic versus normal media; however, there was a significant decrease in intracellular calcium between the GPR68 KO groups in acidic media (KA) compared to cells in normal (KN) media. After one hour (Fig. 19C), there continued to

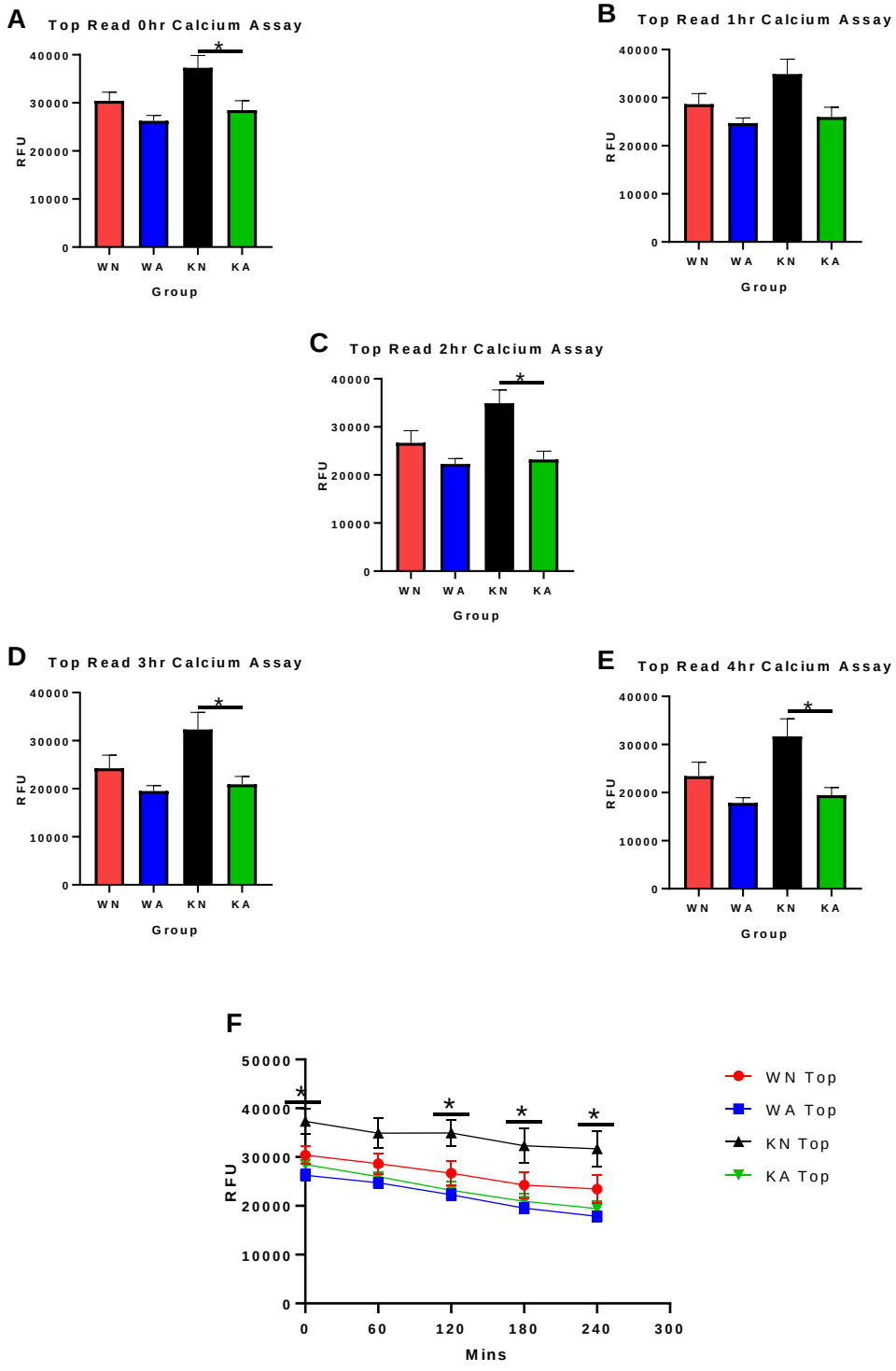

Figure 19. GPR68 KO VSMCs show significantly increased intracellular calcium levels than KO cells in acidic media from top read of plate reader. **A**: 0hr timepoint immediately after 1 hour of incubation in media using top read of plate reader; **B**: 1hr time point using top read plate reader is the only timepoint where there is not significance between the KO groups; **C**: 2hr timepoint top read on plate reader; **D**: 3hr timepoint using top read of plate reader **E**: 4hr timepoint using top read of plate reader; **F**: Time course of WT and KO VSMCs at varying points shows a significant decrease of calcium in the GPR68 KO VSM cells in acidic media (KA) compared to the KO cells in normal media (KN). There a deceasing trend in the WT cells that are in acidic media compared to normal media throughout the time course; n=5-10 technical replicates per group.

be no difference between the WT groups in normal and acidic media. In the KO groups, there was no significant difference, but there was still a marked decrease (p=.06) with the addition of acidic media. After hours 2 (Fig. 19D), 3 (Fig. 19E), and 4 (Fig. 19F) a similar pattern emerged where there were no differences between the WT groups, but a significant decrease in the KO groups in acidic media (KA) compared to KO cells in normal media (KN).

To further explore what effect an acidic environment and subsequent GPR68 activation would have on intracellular calcium levels, after completing the top read Fluorforte Calcium Assay (Enzo) we calculated percent differences of WT and KO cohorts in normal versus acidic media and presented the data as WT/KO ratios (Figure 20). The calcium results received from the top read showed that the normal pH solutions mounted higher intracellular calcium levels than the acidic solutions for both the WT and KO VSMCs. The results show a larger percent reduction in calcium when comparing the GPR68 KO in acidic media to normal media versus the percent change in WT cells in acidic media to normal media. Figure 20A shows a timeline for top read calcium measurements for WN/WA and for KN/KA from time 0 through 4 hours. After the initial read (Fig. 20B) (0 hr) (p=.14) and after a 1 hour (p=.10) incubation period (Fig. 20C), we saw a marked increase (≈45%) in percent reduction of intracellular calcium between the WT cells as compared to the KO cells. After 2 hours (Fig. 20D), we saw significant differences in percent reduction between the groups. At hours 3 (p=.06) (Fig. 20E), and 4 (p=.06) (Fig. 20F) we saw a marked but not significant differences in percent reduction between the WT and the KO groups.

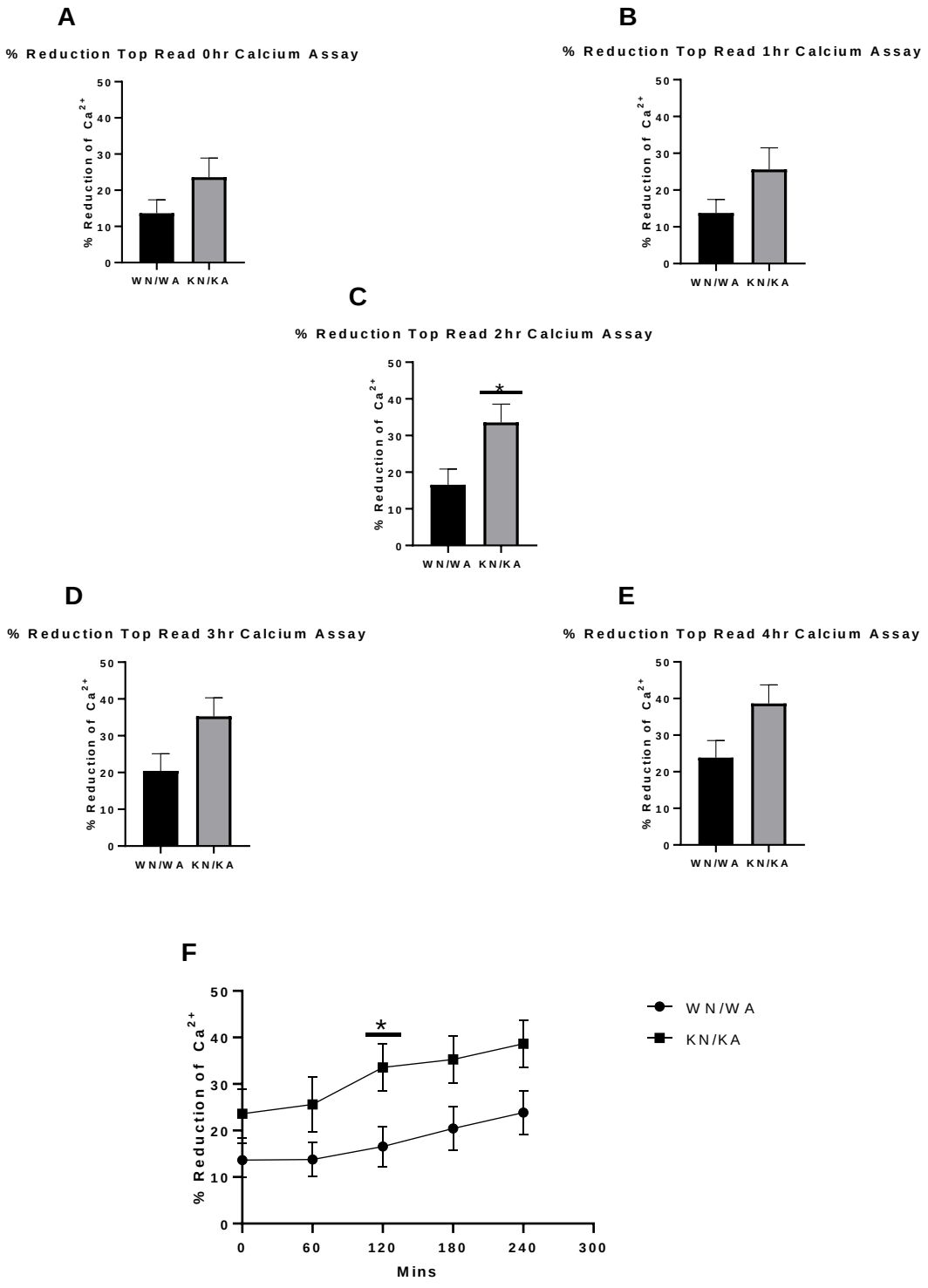

Figure 20. GPR68 KO VSM cells shows a larger calcium reduction in KO cells when normal media is compared to the acidic media when compared to WT cells. A: 0hr timepoint, immediately after 1 hour of incubation in media using top read of plate reader; **B**: 1hr using top read of plate reader ; **C**: 2hr timepoint top read on plate reader ; **D**: 3hr timepoint using top read of plate reader ; **E**: 4hr timepoint using top read of plate reader; **. F**: Time course of WT and KO VSM cells at varying points shows a larger calcium reduction in the ratio of calcium levels in normal media over the levels of calcium in acidic media in KO cells compared to the WT cells in the same ratio of normal media over acidic media; n=5-10 technical replicates per group

A Fluorforte Calcium Assay (Enzo) to measure intracellular calcium levels of both WT and KO cells via 'bottom reading' in real time using a plate reader. In Figure 21, results from the bottom read showed that the GPR68 KO cells displayed significantly higher intracellular calcium levels than any other group throughout the 4-hour period after normalization. Figure 21A shows a timeline for bottom read calcium measurements in WT and GPR68 KO VSMCs from time 0 through 4 hours. After the initial bottom read following the incubation period, (Fig. 21B) there were no differences between the WT VSMC groups, but a trending ($p=.08$) decrease in GPR68 KO cells compared to KO cells in normal media. After one hour (Fig. 21C), there continued to be no differences between the WT groups in normal versus acidic media. In the KO groups, there were no significant differences, but there was a marked decrease of ≈30% with the addition of acidic media (compared to normal media). For hours 2 (Fig. 21D), 3 (Fig. 21E), and 4 (Fig. 21F) a similar pattern emerged where there was no difference between the WT groups, but significant decreases in the KO groups in acidic media compared to the normal media. There were also significant increases in intracellular calcium in the KO VSMCs compared to WT cells in normal media for the same time period 2 to 4 hours after initial incubation (Figs. 21D-F).

To further explore what effect an acidic environment and subsequent GPR68 activation would have on intracellular calcium levels, after completing the bottom read Fluorforte Calcium Assay (Enzo) we calculated the percent differences of WT and KO cohorts in normal versus acidic media and presented the data as WT/KO ratios (Figure 22). The calcium results that we received from the bottom read showed that the normal solutions mounted higher intracellular calcium levels than the acidic solutions in both the WT and

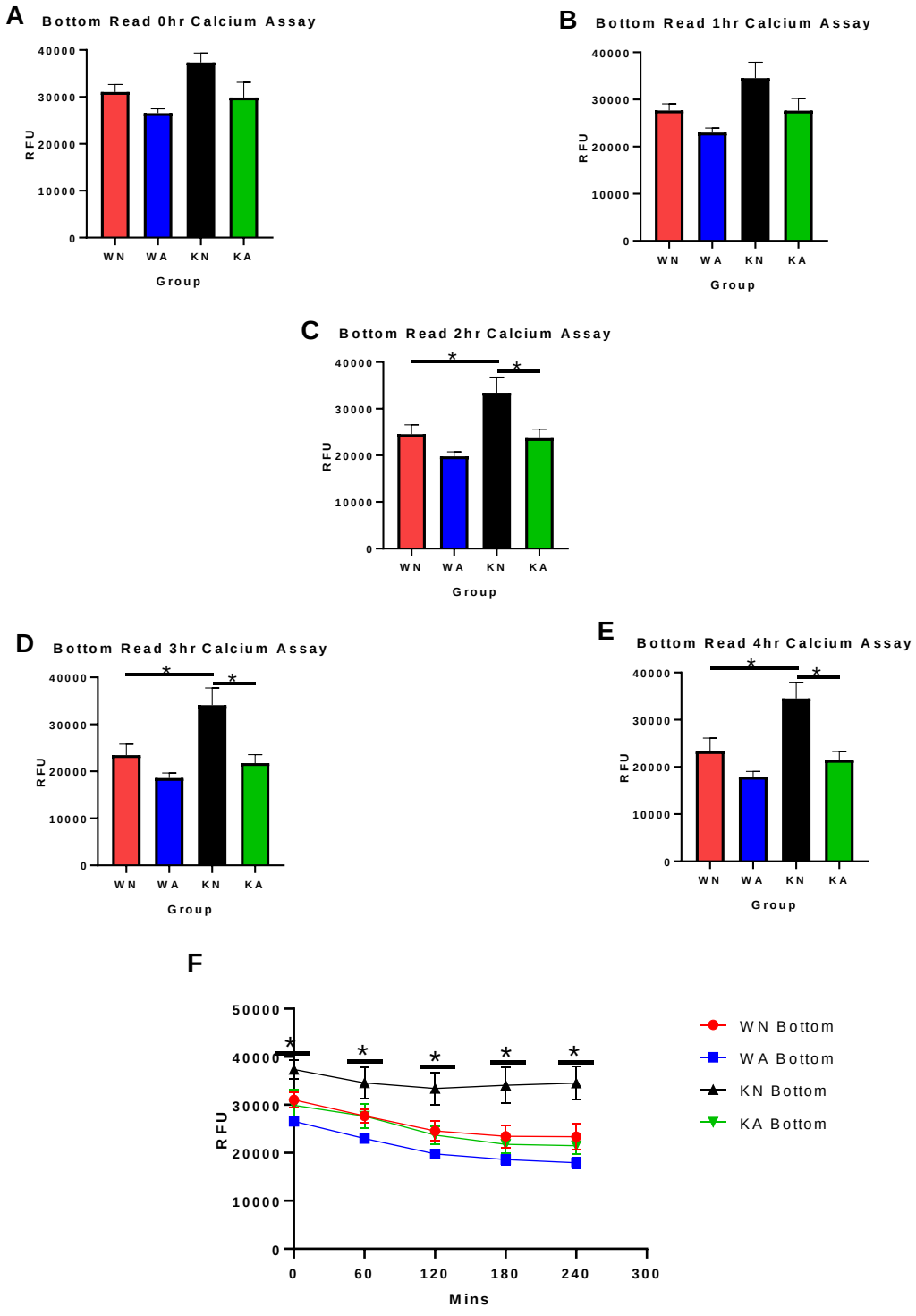

Figure 21. GPR68 KO VSM cells show significantly more calcium than KO cells in acidic based media from bottom read of plate reader. **A**: 0hr timepoint immediately after 1 hour of incubation in media using bottom read of plate reader; **B**: 1hr timepoint using bottom read of plate reader shows a decreasing trend in both the WT and KO groups; **C**: 2hr timepoint bottom read on plate reader ; **D**: 3hr timepoint using bottom read of plate reader ; **E**: 4hr timepoint using bottom read of plate reader; **F**: Time course of WT and KO VSM cells at varying points shows a significant decrease of Calcium in the GPR68 KO VSM cells in acidic media compared to the KO VSM cells in normal media as well as WT cells in normal media after 2 hours from the bottom read of a plate reader. There a deceasing trend in the WT cells that are in acidic media compared to normal media throughout the time course; n=5-10 technical replicates per group

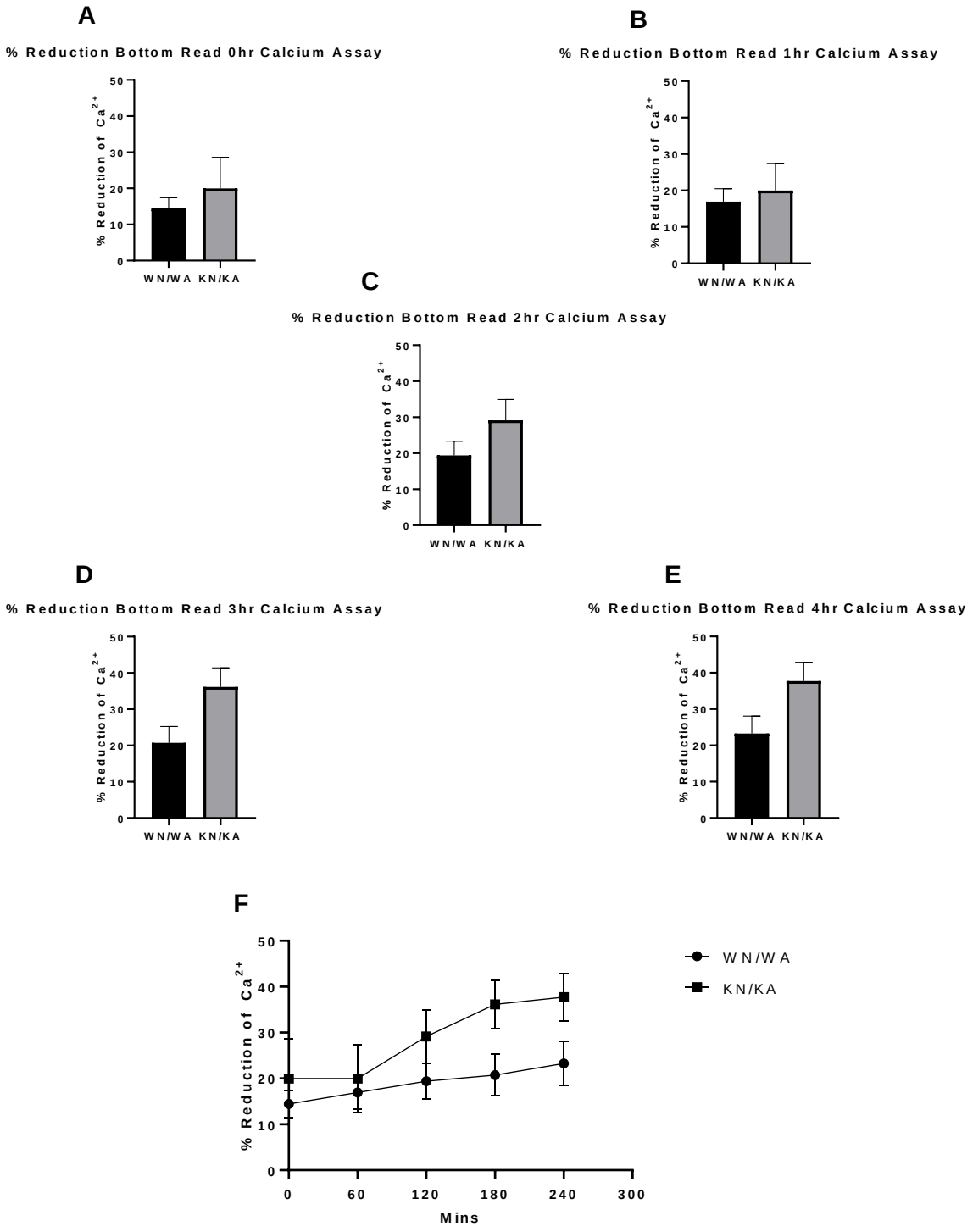

Figure 22. GPR68 KO VSM cells shows a trend toward larger calcium reduction in KO cells when normal media is compared to the acidic media when compared to WT cells. **A**: 0hr timepoint, immediately after 1 hour of incubation in media using bottom read of plate reader; **B**: 1hr using bottom read of plate reader ; **C**: 2hr timepoint bottom read on plate reader; **D**: 3hr timepoint using bottom read of plate reader ; **E**: 4hr timepoint using bottom read of plate reader; **F**: Time course of WT and KO VSM cells at varying points shows a larger calcium reduction in the ratio of calcium levels in normal media over the levels of calcium in acidic media in KO cells compared to the WT cells in the same ratio of normal media over acidic media; n=5-10 technical replicates per group

KO VSMCs. The results show a larger percent reduction in calcium when comparing the GPR68 KO in acidic media to normal media versus the percent change in WT cells in acidic media to normal media. Figure 22A shows a timeline for bottom read calcium measurements for WN/WA and for KN/KA from time 0 through 4 hours. After the initial read (0hr) (Fig. 22B) and after a 1-hour incubation period (Fig. 22C), we saw no significant differences in percent reduction in the WT cells compared to the KO cells. After 2 hours (Fig. 22D), we observed a marked difference ($p=.17$) in percent reduction between the groups. At hours 3 ($p=.051$), and 4 ($p=.07$) we observed marked but not significant differences in percent reduction of intracellular calcium between the WT and the KO groups under normal or acidic conditions (Figs. 22E-F).

A Milliplex MAP Cytokine/Chemokine Panel (EMD Millipore, Billerica, MA) assay was completed to determine potential changes in the cytokine IL-6 in WT and GPR68 KO cells treated with normal or acidic media in the presence of IBMX. After incubation for 5 hours, results in Figure 23 showed a significant increase in IL-6 expression in the WT group in acidic media (WA) compared to its WT counterpart in normal media (WN) as well as compared to KO cells in acidic (KA) or normal (KN) media. No differences were observed in KO cells in normal (KN) versus acidic (KA) media. These cumulative results in primary VSMCs indicate a possible connection between acidic conditions, GPR68, and IL-6 production.

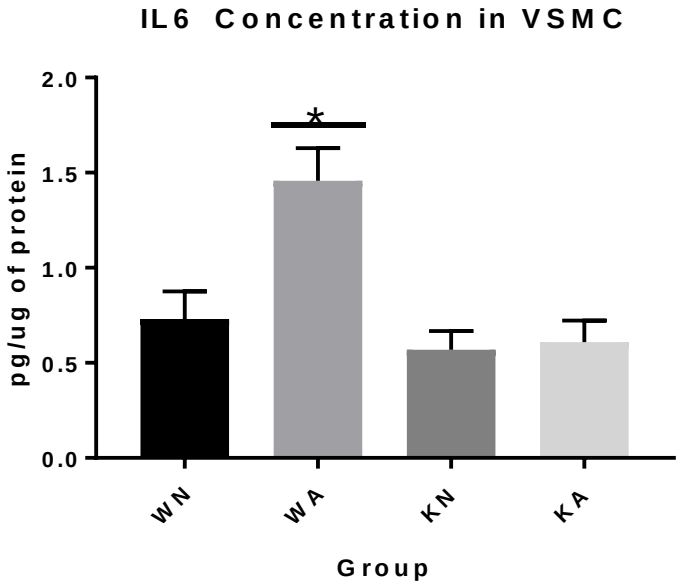

Figure 23. The cytokine IL-6 increases in acidic media in WT VSMCs compared to GPR68 KO cells. WT VSMCs incubated in acidic media (WA) for 5 hours showed a significant increase in IL-6 compared to WT cells in normal media (WN). KO cells saw no change in IL-6 levels in either n, WT cells in acidic media saw a statistically significant increase as compared to their KO counterparts in acidic or normal media; n=6 technical replicates for each group; $p<.05$.

CHAPTER 4

In Vivo Studies on GPR68

Using whole tissue homogenates of injured ischemic left carotid arteries of both WT and GPR68 KO mice harvested 24 hours post-injury, a Milliplex MAP Cytokine/Chemokine Panel (EMD Millipore, Billerica, MA) assay was performed to evaluate potential changes in the cytokine IL-6. As seen in Figure 24, results show no marked differences in IL-6 levels between injured WT and injured KO arterial homogenates at this time point.

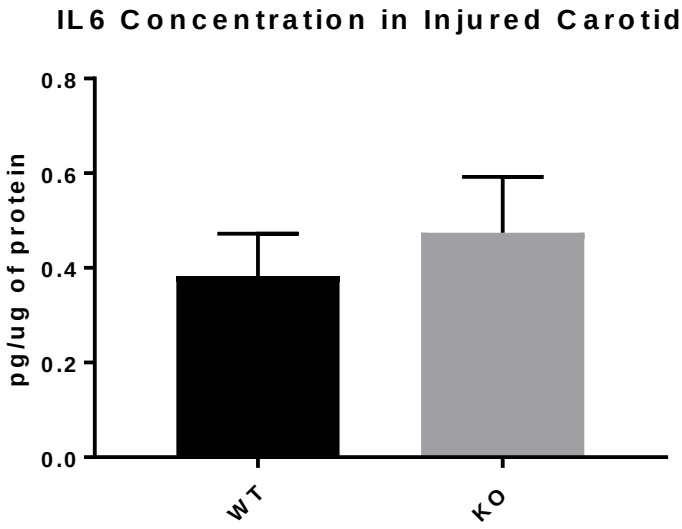

Figure 24. Injured ischemic WT and KO carotid arteries show no differences in IL-6 levels; Ligation-injured left carotid arterial IL-6 content 24 hours post-injury in both WT and GPR68 KO animals showed no statistical differences in IL-6; n=3-4 biological replicates for each group.

To help determine possible phenotypic differences between the C57BL/6J WT and GPR68 KO mice, several key cardiovascular readouts were assessed including heart rate, mean arterial pressure (MAP; an average arterial pressure through a single cardiac cycle), diastolic and systolic blood pressures, the pulse pressure (the difference between diastolic and systolic blood pressures and an indication of stroke volume), and

the rate pressure product (RPP; an indirect index of myocardial oxygen consumption). As seen in Figure 25, no significant differences between the WT and KO mice were observed for any of these systemic cardiovascular phenotypic markers.

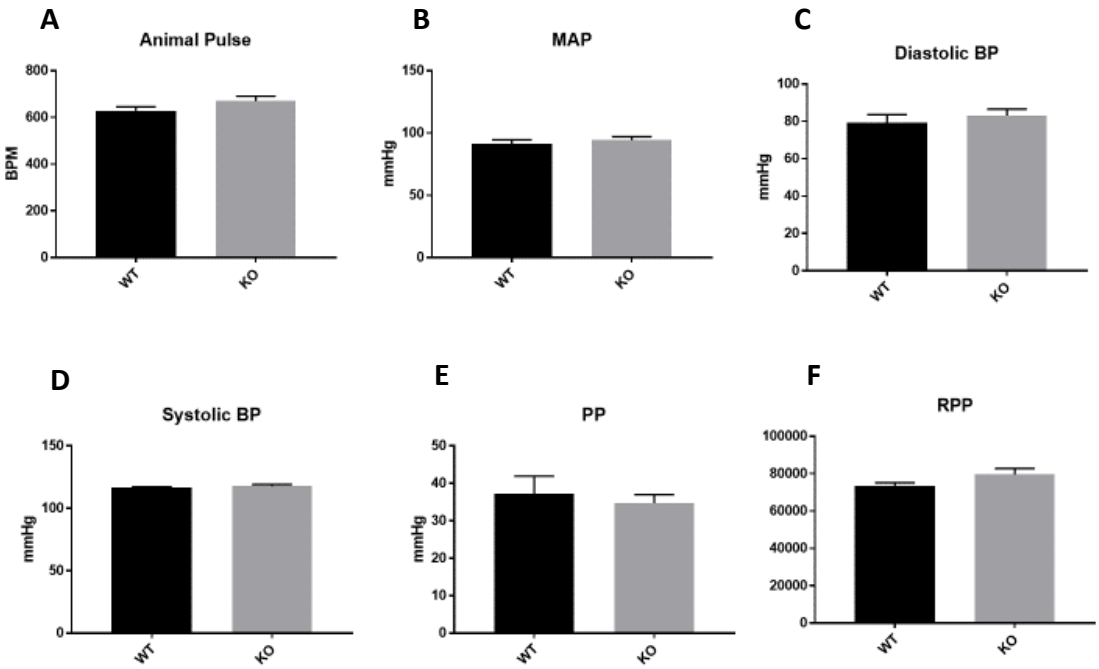

Figure 25. No phenotypic differences in cardiovascular readouts between WT and GPR68 KO animals; Male WT and GPR68 KO animals showed no marked differences in a variety of phenotypic cardiovascular readouts; n=3 biological replicates per group.

To investigate whether balloon-injured arteries create an acidic microenvironment within the vessel, similar to what we have seen in the in vitro acid/base media model, and further in an effort to compare a rat model of arterial distension injury to a mouse arterial ligation ischemia model, rat balloon-injured left carotid arteries (LCAs) were harvested 30 minutes post-injury and probed for GPR68 protein expression using Western blotting. As shown in Figure 26, results showed significantly decreased levels of GPR68 protein expression in injured arterial homogenates compared to their uninjured (naïve) counterparts at this time point.

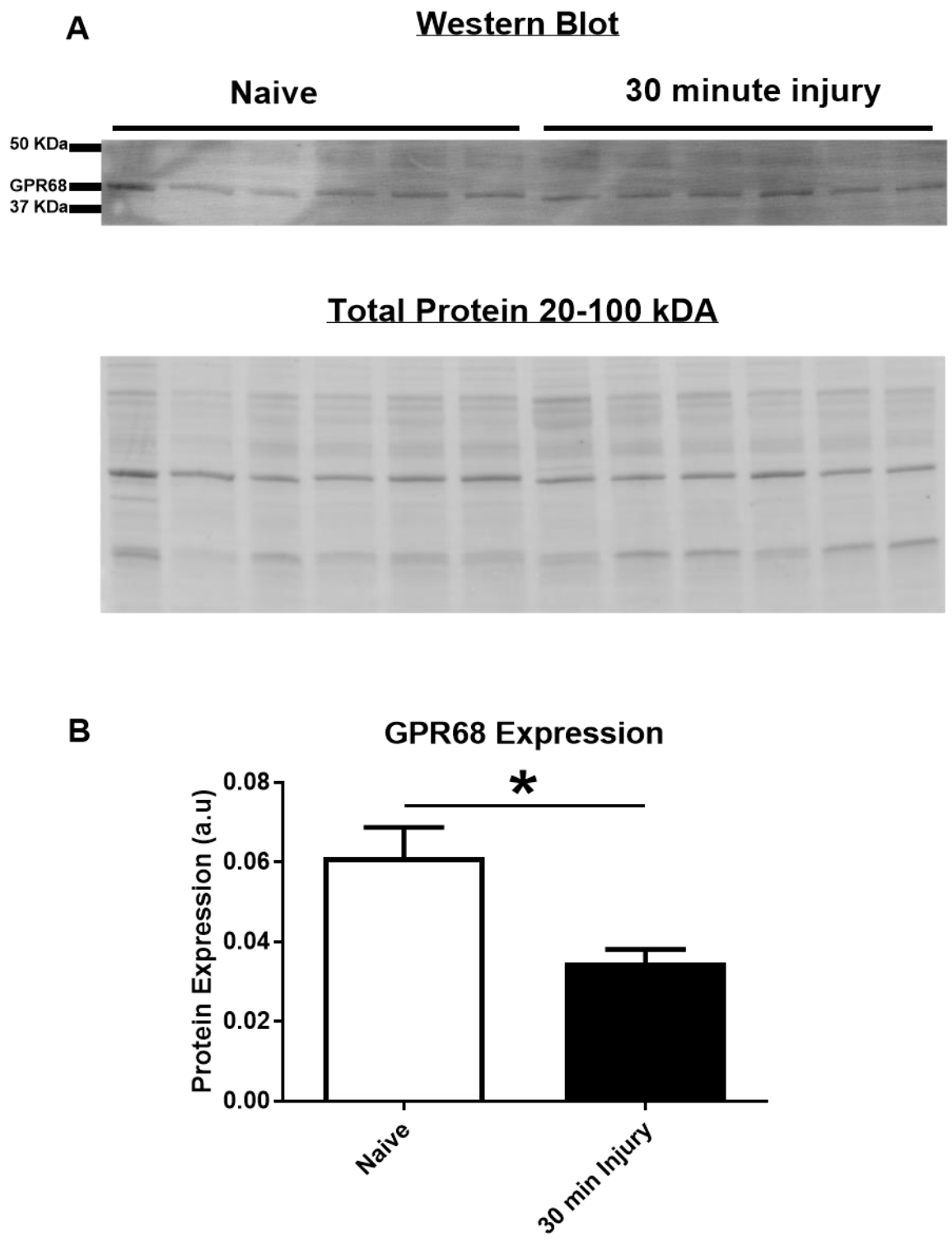

Figure 26. LCA GPR68 expression decreases in 30-minutes following balloon injury compared to uninjured naïve controls. A: GPR68 expression and total protein blot in arterial homogenates harvested 30 minutes after balloon injury or from uninjured controls in male rats. **B**: Quantification shows a significant decrease in GPR68 protein expression in injured vs uninjured controls; n=6 biological replicates per group; *p<.05.

To investigate whether ligation-injured mouse ischemic arteries create an acidic microenvironment similar to what we have seen in the in vitro model of mouse cell culture, and also to compare results to the rat balloon injury mural distension model (see Fig. 26), ligation-injured ischemic LCAs from WT mice were harvested 24 hours post-injury and (along with control uninjured LCAs) probed for GPR68 protein expression using Western blotting. Similar to findings in the rat (see Fig. 26), as shown

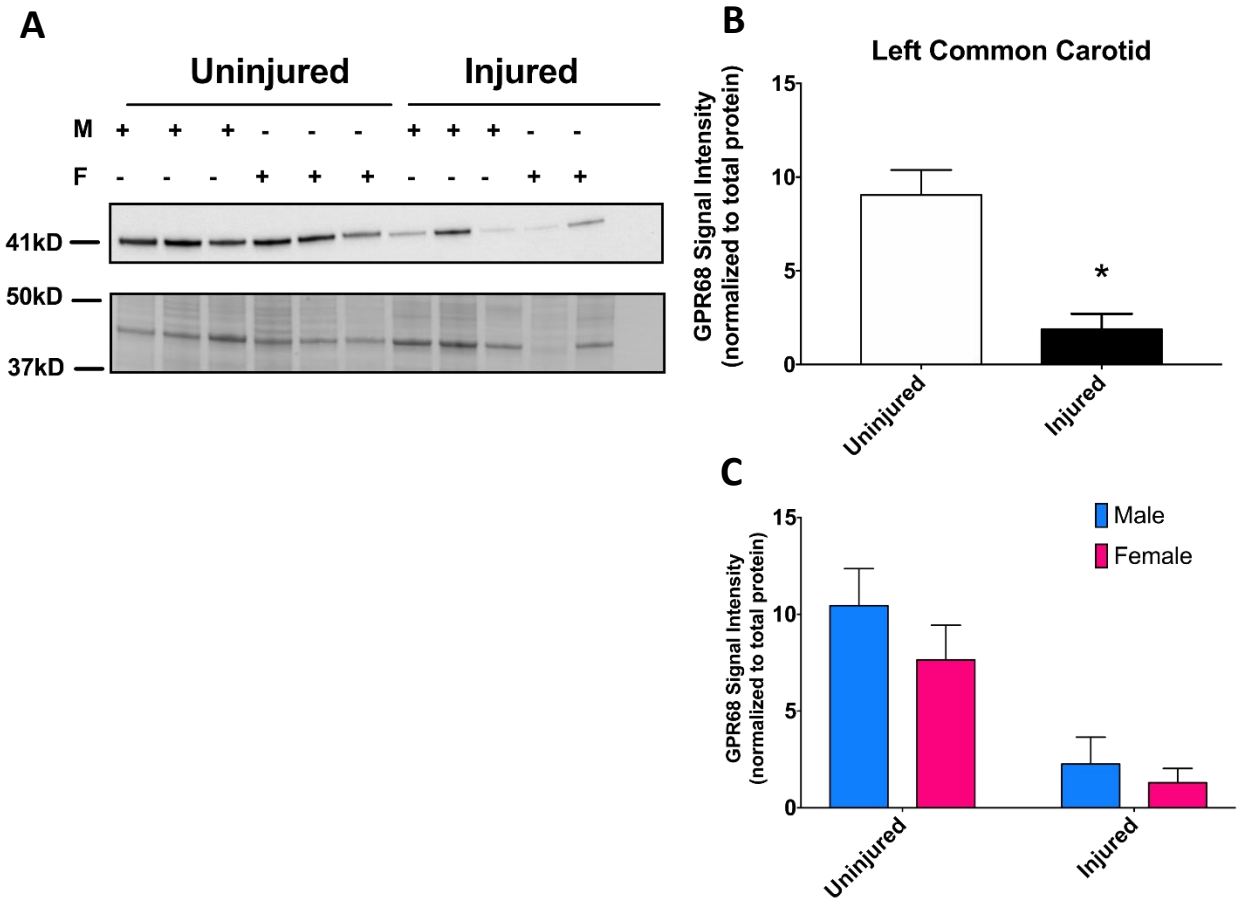

Figure 27. GPR68 expression decreases in injured left carotid arteries (LCA) compared to uninjured LCAs in WT mice. A: GPR68 expression 24 hours after ligation injury or uninjured LCA of both male and female WT mice; Western Blot and total protein blot; **B**: Aggregated data from male and female LCAs show a significant decrease in GPR68 expression in injured vs uninjured controls; **C**: Disaggregated data for male and female cohorts show a decreasing trend in GPR68 in the ligation injury vs uninjured controls but significant sex differences were not discerned; n=3 for female and n=3 for male biological replicates per group.

in Figure 27, results indicate significantly decreased GPR68 protein expression in injured vessels compared to uninjured counterparts. Both males and females were used in these surgeries, and we then sought to determine sex differences between injured and uninjured male and female LCAs. Following disaggregation of data by sex, while there was a trending decrease in injured LCAs compared to uninjured LCAs, no significant differences in sex between the groups were observed (Fig. 27C).

To discern potential impact of GPR68 ablation on vessel wall remodeling following ischemia-induced injury, carotid artery remodeling 4 weeks post-injury was assessed via histomorphometry in uninjured and ligation-injured WT and GPR68 KO mice. Shown in Figure 28A are representative Verhoff-van Gieson stained arterial cross sections 28 days post-injury for uninjured and ligation-injured WT and GPR68 KO animals. Quantification shows marked but not statistically significant ($p=.08$) decrease in neointimal area in injured KO vessels compared to injured WT vessels (Fig. 28B), while WT and KO vessels show similar medial wall areas (Fig. 28C). When assessing neointimal/medial wall area ratios, significant decreases were observed in the injured GPR68 KO mice compared to injured WT controls (Fig. 28D), with corresponding, but not significant, increases in lumen area for the KO (versus WT) arteries (Fig. 28E).

A

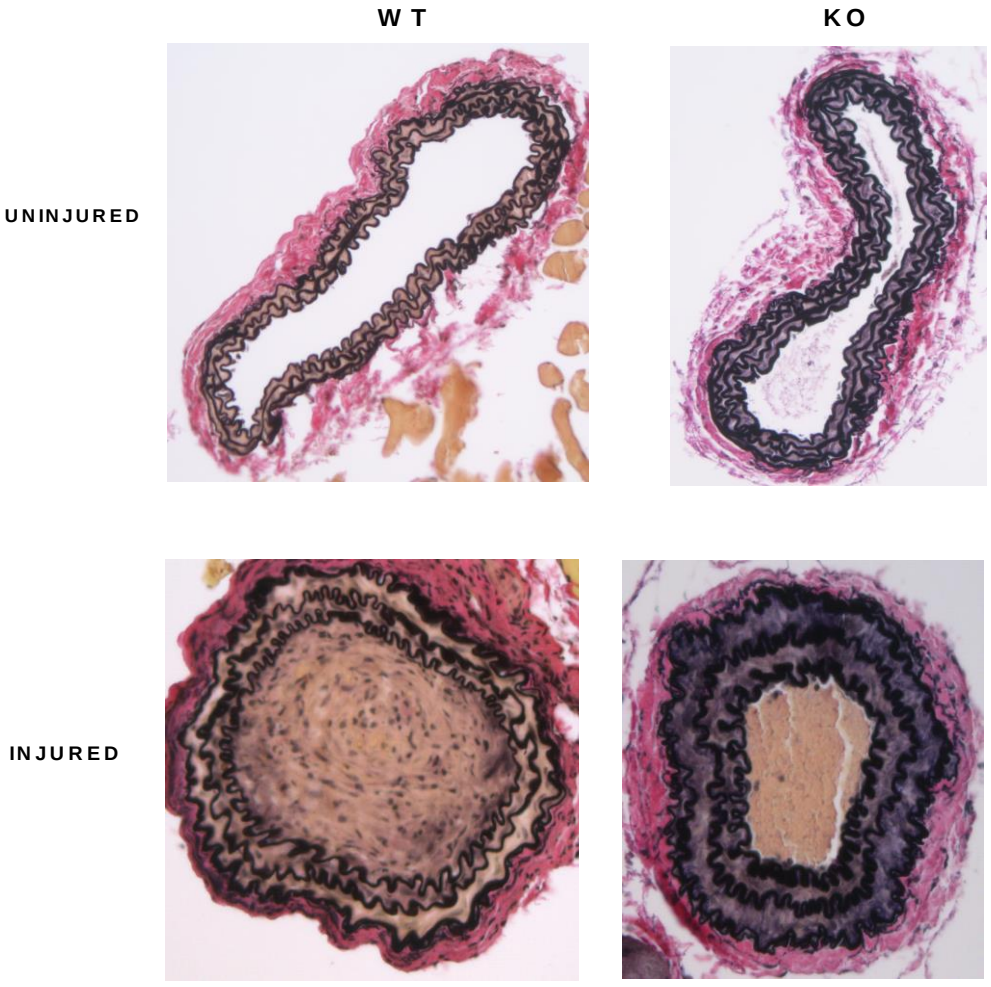

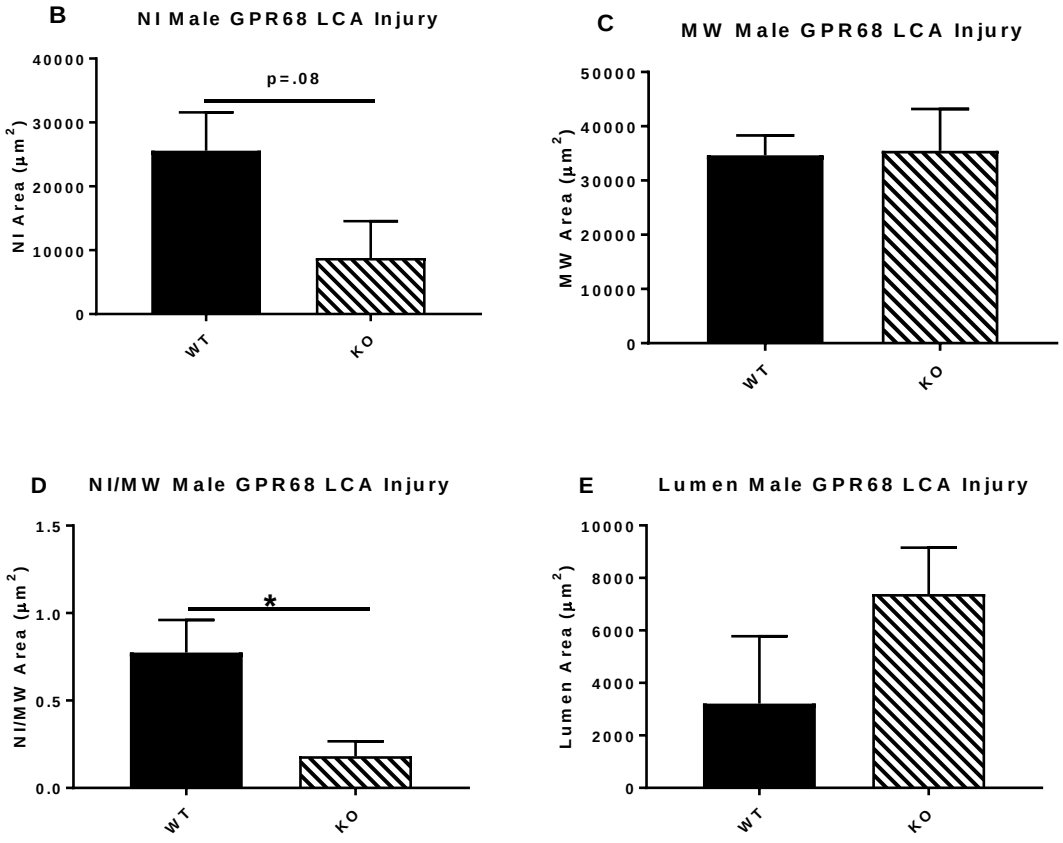

Figure 28. Injured WT vessels have larger neointimal area and increased vessel wall remodeling compared to their KO counterparts following ligation injury. **A**: Photomicrographs of Verhoeff-Van Gieson (VVG)-stained LCA cross-sections from WT and KO mice 28 days after arterial ligation injury.; **B**:LCA neointimal area of WT mice compared to KO mice; **C**: LCA medial wall area of WT mice compared to KO mice; **D**: LCA neointima area/medial wall area ratios of WT mice compared to KO mice ; **E**: LAC lumen area of WT mice compared to KO mice; n=7 biological replicates per group; *p<.05 versus WT.

RESULTS REFERENCES

1. Huang XP, Karpiak J, Kroeze WK, et al. Allosteric ligands for the pharmacologically dark receptors GPR68 and GPR65. *Nature*. 2015;527(7579):477-483. doi:10.1038/nature15699.

CHAPTER 5

Integrated Discussion and Conclusion

Our scientific knowledge of proton sensing GPCRs including GPR68 and their functions within the body and particularly in cardiovascular tissues is just now emerging. Little research exists focused on GPR68 in cardiac and/or vascular diseases such as atherosclerosis, restenosis, and ischemic artery disease, conditions where local acidosis can arise. The experimental strategy for this dissertation project was designed to shed light on GPR68 and its regulatory actions and potential therapeutic utility in the vascular system and in pathologic vascular smooth muscle (VSM) growth. The results from this dissertation project promise insight as to not only the regulatory aspects of GPR68 in VSM cell (VSMC) proliferation and death as foundations of cardiovascular disease (CVD), but also provide evidence for the signaling pathways through which GPR68 alters these clinically important functional outcomes.

The hypothesis of this dissertation is that the pH sensing GPCR, GPR68, when stimulated by acidosis induces cAMP signaling that is protective against pathologic VSM growth in CVD. In order to test this proposal, two Specific Aims were developed: **Aim 1 will determine that acidic activation of GPR68 decreases VSMC proliferation and increases VSMC death; Aim 2 will determine that GPR68 achieves this decrease in VSMC proliferation and increase VSMC death via stimulatory G_s signaling including cAMP and the downstream effectors PKA and EPAC.** Data generated in this dissertation project largely support our hypothesis and suggest that GPR68, when stimulated by acidosis, activates the cAMP and EPAC signaling that is protective against pathological VSM growth in CVD.

IN VITRO STUDIES

Several studies have found a role for GPR68 in tissues such as bone, in conditions such as injury or disease, infections and/or fractures where local, acidic conditions can drop below pH 7.4[1]. These local acidic conditions have been implicated in regulating osteoclast differentiation, enhancing osteoclast survival in acidic conditions as well as increasing Ca^{2+} concentration[2-4]. GPR68 also has been implicated in tumorigenesis and cancer pathobiology[5-7], as well as in vascular reactivity in endothelial cells, where it has shown to be a mechanosensor of shear stress [8]. While these systems have been explored, there has been limited published research on proton sensing GPR68 in the vascular system, and in that context GPR68 is still vastly understudied. With this in mind, to further explore GPR68 and VSM, this dissertation project was performed using whole body GPR68 knockout (KO) mice.

The GPR68 KO mice used for both our in vitro and in vivo studies were purchased as a single breeding pair from the Mutant Mouse Resource and Research Center (MMRRC), where they were derived by Beverly Koller and colleagues at University of North Carolina at Chapel Hill[9]. Briefly, the targeting construct for the *Gpr68* locus consists of a PGK-1 promoter-driven neomycin resistance cassette flanked by two arms of homology with the mouse *Gpr68* locus. The longer arm of homology was generated using a 7,266-bp *PstI* fragment extending from the last intron to the beginning of the last exon. This exon contains the entire coding sequence of the *Gpr68* gene. The 1,335-bp shorter arm was generated by PCR amplification and extends from the downstream end of the long arm into the 3′ untranslated region of the gene. Homologous recombination of the targeting construct with the *Gpr68* locus inserts

the neomycin resistance cassette into codon 78 of the gene, thereby disrupting expression[9]. The GPR68 KO mice that we acquired were derived from C57BL/6J mice as the background strain[9]. To maintain consistency, the GPR68 KO mice were paired with wild type (WT) C57BL/6J mice as a control group, and while true littermate controls were not possible due to time constraints, we paired our KO mice with age-/sex-appropriate C57BL/6J WT controls as to generate repeatable results[10,11] and to avoid biased conclusions.

Following breeding of our original KO pair, and generation of male and female GPR68 KO offspring and establishment of ample numbers of male and female KO mice as well as male and female C57BL/6J WT control mice, we initially wanted to confirm their genetic makeup before using them in experimental protocols. We performed real time quantitative PCR (RT-qPCR) using SYBR Green reagents with custom GPR68 primers that should detect WT GPR68 in the C57BL/6J WT mice but should not detect it in the KO mice if the GPR68 gene was successfully ablated. The housekeeper gene used to normalize our GPR68 gene expression levels was GAPDH. As seen in Figure 2, untreated primary VSMCs from our WT mice showed marked GPR68 expression (measured as relative quantity (RQ)/GAPDH), while our GPR68 KO primary VSMCs failed to show discernable GPR68 expression. Using our custom GPR68 (and GAPDH) primers, RT-qPCR confirmation of our KO and WT models was repeated multiple times in both primary VSMCs as well as intact arteries, and identical results were consistently observed (data not shown). It is important to note, that while confirming the validity of the RT-qPCR primers, extra steps were taken to ensure that our custom primers were properly optimized. Experimental designs were developed for assay efficiency and melt

curve analyses to ensure that the custom primers used with SYBR Green reagents were properly optimized. As shown in Figure 3, we achieved a relative efficiency exceeding 90% for our RQ values using RT-qPCR and SYBR Green reagents. Melt curve analysis was done using a variety of primer concentration levels to ensure that there were no signs of multiple peaks that would be indicative of primer dimers and/or multiple PCR products. Once optimized, the assay efficiency allowed us to determine a consistent doubling of our cDNA which is important for using the ddC_t equation in our RQ results. The results of the melt curve analysis (Fig. 4) determined single PCR products for GPR68 target and GAPDH housekeeping primers and that primer dimers were nonexistent. Both the assay efficiency and melt curve analyses confirmed that our custom target and housekeeping primers were valid and optimized for use for determination of GPR68 (and GAPDH) gene expression in our RT-qPCR experiments.

As an additional quality control effort and with scientific rigor, using the professional services of Transnetyx Automated Genotyping Services (Cordova, Tennessee), we were able to definitively prove that our KO tissues and KO VSMCs were in fact complete genetic knockouts (see Figure 5). In comparison to our RT-qPCR approaches, genotyping performed by Transnetyx confirmed the presence of GPR68 in the WT mice and the lack of GPR68 in the KO mice when using WT-GPR68 primers (and c-JUN housekeeping primers). Further, Transnetyx confirmed the GPR68 KO by probing for neomycin, which was only present in the GPR68 KO mice (as it was inserted during gene modification in the KO models for use as a positive control) and was not expressed in the WT mice. The results from Transnetyx (Fig. 5) confirmed our own data and validated our GPR68 custom primers as a viable approach for measuring GPR68

expression. Further, over time we have repeated our genotyping efforts on both our WT and GPR68 KO models, in an effort to discern potential genetic drift, and our reproducible results further established complete GPR68 gene ablation in our KO mice compared to our WT mice. Taken together, these findings confirm genetic makeup of our unique GPR68 KO models.

Cell Growth

Following determination of the genetic makeup of our KO and WT mice including confirmation of genetic ablation of GPR68 in our KO models, the potential role for GPR68 in cellular growth, specifically VSMC proliferation and cell death, was investigated. As mentioned, VSMC growth and death are normally low and held 'in check' in quiescent adult arteries, but in the progression of CVD they can become imbalanced and manifest into a synthetic, proliferative phenotype[12,13]. In our hands, we wanted to see if there were potential differences in growth between the WT and GPR68 KO VSMCs under various in vitro conditions. Initial experiments used 'normal growth media' consisting of DMEM with 10% FBS growth serum (later experiments utilized normal/acidic growth media, to be discussed later). First, VSMCs of WT and KO mice were incubated in quiescent (0.2% serum) for 24 hours to achieve cytostasis and to ensure that all cells are at the same relative cell cycle stage, and then at 'time 0' quiescent media was replaced with complete growth media (containing 10% FBS). At times 0 and 24 hours, there were no observed differences in cell viability between WT and KO cells (see Figs. 6A, 6B). Interestingly, after 48 hours (Fig. 6C) a significant (~20%) decrease in viability was observed in WT cells compared to the GPR68 KO cells, which seemed to stay consistent (~80% viability) over the same time period. This

is interesting to note, as our WT cells under acidic conditions (pH≈6.5-6.7) failed to show any notable decrease and maintained cell viability over the 48-hour time period (data not shown).

To compare growth characteristics of WT and GPR68 KO VSMCs under serum-stimulated conditions, cells were then compared for a variety of other morphological and growth readouts, including cell circularity (Fig. 7), cell diameter (Fig. 8), and cell numbers (Fig. 8). No marked differences in cell circularity or cell diameter between the WT and GPR68 KO cells were observed over the course of 48 hours (see Figures 7C and 8C). Cell circularity is generally indicative of membrane protrusions such as lamellipodia, filopodia and/or blebs that are relevant in cell morphology and cell function[14]. A cell exhibiting a decrease in circularity can then be related to spreading of cells as occurs during cell migration and growth[14]. A change in the cell diameter could give insight as to how quickly cells are progressing and what phase cells are in the cell cycle, as an increase in diameter could be a sign of a dividing cell entering G_1[15]. As a readout of hyperplastic cellular growth, viable cell numbers were equal for WT and KO cells from the initial induction of growth stimulation (0 hours) through 24 hours (see Figure 9A, B, D). Results after 48 hours (Fig. 9C, D) showed a significant increase in viable cell numbers in the GPR68 KO group compared to the WT group. These experiments were repeated over time by the author and by multiple investigators in addition to the author, using cells of similar or different passages and from both male and female animals as well as under varied growth conditions (10-20% serum), and identical results were found every time. This consistent increase in viable cell numbers in our GPR68 KO cells suggest that in ‘normal’, non-genetically modified tissues under

in vitro, growth-stimulated conditions, GPR68 may be eliciting cytostatic growth-inhibition (as witnessed by exaggerated cell numbers in our GPR68 KOs), in line with our original hypothesis. Upon loss of GPR68 in these growth stimulated conditions, the GPR68 KO cells then experience growth induction, which is greatly exacerbated over a period of 48 hours. A potential concern for our cell number data may involve the apparently reduced cell viability that was seen in the WT cells at 48 hours (see Fig. 6C). However, data are presented for viable cell numbers, and the average cell viabilities for the WT and KO cell over 48 hours that were used in these readouts were not significantly different (WT=73.6% vs KO = 77.9%). Moreover, historical data from our lab using C57BL/6J WT mice as well as other strains of WT mice (and also including rat primaries) show a consistent range of viability between 65% and 85% over 72 hours (data not shown). These observations lend credence to our results and provides the indication that the differences in both cell viability and cell numbers may be the result of changes in cell cycle progression.

The influence of GPR68 on proliferation in primary VSMCs was previously described in a single study[16], yet that report cited no differences in growth between WT VSMCs and GPR68-siRNA knockdown VSMCs using a 3-(4,5-dimethylthiazol-2-yl)-2,5-diphenyltetrazolium bromide, or MTT, assay over 72 hours. The MTT is a tetrazolium salt that is reduced to purple formazan crystals mainly by mitochondrial succinate dehydrogenase and the color intensity of the formazan dye is correlated to the number of viable cells[17]. However, some chemicals or phytochemicals may change the activity of succinate dehydrogenase or interact with MTT directly[18,19]. While the MTT assay itself can be used as an indirect readout of proliferation, it suffers from limitations when

used as a singular proliferation readout and is often used instead as a measure of mitochondrial function, as our lab has previously described[89]. Reports that certain chemical reagents can interact with MTT compounds or interfere with mitochondrial dehydrogenase activity, which could then bias the assay results, have been noted[20-22], and there can be difficulty of removing the cell culture media from the plate wells due to floating cells with MTT formazan on the cell's surface, which can give rise to significant well-to-well errors[23]. Also, cells used in that study were grown in DMEM media in the presence of the mitogenic growth factors LPA and PDGF[16], potent mitogens that can also serve as cellular signaling molecules which could confound the apparent MTT results. In the absence of these additional growth factors, which could add potential confounding effects to the findings observed as well as potentially interfere with the MTT reagents, we witnessed consistently increased cell growth in our KO cells compared to our WT cells over a 48 hour period.

By comparison, in epithelial cells under normal pH conditions, a knockdown/knockout of GPR68 has been reported to increase proliferation[24]. Further, in a knockdown of GPR68 in breast cancer cells an increase in cell proliferation was observed under otherwise normal conditions[25]. Conversely, there have been reports showing increased expression of GPR68 by either acidic media and/or overexpression resulted in inhibited proliferation in endothelial progenitor cells[26] and in Caco-2 epithelial cells[27]. These studies, along with and supporting our results, give rise to the notion that loss or reduced activation of GPR68 results in an increase in proliferation and cellular growth.

In an effort to gain further insight into this observed hyper-proliferation of GPR68 KO cells, we examined cell cycle progression in serum-stimulated WT and KO cells (Fig. 10). Analysis of cell cycle progression, using flow cytometry to decipher individual phases of the cell cycle, was performed on WT and GPR68 KO cells at time 0 and every four hours up through 12 hours under growth-stimulated (10% serum) conditions following a low serum, quiescent period. We analyzed three individual "checkpoints" in the cell cycle: the G_0/G_1 growth phase is the first checkpoint which decides whether cells are ready to enter the S phase or maintain G_0 and is considered the resting phase[28]; the S phase includes DNA replication in which the 23 pairs of chromosomes are duplicated[28]; the G_2/M phase contains the G_2 growth checkpoint before cells continue to the M phase (mitosis) and cytokinesis[28]. Our cell viability and cell number results hint that our KO cells appear to be growing at a faster rate compared to their WT control counterparts. The number of WT cells in quiescent G_0/G_1 was trending upwards ($p=.08$) compared to the number of KO cells at time 0 (Fig. 10A) and after 4 ($p<.05$; Fig. 10B) and 8 hours (Fig. 10C), while the number of KO cells in G_2/M was higher than the number of WT cells in G_2/M at time 0 ($p=.06$; Fig. 10A) and after 4 and 8 hours (Figs. 10B, 10C). Moreover, a trend towards increased KO cells numbers in the synthetic S phase after 4 hours compared to WT cells was observed (Fig. 10B). While most of these comparisons are not statistically significant, these observations may represent biological significance, effects considered by expert judgment as important and meaningful[29]. These results suggest that the GPR68 KO cells are progressing through the cell cycle at higher rates compared to WT control cells, with fewer KO cells in the quiescent phase and more KO cells in the synthetic/proliferative phases from plating

(time 0) through 8 hours. Furthermore, after 12 hours (Fig. 10D), this trend seems to be reversed, with higher numbers of KO cells in G_0/G_1 and lower KO numbers in S compared to their WT counterparts. While longer timepoints and a more thorough cell cycle analysis could help identify discrete cell cycling times for GPR68 KO cells (compared to control cells), these preliminary data suggest that the cell cycling for GPR68 KO cells is much shorter than the control VSMCs, perhaps even shorter than 12 hours (as it appears that WT/KO cell numbers in all phases switch between 8 and 12 hours), which support our proliferative (cell number) data and provide further evidence that GPR KO cells are proliferating at faster rates than our control WT cells.

In a very broad sense, knockout cells exhibiting increased or reduced cellular growth are not uncommon and is usually based on the ablated gene and their functional impact. This has been seen in a wide variety of cell types[30-32] such as caveolin-2 knockout mice, whose mouse lung endothelial cells (MLEC) showed a 2.5x increase in cell numbers compared to their WT counterparts over 96 hours[30]. Specific to GPR68 KOs, hemopoietic stem cells (HSCs) and $CD4^+$ cells from both WT and whole body GPR68 KO mice have been shown to elicit no significant changes in cell survival or proliferation[33,34]. However, we are using different cell types and a different GPR68 KO mouse. Unlike our whole body KO for GPR68, the GPR68 KO used in this study was based on both insertion and intragenic deletion in which *Cre* mediated recombination removed the open reading frame compared to our GPR68 KO in which a neomycin-resistance cassette was inserted, which disrupted the expression of the gene[6,9]. To our knowledge, no reported studies to date have examined VSMC viability in global GPR68 KO mice.

The role of GPR68 in proliferation and/or cell death may involve it partly acting as a cytostatic regulator to avoid aberrant growth and to maintain the physiological conditions of the cell. In cell cycle analysis of endothelial cells with or without siRNA knockdown of GPR68, the authors saw a 25% increase in G_0/G_1 and a 25% decrease in $S+G_2/M$ in acidic media (pH 6.4) compared to normal media (pH 7.4) that was also reversed with the introduction of anti-GPR68 siRNA[35]. Our cell cycle experiments did not include acidic media but rather were designed to compare WT to KO models, and perhaps future cell cycle studies could be performed with/without acidic media exposure to further decipher the role of GPR68 not only in normal physiologic conditions, but also in acidic conditions (as performed in subsequent experiments discussed below). Other proton sensing GPCRs such as GPR132 have been shown to arrest the cell cycle at G_2/M in fibroblasts, which in turn reduces cell cycle progression and cell proliferation[36]. More dissection of the cell cycle, as well as increased attention to cellular viability will need to be done to confirm these regulatory outcomes and mechanisms involved.

Normal vs Acidic Media

While blood vessels maintain a viable pH range between 7.35 and 7.45, which is very closely regulated in the human body, GPR68 is activated in acidic conditions and is fully activated below a pH of 6.8 (and likewise, is fully inactivated at a pH above 7.8)[37-39]. To mimic acidic conditions in the vascular system, acidic media was prepared with a pH≈6.5-6.7 in addition to ‘normal’ pH buffered media (pH 7.4-7.6). To validate the biological ability of our specially prepared media to activate GPR68, we incubated WT cells in acidic (or normal) media over a 5-hour time period and then performed RT-qPCR using two different methods of quantitative gene expression - Taqman and SYBR

Green - to estimate GPR68 gene expression levels (see Figure 11). These two independent approaches produced identical results, with significantly increased activation of GPR68 mRNA expression ~4-fold in cells incubated in acidic media (WA) versus normal media (WN) (see Figure 11). The large increase in GPR68 transcriptional activation provides confidence that our acidic media serves as a reliable agonist of biological GPR68 activation and in turn could be used to induce GPR68 in our cells in subsequent experiments. Our findings agree with other studies in a variety of tissues that have validated activation of GPR68 at pH 6.8 and below including endothelial cells[35], kidney[40], and airway smooth muscle[41].

We then determined whether the acidic media (pH≈6.5-6.7) would have discernable effects on viability in our WT and GPR68 KO cells over the course of 48 hours (see Figure 12). Viability, determined by trypan blue exclusion staining, at plating (0 hrs) was unchanged amongst all groups (Fig. 12A). At the 24-hour time point (Fig. 12B), while we didn't see any differences in viability between acidic and normal media in the KO groups, we did see a significant increase in WT cell viability in acidic media compared to normal media (pH≈7.4-7.6). This was interesting as they were same WT cells seeded over multiple plates, and yet it almost seemed that the acidic media was helping to maintain cell viability in our control cells. Then, at 48 hours (Fig. 12C), there were no significant changes between the WT cells in normal versus acidic media, indicating that GPR68 has a possible role in maintenance of cell viability under acidic conditions. However, at 48 hours, viability in the KO cells in normal media was significantly higher than acidic group. In this case, the KO cells in acidic conditions lacked GPR68 activation helping to maintain viability and thus the cells were dying at a

higher rate. Comparing the WT cells in normal media as compared to KO cells in normal media also reveal a significant increase in viability over the 48-hour time point. What we could be seeing is that GPR68 in basal conditions serves to maintain cell viability, and when activated and overexpressed under acidotic conditions, helps to stabilize cell viability. These results indicate that our cells experience no adverse cytotoxic effects after 5-hour incubation in acidic media when compared to normal pH media. The 48-hour time point is typically when the media would be changed based on our established experimental protocols, so other outside factors such depleted nutrients and a resulting altered pH could be at play. Further investigation of cell viability over longer time periods needs to be done to determine a more precise cause. In previous studies, cancer associated fibroblasts (CAFs) containing an siRNA knockdown of GPR68 or a control non-targeting siRNA were placed in media with a pH between 7.4 and 6.4. The CAFs with siRNA knockdown showed significant decreases in cell viability at pH 6.6 and pH 6.4 when compared to the control siRNA after 48 hours[42]. In another study, viability was assessed in endothelial progenitor cells (EPCs) with or without siRNA knockdown of GPR68[35]. Not only was there about 25% reduction in cell viability after 48 hours in acidic media (pH 6.4) compared to normal media (pH 7.4), but that reduction of cell viability in acidic media was reversed to levels found in normal pH when siRNA knockdown of GPR68 was performed[35]. This again, as previously discussed, may reveal a role for GPR68 in maintenance of cell viability in acidic conditions.

G_s Signaling Pathway

Cyclic AMP (cAMP) is a critical second messenger that plays many key roles in intracellular signaling. Synthesized by adenylyl cyclase (AC) from ATP, cAMP is broken

down and inactivated by hydrolysis to AMP by a family of phosphodiesterases (PDE). It has a variety of functions, including significant roles in proliferation, migration, differentiation, and apoptosis. Its impact on cell proliferation is well documented[43-47], with most research pointing toward capacity of cAMP in reducing proliferation and vascular growth. Cyclic AMP can activate a multiple downstream signaling pathways[48], including notably PKA and EPAC.

In regards to the possible mechanisms by which GPR68 may attenuate VSMC proliferation, considering that scientific evidence[48-50] indicates that cell growth and proliferation are largely activated through stimulatory G_s and that G_s signaling is thought to be correlated with GPPR68[9,33,40,41], in our hands the cAMP signaling system was evaluated under normal or acidic growth-stimulated conditions in primary VSMCs. As shown in Figure 13, using a cAMP-specific ELISA we detected a significant decrease in cAMP levels in WT cells exposed to acidic media (WA) compared to WT cells in physiologically normal (pH = 7.4-7.6) media (WN). In fact, the WT group in normal media had significantly higher cAMP content than the KO groups in normal (KN) or acidic (KA) media as well. Between the KO groups, results showed no differences between cells in normal versus acidic media. These findings give an indication that cAMP is reduced in response to prolonged (5 hours) acidic conditions coincident with acid-mediated activation or perhaps over-expression of GPR68 (see Fig. 11). This reduction of cAMP in KO cells in normal conditions (WN to KN comparison) may be linked to increased cellular growth and proliferation. This reduction of cAMP could be a result of biased signaling which has been reported for GPR68 in other cell types[51]. Biased signaling would occur when prolonged over-exposure of GPR68 eventually

shuts down G_s signaling to reduce cAMP and can also be coupled with an increase in G_i (and/or perhaps other G protein) signaling. This activation of G_i signaling would then reduce cAMP by inactivation of AC and diminished cAMP synthesis. It is known that cAMP is involved in reducing cell proliferation[43-47], and the reduction of cAMP in normal media backs up our viability and cell cycle data (Figs. 4-7). The lack of GPR68 in KO cells does not allow for GPR68-mediated activation of cAMP in normal media, and in turn does not change the activating conditions of acidic media.

In two previous studies involving GPR68 in the VSM[16,52], the authors probed cAMP at a shorter time point (30 min) in media with pH values at 6.3, 6.5, 6.8, and 7.6[16,52] and found that intracellular cAMP was increased between 3-fold and 10-fold at pH 6.3-6.8 (acidic media) compared to pH 7.6 (normal media) with the PDE inhibitor IBMX added to prevent degradation and to maintain intracellular levels of cAMP[16,52]. The only other use of acidic media with regards to cAMP did not involve VSMCs, but instead was done in CAFs that contained siRNA knockdown of GPR68 or a control nontargeting siRNA[42]. However, like the previous publications[16,52], the incubation time in acidic media in that study[42] was short term. Their cAMP assay was performed after an incubation period in a range of media compositions with pH levels between 7.4 and 6.4 for 30 mins, and their results showed up to a 2-fold increase in cAMP in the CAFs with control siRNA at acidic pH between 6.8 and 6.4 when compared to comparatively basic pH levels that were between 7.4 -7.0[42]. There was also at least a 2-fold decrease at acidic pH levels between 7.4 and 6.4 in siRNA knockdown CAFs when compared to the CAFs with control siRNA[42].

In our study, we observed a significant 2-fold reduction in cAMP content in WT cells treated with acidic (pH≈6.5-6.7) media compared to WT cells treated with normal pH media (see Fig. 13). This also occurred with a similar 2-fold decrease in KO cells in either normal (KN) or acidic (KA) media compared to WT cells in normal media. While there is some discrepancy in our findings compared to other studies, it is important to note that the time frames in which the VSMCs were incubated in acidic media, 10-30 minutes in other studies compared to 5 hours in our study, may point to the reason as to why these differences are present between our work and what has been previously published. These acute time points in acidic buffer involved significant increases in GPR68. However, we believe that prolonged exposure to acidic conditions could either promote inactivation of the G_s signaling pathway or promote activation of the G_i signaling pathway through biased signaling, which has been reported for GPR68 in other cell types[40,51]. The decrease in the G_s signaling pathway could then be a cause for the decreased cAMP levels. That inactivation, along with the increased activation of G_i signaling, which inhibits the G_s pathway and cAMP, could therefore be responsible for the decrease in cAMP at 5 hours and our observed increases in cell proliferation. Another point to consider is the use of different cell types and their unique responses to these interventions. We and others[16,52] used primary VSMCs, but one other study used CAFs[42]. In order to address these differences, a time course study using VSMC with cAMP readouts between the 30 min and the 5 hour time point could be done in order to observe the possible changes in cAMP levels over the course from the more acute (30 min) time point to the more prolonged (5 hour) time point to observe if the same effect is occurring that is seen already in the literature.

Following this observation that acidic conditions, which over-expresses GPR68, serve to significantly reduce cAMP content, with lack of effects in our KO cells to verify dependency on GPR68, we wanted to see if cAMP activated its canonical target PKA or if it operated through an alternate signaling route. The only publication available that has examined PKA, cAMP and GPR68 together was in the previously cited paper using CAFs[42], yet in that study PKA was not a readout but instead was pharmacologically manipulated and resulting IL-6 levels were recorded[42]. As of this writing, no publications exist in available scientific databases where PKA levels or activity were examined in VSM under acidic conditions, based on numerous searches on PubMed and Google Scholar. Our PKA activity assay was performed both with and without IBMX, and in general our results suggest that PKA is not largely involved in GPR68/cAMP signaling under acidic conditions (see Figure 14). These results indicate that the canonical PKA pathway through which cAMP exerts many of its effects may not be activated in response to acidic conditions in primary VSMCs.

Several studies using a variety of cell types including arterial SMCs, prostate carcinoma cells, hepatic stellate cells, and rat anterior pituitary cells, have implicated EPAC, as opposed to PKA, in the control of cell proliferation[53-56], and even a synergistic relationship between EPAC and PKA in the inhibition of VSMC proliferation has been theorized[49]. Unfortunately, research findings regarding EPAC and proliferation have been contradictory in the literature, arguing for highly context-specific actions of EPAC. A number of papers implicate its role in inhibiting cell proliferation, with or without concomitant activation of PKA[49,53-55,57]. Other studies suggest a role for EPAC in pro-proliferative processes[56,58]. Whatever the role is for EPAC in mediating VSMC

proliferation, its general role in proliferation and in the face of acidic insult needs to be further studied.

In our studies, following various interventions in WT and KO cells we attempted to quantify EPAC protein expression using four different anti-EPAC antibodies (both polyclonal and monoclonal) from multiple vendors and performing numerous Western blots. Despite using various Western blotting protocols and permutations of our experimental approach, we were unsuccessful in accurately visualizing EPAC protein expression. Our limitations in successfully probing for EPAC had us searching for an alternate, downstream target that could give us an indirect reading of EPAC activity. We determined that Rap1A/1B would serve as a suitable protein for indirect readout of EPAC[59]. A small GTPase, Ras associated protein 1 (Rap1) belongs to the Ras family of proteins which are important in growth, survival and differentiation[60]. Activated by EPAC1, a Rap-GEF that favors GDP/GTP exchange, results in the activation of small GTPases like Rap1A/1B[60]. In turn, to determine a possible role for the cAMP product EPAC in our observed GPR68-mediated VSMC cytostasis, we probed for Rap1A/1B, an effector directly activated by EPAC[59]. Incubation of WT VSMCs in acidic media (WA) significantly decreased Rap1A/1B protein expression levels compared to WT cells treated with normal physiological media (WN) (Figure 15). In the KO cells, there were no significant differences in Rap1A/1B levels in normal versus acidic media, although KO cells exhibited ~30% reduction in Rap1A/1B levels when in acidic media compared to normal media (Fig.15C). In PKA-independent cAMP signaling, EPAC is the primary effector between cAMP and Rap1A/1B, and in turn these results indicate that EPAC is similarly reduced under acidic (versus normal media) conditions similar to cAMP and

Rap1A/1B. The reduction of these proteins when exposed to extracellular acidosis is no longer valid in the KO cells, suggesting a key mechanistic role for GPR68 operating through these signals.

In continued examination of Rap1A/1B, cells treated with ogerin, a PAM of GPR68[9,61,62], demonstrated similar results for Rap1A/1B (see Figure 16) compared to cells not treated with ogerin (see Figure 15). While not statistically significant (p=0.25), the reduction (~50%) of Rap1A/1B in WT cells in acidic media with ogerin was comparable to results in WT cells without ogerin, while KO cells showed no marked differences in acidic versus normal conditions. As a PAM, ogerin operates to promote GPR68 signaling, and in a 'proof of concept' experiment using only KO cells in acidic or normal media with or without ogerin, no significant differences were seen between groups (Fig. 17), providing more evidence for GPR68 specificity of ogerin and further backing up our notion that GPR68 operates primarily through Rap1A/1B subsequent to cAMP/EPAC signaling in primary VSM cells. Use of ogerin in published studies is scarce, as only 6 papers mention the use of ogerin. In the original paper identifying ogerin as a PAM of GPR68, the investigators showed that it promoted GPR68 signaling and suppressed fear conditioning in WT mice but lacked efficacy in GPR68 KO mice[9]. Our current studies support findings of this seminal article, with WT cells with ogerin (Fig. 16, WN) showing ~25% increase in Rap1A/1B expression compared to WT cells without ogerin (Fig. 15, WN), and without discernable influence of ogerin in our GPR68 KO cells. As a PAM, ogerin is the only agonist currently available that specifically targets GPR68[42]. Alternate routes for GPR68 induction, other than our currently used acidic/basic media, could include use of hypoxia (versus normoxia) exposure, use of

extracellular hypercapnia (versus isocapnia), or over-expression through plasmid-driven GPR68-Tango[63].

These results involving Rap1A/1B prompted us to then explore the MEK pathway and extracellular signal-regulated protein kinases 1 and 2 (ERK1/2). This pathway is responsible for indirect cell cycle progression of G_1-S phase progression by activation of S-phase kinase associated protein 2 (Skp2), and is needed in cell proliferation for the activation of cell cycle regulatory proteins such as Elk-1 and Sap-1a[90]. This pathway is also connected to cAMP signaling through the Rap1A/1B and has been shown to modulate ERK1/2 and therefore cell proliferation in VSMCs[91]. Initial results of phosphorylated ERK1/2 show very similar results to the Rap1A/1B, with a significant decrease between the WN and the WA groups, and no significant differences between the KO groups, although there was a marked decrease (p=.071) when comparing the KN group to the KA group (see Fig. 18A). While there were notable differences between the total ERK1/2 groups, there were no statistical differences between them (Fig. 18B). We normalized the pERK1/2 as compared total ERK and again, while we did not see any significant differences between groups, we did see about a ~80% reduction with the WN group when compared to the WA group and a ~40% reduction in the KA group compared to the KN group (Fig. 18C).

Stimulation of GPR68 via acidic conditions has been shown to trigger IL-6 expression through ERK1/2 and p38 activation in human airway SMCs[71]. This activation of both ERK1/2 and p38 has also been linked in the proliferative pathway by upstream activation of EPAC and PKA and by default, cAMP[44]. Our preliminary results seem to back up our assertion that this is an EPAC-Rap1A/1B mediated signaling pathway.

Calcium Signaling

Free intracellular calcium is a universal signaling molecule which is often seen in the vascular system in its ability to regulate vessel tone[64], with signaling primarily through activation of G_q and release of calcium from intracellular stores by activation of IP_3 and PLC[65]. Recently, it was theorized that calcium signaling is linked to growth via activation of the MEK/ERK1/2 pathway[66,67]. Proton-dependent Ca^{2+} release from intracellular stores has been shown to trigger the MEK/ERK1/2 pathway, thereby linking acidification with cell proliferation[66].

This reported connection with both the G_s signaling and the ERK1/2 pathway and the potential importance of acidic conditions in the control of intracellular Ca^{2+} prompted us to investigate the influence of acid exposure on VSMC calcium over a 5-hour experimental period as used with our other cellular signaling protocols. Our calcium assay measurements were taken from both the top and bottom reads at various time points over a 5-hour period (Figs. 19-22), and cumulative results showed consistently higher levels of intracellular Ca^{2+} in the KO cells in normal media (KN) compared to all other groups. In microplate reading, the bottom read is usually preferred when cells are adherent to the bottom of the plate[68]. However, a top read can also be done, which is generally better for reading molecules that are at the surface of lipophilic solutions or in suspension[68]. Using top reads (Figs. 19, 20), across almost the entire 4-hour incubation period (minus the 1-hour time point; see Fig. 19C), we saw a significant decrease in intracellular calcium in the GPR68 KO cells in normal media compared to KO cells in acidic media. One hour after incubation was the only reading that did not reach statistical significance between the KO groups, but it could still be biologically significant

as we saw ~30% reduction in Ca^{2+} in the acidic media compared to the normal media. The same could not be said for the WT groups with the top reads across the 4-hour timeframe. Throughout these time points, we were unable to see any marked differences between the WT VSMCs in normal media compared to WT cells in acidic media. A similar pattern emerged with the bottom readings for Ca^{2+} (Figs. 21, 22). While the first two hours showed no significant differences between all four groups, we did start to see a trending decrease in the KO cells in acidic media compared to KO cells in normal media. However, in hours 2 (Fig. 21D), 3 (Fig. 21E), and 4(Fig. 21F), we saw significant decreases in Ca^{2+} not only between the KO cell groups in acidic and normal media, but we also saw a significant increase in Ca^{2+} in the KO cells in normal media as compared to the WT cell in normal media. These significant decreases in calcium observed in both the top and bottom reads of GPR68 KO cells in acidic media shows that the modulation of $Ca2^{+}$ is at the very least, not all GPR68 mediated. Without GPR68, we should not have seen such a vast decrease between the groups, but it was apparent in both top and bottom reads. However, in both top and bottom reads, we did see increases in Ca^{2+} when GPR68 was removed (i.e., KN versus WN comparisons). This hints that GPR68 is involved in the reduction of intracellular Ca^{2+} at a basal level.

To understand if GPR68 is involved in acidosis-induced Ca2+ reduction, we compared the percent (%) reduction from WT or GPR68 VSMCs in normal media to those in acidic media. In our top reads (Fig. 20), we consistently saw marked increases in the % reduction of Ca^{2+} from 0 – 4 hours in the KO cells compared to WT cells, with significance reached after 2 hours (Fig. 20D). In our bottom reads (Fig. 22), we did not see differences in the % reduction from normal to acidic media between the WT and the

GPR68 KO cells across the time points. For hours 2 (Fig. 22D), 3 (Fig. 22E), and 4 (Fig. 22F), while not significant, we did see marked increases in % reduction of Ca^{2+} in the KO cells compared to the WT cells. Both the top and bottom reads trended toward a larger % reduction of Ca^{2+} in the GPR68 KO cells as compared to their WT counterparts. This hints that GPR68 may be involved in the maintenance of intracellular Ca^{2+} levels under acidic conditions.

It has been reported in endothelial cells that acidosis can serve to inhibit Ca^{2+} influx, which would decrease intracellular calcium levels[69], and the general notion in endothelial cells and other cell types is that acidosis acts to reduce intracellular Ca^{2+} concentrations[38]. Removing GPR68 in basal pH conditions results in higher intracellular calcium levels then their WT counterpart. This could be an indication of the role of GPR68 in modulating calcium levels. Whether this decrease in intracellular calcium by a G_q or G_s mediated activation/inactivation is still unknown. From a few studies assessing GPR68 and calcium, G_q signaling may be initially involved and that modulation of ERK1/2 can occur further downstream. In human airway epithelium, G_q inhibition by the antagonist RGS2 resulted in large reduction in acid-induced, GPR68-dependent increase of intracellular Ca^{2+}[70]. In another study of human airway smooth muscle, G_q was attenuated using both siRNA and an antagonist YM-254890, resulting in decreases in intracellular calcium[71].

A caveat of our Ca^{2+} assay is that it only allows initial detection of Ca^{2+} following a 1-hour incubation time, and in order to maintain consistency, we wanted to measure intracellular calcium levels through 5 hours in acidic (or normal) media. Alternative approaches to detect more acute Ca^{2+} fluxes such as fluorescent dyes and reading on a

plate reader or using fluorescent microscopy is that the changes in Ca^{2+} occur over a matter of seconds[72]. The 1-hour incubation time alone would have missed acute timepoints. Our 'agonist' is acidic buffer, and using the buffers and incubating the calcium binding dye would take at least 1 hour before any results could be accurately taken, thereby presenting a limitation to this approach. We also used a linear system plate reader that reads one at a time instead of a parallel system that could read multiple wells at a single time. It is recommended that we keep the linear reading under an hour total, even then our initial read alone would serve as the best indicator of Ca^{2+} levels[72].

IL-6 Signaling

Interleukin 6 (IL-6) is a multifunctional cytokine that regulates the immune response, acute phase responses, and inflammation, and is produced by a variety of cells[73]. Clinical studies have revealed that an increase in IL-6 is associated with an increase in adjusted relative risks for coronary heart disease death and myocardial infaction[74]. Increased levels of pro-inflammatory IL-6 have been associated with atherosclerosis, vasculitis and other CVDs[48]. Intermittent hypoxia has been shown to increase IL-6 in human coronary VSMCs which suggest that hypoxia induces IL-6-dependent inflammation of the vessel wall and in ischemic/hypoxic tissues[75,76]. Stimulation of GPR68 via acidic conditions has been shown to trigger IL-6 expression through ERK1/2 and p38 activation in human airway SMCs[71]. This activation of both ERK1/2 and p38 has also been linked in the proliferative pathway by upstream activation of EPAC and PKA and by default, cAMP[44]. In our studies using primary VSMCs incubated in normal or acidic buffers, results similarly show a significant

increase of IL-6 protein expression in WT cells in acidic media compared to WT cells in normal physiological media (see Figure 23). In KO cells, however, no marked changes in IL-6 expression were evident in cells incubated in acidic versus normal media, and in fact levels were comparable to WT cells in normal media (WN). These observations suggest that, consistent with what has been reported in airway SMCs[71], in primary WT VSMCs IL-6 is upregulated in acidic conditions concomitant with induced GPR68, yet no differences are detected in the absence of GPR68 in KO cells. This is significant as mouse CAFs have shown increased IL-6 expression that are activated by the cAMP/PKA/CREB pathway[42].

Acid activation of GPR68 seems to be important in the modulation of IL-6 and Ca^{2+}. The results from our in vitro data mimic the increases in IL-6 observed in CAFs, S100B-positive cells of the anterior pituitary gland as well as airway SMCs following extracellular acidification[42,71,77].

Overall, these findings present a number of interesting new discoveries. First, our results support GPR68 acting as a cytostatic brake in VSMCs, slowing down yet maintaining cell proliferation under normal physiological conditions. We have also found that the mechanism for this increased proliferation may lie in cell cycle control. Our cell number readouts and our cell cycle data also back up the notion that GPR68 seems to be important in the reduction of VSMC proliferation and growth.

Furthermore, our data suggest acidic pH activates GPR68 and that it operates likely via G_s signaling in VSMCs. While the exact role of G_s signaling in GPR68-mediated cell growth is still unclear, our data suggest that GPR68 plays a role in reducing proliferation of cultured VSMCs. The reduction of cAMP in WT animals as well

as the reduction of Rap1A/1B and phosphorylated ERK suggest an EPAC-mediated mechanism in the capacity of GPR68 in reducing proliferation in acidic conditions. In normal pH conditions, we have an intact system for GPR68, but it seems to operate at a very low activation level. This in turn increases cAMP signaling which reduces cell growth. Under acidic conditions, GPR68 is fully activated which either then reduces G_s signaling or possibly increases G_i signaling via biased signaling, which reduces cAMP signaling and activity, in turn increase cellular growth. In the KO cells, there is none of this, as GPR68 is absent. Interestingly the primary activation pathway is up for some debate, with some studies finding G_q coupled signaling, while there are some others suggesting G_s signaling[37]. Regardless, our findings contend that cAMP is involved in and acidic pH activated GPR68 signaling in VSM.

Our observations are the first to contend increased IL-6 expression in VSMCs under acidic conditions. However, we did not see increased Ca^{2+} but rather we observed marked decreases in phosphorylated ERK under acidic conditions that were not seen in airway SMCs under extracellular activation[71].

IN VIVO STUDIES

While using in vitro methods has afforded us with new insight using the controlled in vitro setting of primary culture, there are also limitations to such approaches. By using a solitary cell type such as VSMCs, the lack of other resident cell types and/or lack of circulating factors that are associated with in vivo studies are not considered. Therefore, we desired to test some of these same endpoints in intact tissue/live animal in vivo models to provide further context for what was discerned from our cell culture studies.

Along the same line, we were curious to see if the increase in IL-6 in response to acidic conditions in cultured cells could be translated to a whole vessel in vivo model. Using an arterial ligation model to create an ischemic vessel and to mimic an acidic in vivo microenvironment, we were unable to detect significant differences in IL-6 expression in WT versus GPR68 KO injured arteries (see Figure 24). While there are substantial differences between clonal homogenous cultured primary VSMCs and intact whole vessels that contain numerous different cell types including the influence of circulating factors and neurohumoral input, these results, combined with our in vitro IL-6 data, are a necessary starting point in determining a potential role for IL-6 with GPR68 in cell growth.

By using our GPR68 KO to WT comparisons we can see what effects the knockout has on protein and expression levels to elucidate mechanisms as well as to see cause and effect relationships to discern function. However, assessing potential systemic influence on our desired vascular readouts is important because of their possible confounding effects on VSMCs in our studies. If confounding systemic influence is not considered in vivo, false positives and invalid readouts could be generated with disregard of true, genuine differences[78]. In our studies, systemic parameters such as heart rate and blood pressure were compared between WT and KO animals. By understanding possible differences in the system that we are interested in ahead of time, we can then read the results of in vivo studies as genuine rather than a byproduct of the knockout of the gene of interest.

In GPR68 KO mouse models, there are very few reported phenotypic differences compared to WT mice. The most common functional difference that has been reported

is that GPR68 KO mice produce more osteoblasts and osteoclasts and exhibit increased bone density[79]. GPR68 KO mice have also shown significantly decreased plasma insulin levels[80]. In the vascular system, GPR68 has been suggested as a mechanosensor of shear stress in vascular endothelial cells[8] and of mechanical stretch in other cell types[81]. To try to determine potential differences in our WT animals compared to our GPR68 KO animals in an in vivo setting, in our hands several critical cardiovascular readings were assessed in order to not only shed light on why it seems that the KO animal cells were proliferating faster, but to see if we could determine any general differences, at least in cardiovascular tissues, between the WT and the GPR68 KO animals.

The systemic parameters that were directly measured in our studies included heartrate (HR) and systolic and diastolic blood pressures (SBP, DBP). From these values the mean arterial pressure (MAP), a readout of average arterial pressure from systole to diastole through one cardiac cycle, pulse pressure (PP), a readout of the difference between the systolic and the diastolic blood pressure, and rate pressure product (RPP), which is a readout of cardiac work, were calculated. These readouts give us an indication on possible alterations of vascular tone, vascular resistance, plasticity, and cardiac work which may go on to alter cell growth such as proliferation and cell signaling including cAMP and could be the explanation as to why we are seeing changes in cell growth and G_s signaling[82,83,84]. However, these results did not discern any noticeable differences between the WT and KO animals (Fig. 25). These similar phenotypic data between our WT and GPR68 KO models minimize the influence of

potential systemic confounders such as alterations in blood pressure profiles or heart rate, in the observations discussed previously.

While we did not see any discernable phenotypic differences between our WT and GPR68 KO animals with regards to HR and BP under normal physiological conditions, we looked at in vivo injury and remodeling using two distinct injury models in the common carotid artery which could potentially impact GPR68 signaling. While these models are used to study a response to a primary injury, they also serve as models to study the pathophysiology of vascular disease in the intact whole-body system. Moreover, these in vivo findings will allow us to extrapolate our in vitro observations to the in vivo, whole body setting. For these studies we used a rat carotid artery balloon injury model[85,86] and a mouse carotid artery ligation ischemia model[86].

The rat carotid artery balloon injury model allows us to study both vascular growth and remodeling subsequent to mural wall mechanical distension, and mechanical stretch has been shown to modulate GPR68 under in vitro conditions[81]. This approach consists of carotid artery access and isolation of the common carotid artery, followed by insertion of a balloon embolectomy catheter through an external branch arteriotomy and catheter-induced endothelial denudation, medial wall expansion and distension of the common carotid artery. This model allows evaluation of in vivo VSM proliferation and migration and apoptosis as well as endothelial cell regeneration and biology of extracellular matrix components[85,86]. In this rat injury model, our results showed a significant decrease in carotid artery homogenate GPR68 protein expression compared to uninjured naïve vessels over an acute (30 min) timepoint (Fig. 26B). Several caveats exist though concerning these findings. First, this model was

performed in a different species (rat) than what was used for our in vitro studies (mouse) discussed to this point. The rat was used based on previous knowledge of the balloon injury model and to generate results using a different species to see how they relate to the mouse model. The second factor is the acute time point of 30 mins compared to the in vitro timepoint of 5 hours. What could be happening in the whole body in an acute timepoint of 30 minutes may not be what is occurring is a longer 5-hour timepoint under cell culture conditions. This initial decrease in GPR68 expression could potentially become an increase in GPR68 expression at a more prolonged time point. A third factor is that GPR68 protein readings might not be VSMC-specific. The heterogenous vascular environment in vivo also includes the extracellular matrix and the endothelial cells, both which may have contributed to the drop in GPR68 expression. Also, and perhaps the most important limitation to these data, is that in vivo confirmation that vessel wall distension injury creates an acidic microenvironment has yet to be done. Finally, antibodies for GPCRs have been known to be finicky and promiscuous[87]. Primary antibodies for GPCRs tend to not be very specific and generally target more conserved regions of GPCRs, in turn often giving inaccurate readouts[87]. There is also the issue with how quickly a membrane localized GPCR can be internalized and degraded[88]. This internalization and degradation can happen within minutes through ubiquitination and/or β-arrestin-mediated processes, and limited membrane residency and this GPCR recycling add limitations to accurate GPCR detection[88].

The mouse ligation injury is a model in which reducing flow with a ligature creates minimal/zero blood flow in the common carotid artery and subsequently

provokes an ischemic environment that may be similar to the in vitro approach of acidic media (pH≈6.5-6.7) used with our VSMCs. The mouse ligation model is used to induce flow cessation and vessel ischemia in the setting of an intact vessel architecture, and endpoints can vary different based on the exact site of the ligature placement as our lab has detailed[86]. This means the operator could obtain vastly different outcomes if observing a particular section of the carotid closer to the ligation than if observing carotid tissue more distal to the ligation; therefore, consistency in tissue harvest in relation to the precise ligature site is necessary[86]. Performed in our WT and GPR68 KO mice and using these strict procedures, our results showed a significant decrease in arterial wall homogenate GPR68 protein expression over an intermediate (24 hr) timepoint (Fig. 27). We also performed the same ligation injury on both male and female mice to discern if sex influences the protein levels of GPR68 both injured and in uninjured mice. These disaggregated results showed no significant difference in GPR68 expression between males and females for both the uninjured and injured cohorts (Fig. 27C).

The decrease in GPR68 protein expression observed in the mouse model over an intermediate timepoint was similar to what was seen in the rat model at a more acute timepoint. However, the intermediate timepoint was much longer than the 5-hour timepoint used for our in vitro VSMC studies. Given the rapid nature of GPCR recycling, what we are seeing might be a result of prolong exposure to acidic conditions that are not necessarily seen in the more acute 5-hour time point. The acute response to acidic conditions could activate GPR68 and may be initially growth protective over the first few hours of acidosis, such as what was seen at the 5-hour in vitro data. However, over 24

hours of prolonged exposure to acidotic conditions, GPR68 might then be implicated in the increase of VSMC proliferation. Also, as we are dealing with not only VSMCs, but a number of other cell types, including endothelial cells, collagen and elastic fibers, the outcomes seen in VSMCs may not directly translate to an in vivo environment where there is crosstalk between VSMCs and these other cell types including namely endothelial cells. The ligation injury model creates an ischemic environment by partially or completing blocking blood flow to the carotid artery. This is lack of blood flow in theory would allow for acidic conditions to arise in the vasculature[86].

Using WT and GPR68 KO mice, we performed the carotid artery ligation ischemic model and harvested tissues after 4 weeks to see the effects of GPR68 ablation on cell proliferation and death as key components in vascular remodeling. Our results showed that the KO animals with carotid artery ligation injury showed significantly less neointimal growth when compared to their WT counterparts (Fig. 28). These results would suggest that deletion of GPR68 could in fact be instrumental in slowing down neointimal growth and that the addition of GPR68 is not so much growth-protective, but may help in increasing VSMC proliferation and/or decreasing cell death in the in vivo setting. Further, the fact that the in vitro studies involve VSMCs while in vivo studies involve a whole variety of cells in the heterogenous vessel wall may have profound effects on the outcome of vascular remodeling and neointimal formation in cell-specific fashion. There is even a possibility of an influence from other proton-sensing GPCRs, particularly GPR4, which share high homology and have been shown to form weak heterodimers with GPR68[92].

Lastly, the increase in neointimal growth and the resulting inference that GPR68 is not growth protective in vivo seems to contradict our in vitro results that GPR68 is growth protective. However, this can at least be partially explained by differences in timing as the in vivo ligation injury for the mice used a 4-week timeframe for tissue harvest while the signaling pathways were assessed over 5 hours. What we could be observing, considering the rapid nature of GPCRs including G_s signaling, is more a snapshot of the moment. The acute response to acidic conditions, that is, activated GPR68, may be initially growth protective, such as what was seen with our 5-hour in vitro data; however, over 4 weeks of prolonged exposure to ischemic acidosis, GPR68 might then be implicated in the increase of VSMC proliferation. Also, with our in vivo studies we are dealing with not only VSMCs, but a number of other cell types, including endothelial cells, collagen and elastic fibers, the outcomes seen in VSMC may not directly translate to an in vivo environment where there is interaction between endothelial cells and VSMCs. Finally, we are unsure precisely what the true acidic conditions were in our in vivo ischemia model. While we are able to control conditions in an in vitro setting, as of now we can speculate the conditions that arise with the ligation ischemia model. The only other in vivo model of a vascular system has shown that GPR68 acts as a mechanosensor and acts in shear stress and that flow mediated outward remodeling of small arteries occurred in vivo[8].

Acidosis is a major hallmark of ischemic CVD which could potentially be a key regulator of CVD pathogenesis. Historically associated with CVD, acidosis has predominantly been considered a side-effect rather than an active player in CVD pathogenesis, yet those studies are just now emerging. Our GPR68 KO VSMC studies

are unique in that, at the time of this writing, only one other study exists in the scientific literature that specifically targeted GPR68 in VSM, yet it focused primarily on vascular endothelial cells and theorized GPR68 as a sensor for endothelium-mediated shear stress mechanotransduction[8]. Altogether, our study will help advance our knowledge of GPR68 in VSM and will help characterize utility of our GPR68 KO models. We also implicate a role for GPR68 in the remodeling process and although its final impact in the in vivo setting is unclear, it seems that it may play a proliferative role in neointimal formation.

Conclusions & Future Directions

In conclusion, in this dissertation we have explored GPR68, a proton sensing GPCR whose roles in the cardiovascular system are just now coming to light. While at this moment, our knowledge of GPR68 in VSM and its role(s) in mediating varied aspects of CVD is limited, we have been able to make small steps towards understanding its impact and the mechanisms by which it works. Our grasp of the true role of GPR68 in the cardiovascular system is in its infancy. The precise mechanisms by which GPR68 is activated and the downstream regulatory outcomes are only going to increase with continued research efforts. In our hands, we have started this process, by not only beginning to characterize the GPR68 KO mouse model with particular focus on VSM, but we've also begun to dissect the role that G_s signaling and the cAMP pathway may play in acidic pH activated GPR68 in VSMC proliferation and cell death. A complete overview of the key signaling pathways (Fig. 29) is shown below. Thus, the GPR68 receptor could be a novel therapeutic target for vascular ischemic disorders, such as stroke and restenosis, in which extracellular acidification may lead to vascular

dysfunction and disease. It could also be a target in ischemic vascular diseases such as carotid artery and peripheral arterial disease, in which the lack of oxygen from plaque build-up can lead to an altered metabolism and the resulting acidification.

While we are just beginning to discern how GPR68 is involved in both the vascular system and in CVD, work still needs to be continued in a number of areas. In cellular growth, our study included estimations of cell death but further exploration into programed cell death and apoptosis and necroptosis needs to be explored. This will allow more insight into whether GPR68 and some of the many forms of cell death are linked. Continued work is needed on cell proliferation, including readings of cell cycle proteins (cyclins, cyclin-dependent kinases, etc.) that are important checkpoints in the various stages of the cell cycle. Finally, the connection of GPR68 and cAMP to signaling molecules such as IL-6 and $Ca^{2+}$and their subsequent pathways needs work to decipher if/how they are involved in cellular growth.

In our in vivo models we need more confirmation that our ligation injury model properly mimics an acidic environment that the in vitro cell culture studies undergo so that the ligation injury model can be properly assessed in the creation of an acidic in vivo environment. There is more work needed for the acute, intermediate, and chronic timepoints to fully link the signaling pathways with in vivo remodeling events. The disconnect that was observed between our observations in vitro and those in vivo warrant further investigation to gain better insight of the complex interactions that occur in different time points as well as these different environments including the in vivo milieu versus in vitro platforms.

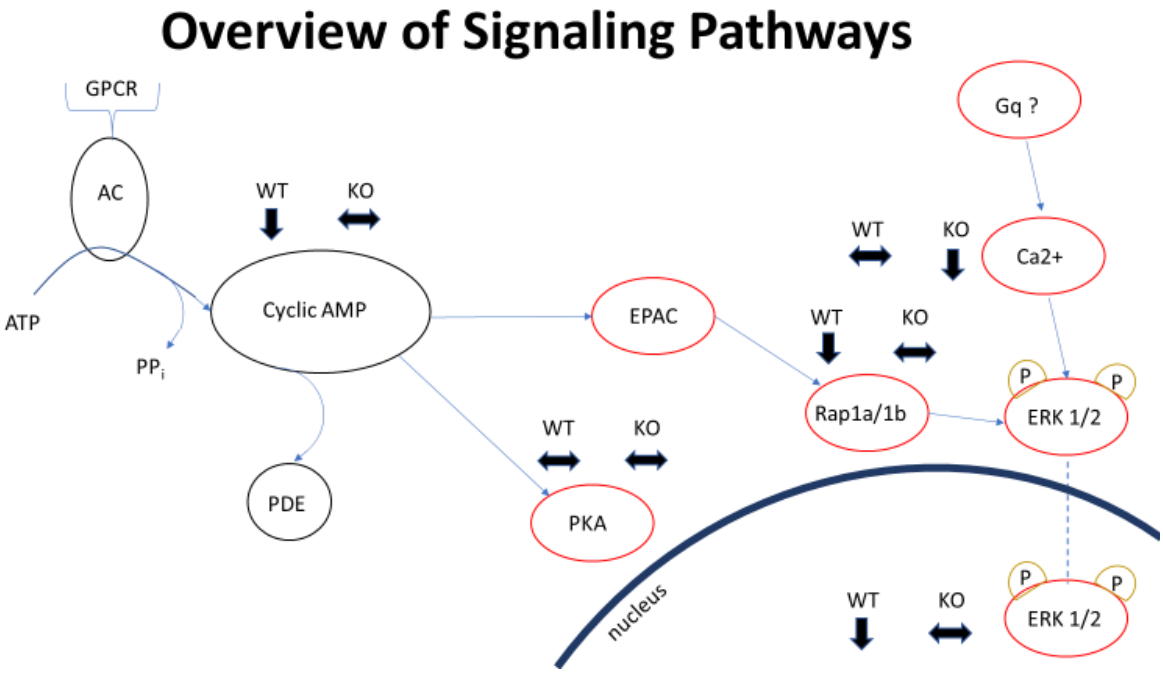

Figure 29. Overview of signaling pathways. An overview of all signaling pathways and corresponding directional results upon exposure to acidic conditions as compared to normal conditions for wild type (WT) and knockout (KO) VSMCs.

DISCUSSION REFERENCES

1. Kato K, Morita I. Promotion of osteoclast differentiation and activation in spite of impeded osteoblast-lineage differentiation under acidosis: effects of acidosis on bone metabolism. *Biosci Trends*. 2013;7(1):33-41.

2. Yang M, Mailhot G, Birnbaum MJ, MacKay CA, Mason-Savas A, Odgren PR. Expression of and role for ovarian cancer G-protein-coupled receptor 1 (OGR1) during osteoclastogenesis. *J Biol Chem*. 2006;281(33):23598-23605. doi:10.1074/jbc.M602191200.

3. Iwai K, Koike M, Ohshima S, et al. RGS18 acts as a negative regulator of osteoclastogenesis by modulating the acid-sensing OGR1/NFAT signaling pathway. *J Bone Miner Res*. 2007;22(10):1612-1620. doi:10.1359/jbmr.070612.

4. Pereverzev A, Komarova SV, Korcok J, et al. Extracellular acidification enhances osteoclast survival through an NFAT-independent, protein kinase C-dependent pathway. *Bone*. 2008;42(1):150-161. doi:10.1016/j.bone.2007.08.044.

5. Yan L, Singh LS, Zhang L, Xu Y. Role of OGR1 in myeloid-derived cells in prostate cancer. *Oncogene*. 2014;33(2):157-164. doi:10.1038/onc.2012.566.

6. Li H, Wang D, Singh LS, et al. Abnormalities in osteoclastogenesis and decreased tumorigenesis in mice deficient for ovarian cancer G protein-coupled receptor 1 [published correction appears in PLoS One. 2015;10(4):e0125463]. *PLoS One*. 2009;4(5):e5705. Published 2009 May 28. doi:10.1371/journal.pone.0005705.

7. Insel PA, Sriram K, Wiley SZ, et al. GPCRomics: GPCR expression in cancer cells and tumors identifies new, potential biomarkers and therapeutic targets. *Front Pharmacol*. 2018;9:431. Published 2018 May 22. doi:10.3389/fphar.2018.00431.

8. Xu J, Mathur J, Vessières E, et al. GPR68 senses flow and is essential for vascular physiology. *Cell*. 2018;173(3):762-775.e16. doi:10.1016/j.cell.2018.03.076.

9. Huang XP, Karpiak J, Kroeze WK, et al. Allosteric ligands for the pharmacologically dark receptors GPR68 and GPR65. *Nature*. 2015;527(7579):477-483. doi:10.1038/nature15699.

10. Fontaine DA, Davis DB. Attention to background strain is essential for metabolic research: C57BL/6 and the International Knockout Mouse Consortium. *Diabetes*. 2016;65(1):25-33. doi:10.2337/db15-0982.

11. Taft RA, Davisson M, Wiles MV. Know thy mouse. *Trends Genet*. 2006;22(12):649-653. doi:10.1016/j.tig.2006.09.010.

12. Holt, D., Tulis, D. Vascular smooth muscle as a therapeutic target in disease pathology. *Muscle Cell and Tissue*, Chapter 1, pp. 3-26, Ed. K. Sakuma, InTech Open Access Publishers, ISBN 978-953-51-2156-5, doi: 10.5772/60878;

http://www.intechopen.com/ articles/show/title/vascular-smooth-muscle-as-a-therapeutic-target-in-disease-pathology, 2015.

13. Wehbe N, Nasser SA, Al-Dhaheri Y, et al. EPAC in vascular smooth muscle cells. *Int J Mol Sci*. 2020;21(14):5160. Published 2020 Jul 21. doi:10.3390/ijms21145160.

14. Hart ML, Lauer JC, Selig M, Hanak M, Walters B, Rolauffs B. Shaping the cell and the future: recent advancements in biophysical aspects relevant to regenerative medicine. *J Funct Morphol Kinesiol.* 2018; 3(1):2.

15. Guertin DA, Sabatini DM. Chapter 12 - Cell Growth. In: Mendelsohn J, Howley PM, Israel MA, Gray JW, Thompson CB, editors. The molecular basis of cancer. 3rd edition. Philadelphia, W.B.: Saunders; 2008. pp. 169–175.

16. Liu JP, Komachi M, Tomura H, et al. Ovarian cancer G protein-coupled receptor 1-dependent and -independent vascular actions to acidic pH in human aortic smooth muscle cells. *Am J Physiol Heart Circ Physiol*. 2010;299(3):H731-H742. doi:10.1152/ajpheart.00977.2009.

17. Wang HZ, Chang CH, Lin CP, Tsai MC. Using MTT viability assay to test the cytotoxicity of antibiotics and steroid to cultured porcine corneal endothelial cells. *J Ocul Pharmacol Ther*. 1996;12(1):35-43. doi:10.1089/jop.1996.12.35.

18. Devika PT, Stanely Mainzen Prince P. (-)Epigallocatechin-gallate (EGCG) prevents mitochondrial damage in isoproterenol-induced cardiac toxicity in albino Wistar rats: a transmission electron microscopic and in vitro study. *Pharmacol Res*. 2008;57(5):351-357. doi:10.1016/j.phrs.2008.03.008.

19. Hsu S, Bollag WB, Lewis J, et al. Green tea polyphenols induce differentiation and proliferation in epidermal keratinocytes. *J Pharmacol Exp Ther*. 2003;306(1):29-34. doi:10.1124/jpet.103.049734.

20. Liu Y, Peterson DA, Kimura H, Schubert D. Mechanism of cellular 3-(4,5-dimethylthiazol-2-yl)-2,5-diphenyltetrazolium bromide (MTT) reduction. *J Neurochem*. 1997;69(2):581-593. doi:10.1046/j.1471-4159.1997.69020581.x.

21. Ulukaya E, Ozdikicioglu F, Oral AY, Demirci M. The MTT assay yields a relatively lower result of growth inhibition than the ATP assay depending on the chemotherapeutic drugs tested. *Toxicol In Vitro*. 2008;22(1):232-239. doi:10.1016/j.tiv.2007.08.006.

22. Weyermann J, Lochmann D, Zimmer A. A practical note on the use of cytotoxicity assays. *Int J Pharm*. 2005;288(2):369-376. doi:10.1016/j.ijpharm.2004.09.018.

23. Aslantürk ÖS. In Vitro Cytotoxicity and Cell Viability Assays: Principles, Advantages, and Disadvantages. In Genotoxicity-A Predictable Risk to Our Actual World. IntechOpen. 2017; DOI: 10.5772/intechopen.71923.

24. Zhu C, Wang L, Zhu J, et al. OGR1 negatively regulates β-casein and triglyceride synthesis and cell proliferation via the PI3K/AKT/mTOR signaling pathway in goat mammary epithelial cells [published online ahead of print, 2020 Mar 13]. *Anim Biotechnol*. 2020;1-10. doi:10.1080/10495398.2020.1737099.

25. Zhang J, Che L, Sun W, Shang J, Hao M, Tian M. Correlation of OGR1 with proliferation and apoptosis of breast cancer cells. *Oncol Lett*. 2019;17(5):4335-4340. doi:10.3892/ol.2019.10121.

26. Ding S, Xu J, Zhang Q, et al. OGR1 mediates the inhibitory effects of acidic environment on proliferation and angiogenesis of endothelial progenitor cells. *Cell Biol Int*. 2019;43(11):1307-1316. doi:10.1002/cbin.11179.

27. de Vallière C, Vidal S, Clay I, et al. The pH-sensing receptor OGR1 improves barrier function of epithelial cells and inhibits migration in an acidic environment. *Am J Physiol Gastrointest Liver Physiol*. 2015;309(6):G475-G490. doi:10.1152/ajpgi.00408.2014.

28. Alberts B, Johnson A, Lewis J, et al. Molecular Biology of the Cell. 4th edition. New York: Garland Science; 2002. An Overview of the Cell Cycle. Available from: https://www.ncbi.nlm.nih.gov/books/NBK26869/.

29. Lovell DP. Biological importance and statistical significance. *J Agric Food Chem*. 2013;61(35):8340-8348. doi:10.1021/jf401124y.

30. Xie L, Frank PG, Lisanti MP, Sowa G. Endothelial cells isolated from caveolin-2 knockout mice display higher proliferation rate and cell cycle progression relative to their wild-type counterparts. *Am J Physiol Cell Physiol*. 2010;298(3):C693-C701. doi:10.1152/ajpcell.00401.2009.

31. Khaodee W, Udomsom S, Kunnaja P, Cressey R. Knockout of glucosidase II beta subunit inhibits growth and metastatic potential of lung cancer cells by inhibiting receptor tyrosine kinase activities. *Sci Rep*. 2019;9(1):10394. Published 2019 Jul 17. doi:10.1038/s41598-019-46701-y.

32. McKinley KL, Cheeseman IM. Large-scale analysis of CRISPR/Cas9 cell-cycle knockouts reveals the diversity of p53-dependent responses to cell-cycle defects. *Dev Cell*. 2017;40(4):405-420.e2. doi:10.1016/j.devcel.2017.01.012.

33. He X, Hawkins C, Lawley L, et al. Whole body deletion of Gpr68 does not change hematopoietic stem cell function [published online ahead of print, 2020 Jun 20]. *Stem Cell Res*. 2020;47:101869. doi:10.1016/j.scr.2020.101869.

34. D'Souza CA, Zhao FL, Li X, Xu Y, Dunn SE, Zhang L. OGR1/GPR68 Modulates the severity of experimental autoimmune encephalomyelitis and regulates nitric oxide production by macrophages. *PLoS One*. 2016;11(2):e0148439. Published 2016 Feb 1. doi:10.1371/journal.pone.0148439.

35. Ding S, Xu J, Zhang Q, et al. OGR1 mediates the inhibitory effects of acidic environment on proliferation and angiogenesis of endothelial progenitor cells. *Cell Biol Int*. 2019;43(11):1307-1316. doi:10.1002/cbin.11179.

36. Weng Z, Fluckiger AC, Nisitani S, et al. A DNA damage and stress inducible G protein-coupled receptor blocks cells in G2/M. *Proc Natl Acad Sci U S A*. 1998;95(21):12334-12339. doi:10.1073/pnas.95.21.12334.

37. Wiley SZ, Sriram K, Salmerón C, Insel PA. GPR68: An emerging drug target in cancer. *Int J Mol Sci*. 2019;20(3):559. Published 2019 Jan 28. doi:10.3390/ijms20030559.

38. Celotto AC, Capellini VK, Baldo CF, Dalio MB, Rodrigues AJ, Evora PR. Effects of acid-base imbalance on vascular reactivity. *Braz J Med Biol Res*. 2008;41(6):439-445. doi:10.1590/s0100-879x2008005000026.

39. Singh V, Khatana S, Gupta P. Blood gas analysis for bedside diagnosis. *Natl J Maxillofac Surg*. 2013;4(2):136-141. doi:10.4103/0975-5950.127641.

40. Ludwig MG, Vanek M, Guerini D, et al. Proton-sensing G-protein-coupled receptors. *Nature*. 2003;425(6953):93-98. doi:10.1038/nature01905.

41. Saxena H, Deshpande DA, Tiegs BC, et al. The GPCR OGR1 (GPR68) mediates diverse signalling and contraction of airway smooth muscle in response to small reductions in extracellular pH. *Br J Pharmacol*. 2012;166(3):981-990. doi:10.1111/j.1476-5381.2011.01807.x.

42. Wiley SZ, Sriram K, Liang W, et al. GPR68, a proton-sensing GPCR, mediates interaction of cancer-associated fibroblasts and cancer cells. *FASEB J*. 2018;32(3):1170-1183. doi:10.1096/fj.201700834R.

43. Palmer D, Tsoi K, Maurice DH. Synergistic inhibition of vascular smooth muscle cell migration by phosphodiesterase 3 and phosphodiesterase 4 inhibitors. *Circ Res*. 1998;82:852–861.

44. Smith SA, Newby AC, Bond M. Ending restenosis: inhibition of vascular smooth muscle cell proliferation by cAMP. *Cells*. 2019;8(11):1447. Published 2019 Nov 16. doi:10.3390/cells8111447,

45. Dong H, Claffey KP, Brocke S, Epstein PM. Inhibition of breast cancer cell migration by activation of cAMP signaling. *Breast Cancer Res Treat*. 2015;152(1):17-28. doi:10.1007/s10549-015-3445-9.

46. Lee JW, Lee J, Moon EY. HeLa human cervical cancer cell migration is inhibited by treatment with dibutyryl-cAMP. *Anticancer Res*. 2014;34(7):3447-3455.

47. Schmitt JM, Stork PJ. Cyclic AMP-mediated inhibition of cell growth requires the small G protein Rap1. *Mol Cell Biol*. 2001;21(11):3671-3683. doi:10.1128/MCB.21.11.3671-3683.2001.

48. Holland NA, Francisco JT, Johnson SC, et al. Cyclic nucleotide-directed protein kinases in cardiovascular inflammation and growth. *J Cardiovasc Dev Dis*. 2018;5(1):6. Published 2018 Jan 23. doi:10.3390/jcdd5010006.

49. Hewer RC, Sala-Newby GB, Wu YJ, Newby AC, Bond M. PKA and Epac synergistically inhibit smooth muscle cell proliferation. *J Mol Cell Cardiol*. 2011;50:87–98. doi: 10.1016/j.yjmcc.2010.10.010.

50. Wehbe N, Nasser SA, Al-Dhaheri Y, et al. EPAC in vascular smooth muscle cells. *Int J Mol Sci*. 2020;21(14):5160. Published 2020 Jul 21. doi:10.3390/ijms21145160.

51. Pera T, Deshpande DA, Ippolito M, et al. Biased signaling of the proton-sensing receptor OGR1 by benzodiazepines. *FASEB J*. 2018;32(2):862-874. doi:10.1096/fj.201700555R

52. Tomura H, Wang JQ, Komachi M, et al. Prostaglandin I(2) production and cAMP accumulation in response to acidic extracellular pH through OGR1 in human aortic smooth muscle cells. *J Biol Chem*. 2005;280(41):34458-34464. doi:10.1074/jbc.M505287200.

53. Mayer P, Hinze AV, Harst A, von Kügelgen I. A_2B receptors mediate the induction of early genes and inhibition of arterial smooth muscle cell proliferation via Epac. *Cardiovasc Res*. 2011;90(1):148-156. doi:10.1093/cvr/cvq371.

54. Grandoch M, Rose A, ter Braak M, et al. Epac inhibits migration and proliferation of human prostate carcinoma cells. *Br J Cancer*. 2009;101(12):2038-2042. doi:10.1038/sj.bjc.6605439.

55. Yang Y, Yang F, Wu X, Lv X, Li J. EPAC activation inhibits acetaldehyde-induced activation and proliferation of hepatic stellate cell via Rap1. *Can J Physiol Pharmacol*. 2016;94(5):498-507. doi:10.1139/cjpp-2015-0437.

56. Sun W, Jiao W, Huang Y, et al. Exchange proteins directly activated by cAMP induce the proliferation of rat anterior pituitary GH3 cells via the activation of extracellular signal-regulated kinase. *Biochem Biophys Res Commun*. 2017;485(2):355-359. doi:10.1016/j.bbrc.2017.02.075.

57. Roscioni SS, Prins AG, Elzinga CR, et al. Protein kinase A and the exchange protein directly activated by cAMP (Epac) modulate phenotype plasticity in human airway smooth muscle. *Br J Pharmacol*. 2011;164(3):958-969. doi:10.1111/j.1476-5381.2011.01354.x.

58. Wang X, Luo C, Cheng X, Lu M. Lithium and an EPAC-specific inhibitor ESI-09 synergistically suppress pancreatic cancer cell proliferation and survival. *Acta Biochim Biophys Sin (Shanghai)*. 2017;49(7):573-580. doi:10.1093/abbs/gmx045.

59. Kawasaki H, Springett GM, Mochizuki N, et al. A family of cAMP-binding proteins that directly activate Rap1. *Science*. 1998;282(5397):2275-2279. doi:10.1126/science.282.5397.227.

60. Lezoualc'h F, Fazal L, Laudette M, Conte C. Cyclic AMP sensor EPAC proteins and their role in cardiovascular function and disease. *Circ Res*. 2016;118(5):881-897. doi:10.1161/CIRCRESAHA.115.306529

61. Yu X, Huang XP, Kenakin TP, et al. Design, synthesis, and characterization of ogerin-based positive allosteric modulators for G protein-coupled receptor 68 (GPR68). *J Med Chem*. 2019;62(16):7557-7574. doi:10.1021/acs.jmedchem.9b00869.

62. Huang XP, Kenakin TP, Gu S, Shoichet BK, Roth BL. Differential roles of extracellular histidine residues of GPR68 for proton-sensing and allosteric modulation by divalent metal ions. *Biochemistry*. 2020;59(38):3594-3614. doi:10.1021/acs.biochem.0c00576.

63. Kroeze WK, Sassano MF, Huang XP, et al. PRESTO-Tango as an open-source resource for interrogation of the druggable human GPCRome. *Nat Struct Mol Biol*. 2015;22(5):362-369. doi:10.1038/nsmb.3014.

64. Amberg GC, Navedo MF. Calcium dynamics in vascular smooth muscle. *Microcirculation*. 2013;20(4):281-289. doi:10.1111/micc.12046.

65. Wynne BM, Chiao CW, Webb RC. Vascular smooth muscle cell signaling mechanisms for contraction to angiotensin II and endothelin-1. *J Am Soc Hypertens*. 2009;3(2):84-95. doi:10.1016/j.jash.2008.09.002.

66. Huang WC, Swietach P, Vaughan-Jones RD, Ansorge O, Glitsch MD. Extracellular acidification elicits spatially and temporally distinct Ca2+ signals. *Curr Biol*. 2008;18(10):781-785. doi:10.1016/j.cub.2008.04.049.

67. Apáti A, Jánossy J, Brózik A, Bauer PI, Magócsi M. Calcium induces cell survival and proliferation through the activation of the MAPK pathway in a human hormone-dependent leukemia cell line, TF-1. *J Biol Chem*. 2003;278(11):9235-9243. doi:10.1074/jbc.m205528200.

68. Jones E, Michael S, Sittampalam GS. Basics of Assay Equipment and Instrumentation for High Throughput Screening. In: Markossian S, Sittampalam GS, Grossman A, et al., eds. *Assay Guidance Manual*. Bethesda (MD): Eli Lilly & Company and the National Center for Advancing Translational Sciences; May 1, 2012.

69. Demirel E, Laskey RE, Purkerson S, van Breemen C. The passive calcium leak in cultured porcine aortic endothelial cells. *Biochem Biophys Res Commun*. 1993;191(3):1197-1203. doi:10.1006/bbrc.1993.1344.

70. Liu C, Li Q, Zhou X, Kolosov VP, Perelman JM. Regulator of G-protein signaling 2 inhibits acid-induced mucin5AC hypersecretion in human airway epithelial cells. *Respir Physiol Neurobiol*. 2013;185(2):265-271. doi:10.1016/j.resp.2012.10.003

71. Ichimonji I, Tomura H, Mogi C, et al. Extracellular acidification stimulates IL-6 production and Ca(2+) mobilization through proton-sensing OGR1 receptors in human airway smooth muscle cells. *Am J Physiol Lung Cell Mol Physiol*. 2010;299(4):L567-L577. doi:10.1152/ajplung.00415.2009.

72. Heusinkveld HJ, Westerink RH. Caveats and limitations of plate reader-based high-throughput kinetic measurements of intracellular calcium levels. *Toxicol Appl Pharmacol*. 2011;255(1):1-8. doi:10.1016/j.taap.2011.05.020.

73. Mihara M, Hashizume M, Yoshida H, Suzuki M, Shiina M. IL-6/IL-6 receptor system and its role in physiological and pathological conditions. *Clin Sci (Lond)*. 2012;122(4):143-159. doi:10.1042/CS20110340.

74. Kaptoge S, Seshasai SR, Gao P, et al. Inflammatory cytokines and risk of coronary heart disease: new prospective study and updated meta-analysis. *Eur Heart J*. 2014;35(9):578-589. doi:10.1093/eurheartj/eht367.

75. Kyotani Y, Itaya-Hironaka A, Yamauchi A, et al. Intermittent hypoxia-induced epiregulin expression by IL-6 production in human coronary artery smooth muscle cells. *FEBS Open Bio*. 2018;8(5):868-876. Published 2018 Apr 19. doi:10.1002/2211-5463.12430.

76. Kyotani Y, Takasawa S, Yoshizumi M. Proliferative pathways of vascular smooth muscle cells in response to intermittent hypoxia. *Int J Mol Sci*. 2019;20(11):2706. Published 2019 Jun 1. doi:10.3390/ijms20112706.

77. Horiguchi K, Higuchi M, Yoshida S, et al. Proton receptor GPR68 expression in dendritic-cell-like S100β-positive cells of rat anterior pituitary gland: GPR68 induces interleukin-6 gene expression in extracellular acidification. *Cell Tissue Res*. 2014;358(2):515-525. doi:10.1007/s00441-014-1958-x.

78. Brommage R, Liu J, Hansen GM, et al. High-throughput screening of mouse gene knockouts identifies established and novel skeletal phenotypes. *Bone Res*. 2014;2:14034. Published 2014 Oct 28. doi:10.1038/boneres.2014.34.

79. Krieger NS, Yao Z, Kyker-Snowman K, Kim MH, Boyce BF, Bushinsky DA. Increased bone density in mice lacking the proton receptor OGR1. *Kidney Int*. 2016;89(3):565-573. doi:10.1016/j.kint.2015.12.020.

80. Nakakura T, Mogi C, Tobo M, et al. Deficiency of proton-sensing ovarian cancer G protein-coupled receptor 1 attenuates glucose-stimulated insulin secretion. *Endocrinology*. 2012;153(9):4171-4180. doi:10.1210/en.2012-1164.

81. Wei WC, Bianchi F, Wang YK, Tang MJ, Ye H, Glitsch MD. Coincidence detection of membrane stretch and extracellular pH by the proton-sensing receptor OGR1 (GPR68). *Curr Biol*. 2018;28(23):3815-3823.e4. doi:10.1016/j.cub.2018.10.046.

82. Touyz RM, Alves-Lopes R, Rios FJ, et al. Vascular smooth muscle contraction in hypertension. *Cardiovasc Res*. 2018;114(4):529-539. doi:10.1093/cvr/cvy023.

83. DeMers D, Wachs D. Physiology, Mean Arterial Pressure. [Updated 2020 Aug 22]. In: StatPearls [Internet]. Treasure Island (FL): StatPearls Publishing; 2020 Jan-. Available from: https://www.ncbi.nlm.nih.gov/books/NBK538226/.

84. Homan TD, Bordes S, Cichowski E. Physiology, Pulse Pressure. [Updated 2020 Jun 7]. In: StatPearls [Internet]. Treasure Island (FL): StatPearls Publishing; 2020 Jan-. Available from: https://www.ncbi.nlm.nih.gov/books/NBK482408/.

85. Tulis DA. Rat carotid artery balloon injury model. *Methods Mol Med*. 2007;139:1-30. doi:10.1007/978-1-59745-571-8_1.

86. Holt AW, Tulis DA. Experimental rat and mouse carotid artery surgery: injury & remodeling Studies. *ISRN Minim Invasive Surg*. 2013;2013:167407. doi:10.1155/2013/167407.

87. Michel MC, Wieland T, Tsujimoto G. How reliable are G-protein-coupled receptor antibodies?. *Naunyn Schmiedebergs Arch Pharmacol*. 2009;379(4):385-388. doi:10.1007/s00210-009-0395-y.

88. Drake MT, Shenoy SK, Lefkowitz RJ. Trafficking of G protein-coupled receptors. *Circ Res*. 2006;99(6):570-582. doi:10.1161/01.RES.0000242563.47507.ce.

89. Stone, J.D., Narine, A., Tulis, D.A. Inhibition of vascular smooth muscle growth via signaling crosstalk between AMP-activated protein kinase and cAMP-dependent protein kinase. Front. Physiol. 3:409; doi:10.3389/fphys.2012.00409; 20

90. Mebratu Y, Tesfaigzi Y. How ERK1/2 activation controls cell proliferation and cell death: Is subcellular localization the answer? *Cell Cycle*. 2009;8(8):1168-1175. doi:10.4161/cc.8.8.8147

91. Li Q, Teng Y, Wang J, Yu M, Li Y, Zheng H. Rap1 promotes proliferation and migration of vascular smooth muscle cell via the ERK pathway. *Pathol Res Pract*. 2018;214(7):1045-1050. doi:10.1016/j.prp.2018.04.007

92. Zaslavsky A, Singh LS, Tan H, Ding H, Liang Z, Xu Y. Homo- and hetero-dimerization of LPA/S1P receptors, OGR1 and GPR4. *Biochim Biophys Acta*. 2006;1761(10):1200-1212. doi:10.1016/j.bbalip.2006.08.011.

APPENDIX: ANIMAL CARE AND USE APPROVAL LETTERS

ECU
Animal Care and Use Committee
003 Ed Warren Life Sciences Building | East Carolina University | Greenville NC 27354 - 4354
252-744-2436 office | 252-744-2355 fax

May 20, 2020

Dave Tulis, Ph.D.
Department of Physiology, ECU

Dear Dr. Tulis:

Your Animal Use Protocol entitled, " NO-independent cGMP regulation of vascular remodeling in mice" (AUP #Q261d) was reviewed by this institution's Animal Care and Use Committee on 05/20/2020. The following action was taken by the Committee:

"Approved as submitted"

****Please contact Aaron Hinkle prior to any hazard use****

A copy of the protocols is enclosed for your laboratory files. Please be reminded that all animal procedures must be conducted as described in the approved Animal Use Protocol. Modifications of these procedures cannot be performed without prior approval of the ACUC. The Animal Welfare Act and Public Health Service Guidelines require the ACUC to suspend activities not in accordance with approved procedures and report such activities to the responsible University Official (Vice Chancellor for Health Sciences or Vice Chancellor for Academic Affairs) and appropriate federal Agencies. **Please ensure that all personnel associated with this protocol have access to this approved copy of the AUP/Amendment and are familiar with its contents.**

Sincerely yours,

SBMcRae

Susan McRae, Ph.D.
Chair, Animal Care and Use Committee

SM/GD

enclosure

ECU
Animal Care and Use Committee
003 Ed Warren Life Sciences Building | East Carolina University | Greenville NC 27354 - 4354
252-744-2436 office | 252-744-2355 fax

May 19, 2020

Dave Tulis, Ph.D.
Department of Physiology, ECU

Dear Dr. Tulis:

Your Animal Use Protocol entitled, "NO-independent cGMP regulation of vascular remodeling in rats " (AUP #Q360) was reviewed by this institution's Animal Care and Use Committee on 05/19/2020. The following action was taken by the Committee:

"Approved as submitted"

****Please contact Aaron Hinkle prior to any hazard use****

A copy of the protocols is enclosed for your laboratory files. Please be reminded that all animal procedures must be conducted as described in the approved Animal Use Protocol. Modifications of these procedures cannot be performed without prior approval of the ACUC. The Animal Welfare Act and Public Health Service Guidelines require the ACUC to suspend activities not in accordance with approved procedures and report such activities to the responsible University Official (Vice Chancellor for Health Sciences or Vice Chancellor for Academic Affairs) and appropriate federal Agencies. **Please ensure that all personnel associated with this protocol have access to this approved copy of the AUP/Amendment and are familiar with its contents.**

Sincerely yours,

SBMcRae

Susan McRae, Ph.D.
Chair, Animal Care and Use Committee

SM/GD

enclosure